

CCEER 97-1-B

**FULL-SCALE FIELD RESONANCE TESTS
OF A RAILWAY BRIDGE**

by

Emmanuel "Manos" Maragakis
Bruce M. Douglas
U. Sandirasegaram

A Report to the

**ASSOCIATION OF AMERICAN
RAILROADS**

Civil Engineering Department
University Of Nevada, Reno
May 1997

ABSTRACT

Field dynamic resonance tests of the Strawberry Park Underpass, a two span simply supported railway bridge located in Los Angeles, were performed by using an eccentric mass dynamic shaker. The east span of the structure and the adjacent road bed were instrumented with twenty four FBA-11 accelerometers. The bridge was shaken in both the longitudinal and the transverse directions. To identify the influence of the rails, the tests were performed initially with the rails in place and then with the rails cut at the abutments. The natural frequencies and the corresponding modal damping values of the first and second transverse, the first longitudinal and the first vertical modes were calculated. Significant participation of the adjacent roadbed, indicating a strong interaction between the structure and the soil, was also observed. A three dimensional finite element program was developed, in order to predict the experimentally developed results. These predictions were reasonably accurate. This model will be the first step towards further analytical studies, which are currently under development. This report describes the experimental procedures, the analysis of the data and its results and the development of the analytical model.

ACKNOWLEDGMENTS

This study was funded by the Association of American Railroads a support that is gratefully acknowledged. The purchase of the dynamic shaker by the College of Engineering at the University of Nevada, Reno is also appreciated. The help of Messrs. John Choros and Vinaya Sharma at the initial stages of this project, as well as of Messrs. Semih Kalay, Bill Byers, and Drs. Bob Sweeney and Duane Otter throughout this study is greatly appreciated. Many thanks to Souther Pacific engineers Ken Wammel and Roger Boraas, as well as the Caltrans Engineer, Dan Freeman, for their help with the arrangements for the field tests, as well as Mr. Steve Keowen of ANCO for his help with the shaker operation.

TABLE OF CONTENTS

CHAPTER 1 INTRODUCTION

PAGE

1.1	Background	1
1.2	Objective	2
1.3	Location and description of the bridge	2

CHAPTER 2 EXPERIMENTAL SET UPS AND PROCEDURES

2.1	Introduction	6
2.2	General System Description	6
2.3	Mounting of the Shaker to the Test Structure	7
2.4	Installing Weights and Setting Eccentricity	8
2.5	Hardware System Used in the Test	9
2.6	Installation of the Accelerometers on the Bridge	9
2.7	Accelerometer Setups	10
2.7.1	Transverse Direction Experiment	10
2.7.2	Longitudinal Direction Experiment	12

CHAPTER 3 ANALYSIS OF FIELD DATA

3.1	Response Curves	21
3.2	Plotting Mode Shapes	26

CHAPTER 4 RESPONSE OF THE BRIDGE IN THE TRANSVERSE DIRECTION

4.1	First Mode - Rails In Place	26
4.2	Second Mode -Rails In Place.....	28
4.3	First Mode -Rails Cut	31

CHAPTER 5 RESPONSE OF THE BRIDGE IN THE LONGITUDINAL DIRECTION

5.1	Introduction	64
5.2	First Mode - Rails In Place	65
5.3	First Vertical Mode -Rails In Place	67
5.4	First Longitudinal and Vertical Modes - Rails Cut	69

CHAPTER 6 ANALYTICAL MODELING OF THE BRIDGE

6.1	Introduction	79
6.2	Two Main Girders.....	80
6.3	Floor Beams.....	81
6.4	Ballast Pan.....	81
6.5	Knee Bracket Supports	82
6.6	Track Structure.....	82
6.7	Main Girder Stiffeners	82
6.8	First Vertical Mode Shape of the Model.....	83
6.9	Transverse Mode Shape of the Model.....	83

CHAPTER 7 SUMMARY AND CONCLUSIONS.....	93
REFERENCES	99
APPENDIX	100
LIST OF CCEER PUBLICATIONS.....	130

List of Tables

4.1	Dynamic Properties of the Bridge in the First Transverse Mode.....
4.2	Dynamic Properties of the Bridge in the Second Transverse Mode.....
4.3	Vertical Response of the Bridge in the Second Transverse Mode.....
4.4	Response Parameters of the Bridge for the Cut Rail Transverse Case(Six Variables).....
4.5	Response Parameters of the Bridge for the Cut Rail Transverse Case(Nine Variables).....
5.1	Response Parameters of the Bridge for the Longitudinal Direction.....
5.2	Response Parameters for the Longitudinal Response with Noise Effect.....
5.3	Vertical Response Parameters of the Bridge with Rails in their as built Condition.
7.1	Summary of the Experimental Results.....

List of Figures

1.1	Elevation View of Strawberry Bridge.....
1.2	Plan View of Strawberry Bridge.....
1.3	Abutment Bearings.....
2.1	Setup#1 in the Transverse Direction.....
2.2	Configurations of Shaker Weights.....
2.3	Setup#2 in the Transverse Direction.....
2.4	Setup#3 in the Transverse Direction.....
2.5	Setup#4 in the Transverse Direction.....
2.6	Setup#1 in the Longitudinal Direction.....
2.7	Setup#2 in the Longitudinal Direction.....
2.8	Setup#3 in the Longitudinal Direction.....
2.9	Setup#4 in the Longitudinal Direction.....
2.10	Setup#5 in the Longitudinal Direction.....
2.11	Setup#6 in the Longitudinal Direction.....
3.1	Equivalent SDOF System.....
4.1	CH2 Response Curve- First Transverse Mode.....
4.2	CH3 Response Curve- First Transverse Mode.....
4.3	CH7 Response Curve- First Transverse Mode.....
4.4	CH8 Response Curve- First Transverse Mode.....
4.5	CH9 Response Curve- First Transverse Mode.....
4.6	CH11 Response Curve- First Transverse Mode.....

4.7	CH12 Response Curve- First Transverse Mode.....
4.8	CH14 Response Curve- First Transverse Mode.....
4.9	CH15 Response Curve- First Transverse Mode.....
4.10	Average Response - First Transverse Mode.....
4.11	First Transverse Mode Shape.....
4.12	CH7 Test Response- Transverse Direction.....
4.13	CH7 Acceleration Response- Transverse Direction.....
4.14	CH8 Test Response- Transverse Direction.....
4.15	CH8 Acceleration Response- Transverse Direction.....
4.16	CH7 Response Curve- Second Transverse Mode.....
4.17	CH8 Response Curve- Second Transverse Mode.....
4.18	CH12 Vertical Response - Second Mode.....
4.19	CH21 Vertical Response - Second Mode.....
4.20	Cross Section- Second Transverse Mode.....
4.21	Second Transverse Mode Shape.....
4.22	CH2 Response Curve- Cut Rail Transverse (3 Variables).....
4.23	CH3 Response Curve- Cut Rail Transverse (3 Variables).....
4.24	CH7 Response Curve- Cut Rail Transverse (3 Variables).....
4.25	CH8 Response Curve- Cut Rail Transverse (3 Variables).....
4.26	CH9 Response Curve- Cut Rail Transverse (3 Variables).....
4.27	CH11 Response Curve- Cut Rail Transverse (3 Variables).....

4.28	CH12 Response Curve- Cut Rail Transverse (3 Variables).....
4.29	CH14 Response Curve- Cut Rail Transverse (3 Variables).....
4.30	CH15 Response Curve- Cut Rail Transverse (3 Variables).....
4.31	CH16 Response Curve- Cut Rail Transverse (3 Variables).....
4.32	CH3 Acceleration Response - Cut Rail Transverse
4.33	CH9 Acceleration Response - Cut Rail Transverse
4.34	CH11 Acceleration Response - Cut Rail Transverse
4.35	CH12 Acceleration Response - Cut Rail Transverse
4.36	CH15 Acceleration Response - Cut Rail Transverse
4.37	CH8 FFT Response - Cut Rail Transverse
4.38	CH2 Response Curve- Cut Rail Transverse (6 Variables).....
4.39	CH3 Response Curve- Cut Rail Transverse (6 Variables).....
4.40	CH6 Response Curve- Cut Rail Transverse (6 Variables).....
4.41	CH7 Response Curve- Cut Rail Transverse (6 Variables).....
4.42	CH8 Response Curve- Cut Rail Transverse (6 Variables).....
4.43	CH11 Response Curve- Cut Rail Transverse (6 Variables).....
4.44	CH14 Response Curve- Cut Rail Transverse (6 Variables).....
4.45	CH16 Response Curve- Cut Rail Transverse (6 Variables).....
4.46	CH2 Response Curve- Cut Rail Transverse (9 Variables).....
4.47	CH3 Response Curve- Cut Rail Transverse (9 Variables).....
4.48	CH6 Response Curve- Cut Rail Transverse (9 Variables).....

4.49	CH7 Response Curve- Cut Rail Transverse (9 Variables).....
4.50	CH8 Response Curve- Cut Rail Transverse (9 Variables).....
4.51	CH11 Response Curve- Cut Rail Transverse (9 Variables).....
4.52	CH14 Response Curve- Cut Rail Transverse (9 Variables).....
4.53	CH16 Response Curve- Cut Rail Transverse (9 Variables).....
4.54	First Transverse Mode Shapes for Rail and Cut Rail Cases.....
5.1	Longitudinal Response at 8.0Hz- Uncut Rail.....
5.2	Longitudinal Response at 8.0Hz- Cut Rail.....
5.3	CH2 Response Curve- First Longitudinal Mode.....
5.4	CH3 Response Curve- First Longitudinal Mode.....
5.5	CH4 Response Curve- First Longitudinal Mode.....
5.6	CH5 Response Curve- First Longitudinal Mode.....
5.7	CH2 Response Curve- First Longitudinal Mode(6 Variables).....
5.8	CH3 Response Curve- First Longitudinal Mode(6 Variables).....
5.9	CH4 Response Curve- First Longitudinal Mode(6 Variables).....
5.10	CH5 Response Curve- First Longitudinal Mode(6 Variables).....
5.11	Longitudinal Mode Shape at 6.6Hz.....
5.12	CH6 Response Curve- First Vertical Mode(Lon.Setup).....
5.13	CH7 Response Curve- First Vertical Mode(Lon.Setup).....
5.14	CH8 Response Curve- First Vertical Mode(Lon.Setup).....
5.15	Vertical Mode Shape at 6.0Hz.....

5.16 Vertical Mode Shape at 6.0Hz " Sinusoidal Fitting ".....

5.17 CH2 Response Curve- Cut Rail Longitudinal.....

5.18 CH3 Response Curve- Cut Rail Longitudinal.....

6.1 Cross Section of Main Girder with a Model of The Plates.....

6.2 Three Dimensional Model of the Bridge.....

6.3 Part of the Model Showing Floor Beams Connected to the Main Girders.....

6.4 Part of the Model Showing the Brackets, Ballast Pan and Stiffeners.....

6.5 First Vertical Mode Shape of the Model at 5.9Hz.....

6.6 Cross Section of the Vertical Mode at 5.9Hz.....

6.7 First Transverse Mode Shape of the Model at 7.0Hz.....

6.8 Cross Section of the Model at 7.0Hz.....

6.9 Mode Shape of the Model at 9.2Hz.....

6.10 Cross Section of the Model at 9.2Hz.....

6.11 Vertical Amplitudes at 5.9Hz.....

6.12 Transverse Amplitudes at 5.9Hz.....

6.13 Comparison of the Amplitudes at 5.9Hz.....

6.14 Transverse Amplitudes at 7.0Hz.....

6.15 Vertical Amplitudes at 7.0Hz.....

6.16 Comparison of the Amplitudes at 7.0Hz.....

CHAPTER 1

INTRODUCTION

1.1 BACKGROUND

During the last two decades, significant research has been conducted to investigate the seismic response of highway bridges and to address their seismic retrofitting requirements. This research has included several experimental and analytical studies. During this time, no significant studies have been performed to identify the dynamic properties of railway bridges, their ultimate strength, and their response under earthquake excitations. One important difference between highway and railway bridges is that, in the case of railway bridges, the rails, ties, ballast and ballast pan provide a connection between the bridge structure and the adjacent roadbed. The presence of the track structure could provide significant benefits in terms of providing additional restraint and a mechanism for transferring seismic loads to the roadbed. Thus, the structural elements of the railway bridges might be relieved from the demand to carry all of the seismic load.

The Association of American Railroads (AAR) funded a study with the University of Nevada, Reno, to perform full scale resonance tests on the Strawberry Park Underpass, a railway bridge located in Los Angeles, California. The bridge was scheduled for removal in Spring 1995. A new bridge, next to the Strawberry Underpass, was under construction during the test.

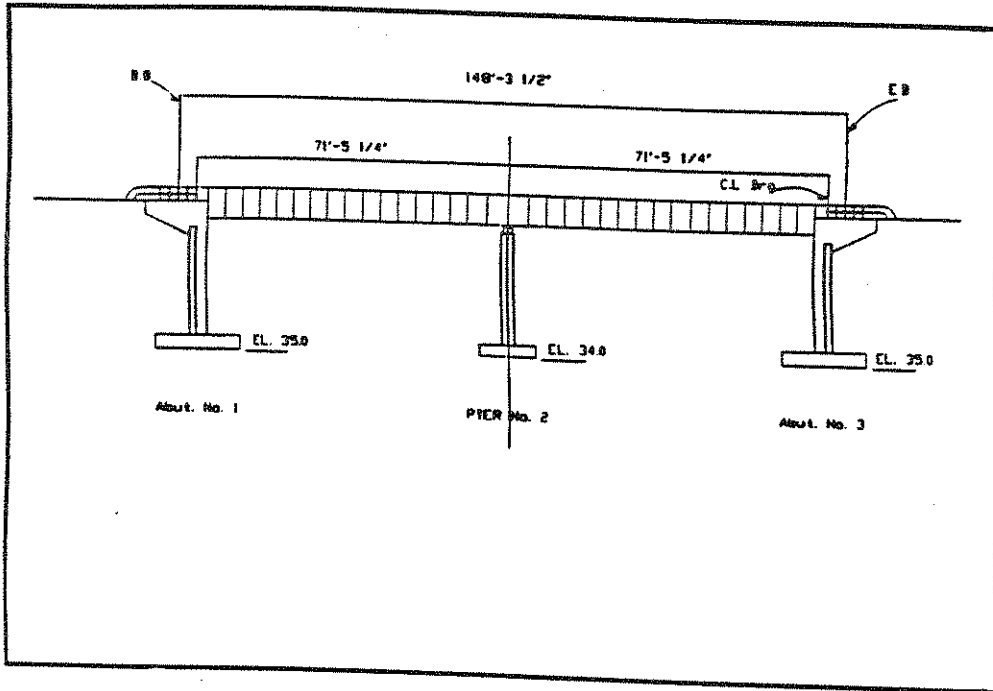


Fig 1.1 : Elevation view of Strawberry Bridge.

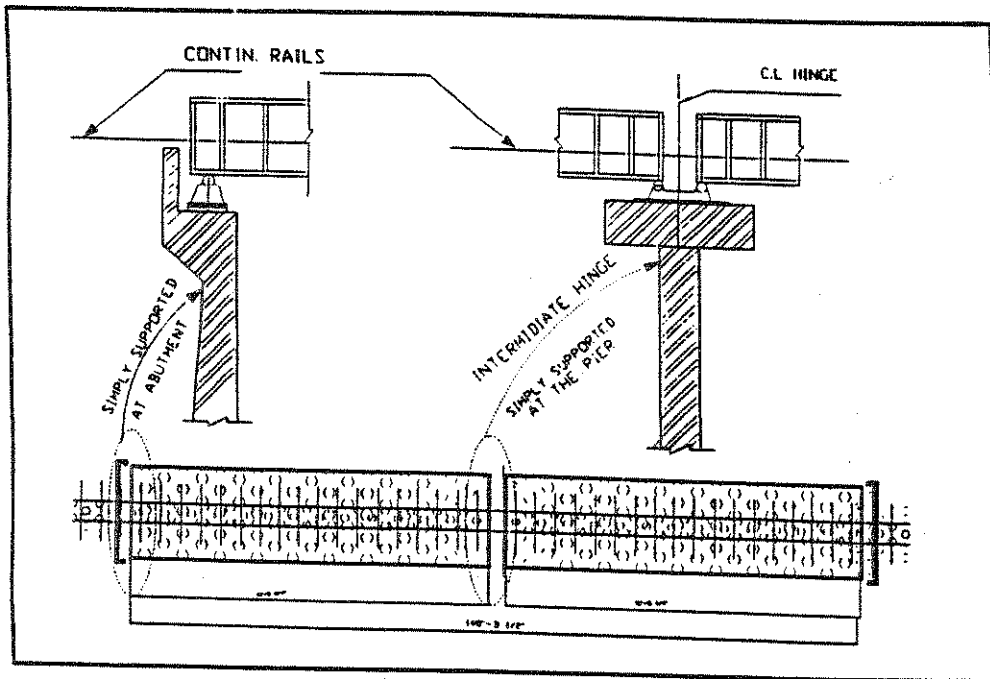


Fig 1.2: Plan view of strawberry Bridge.

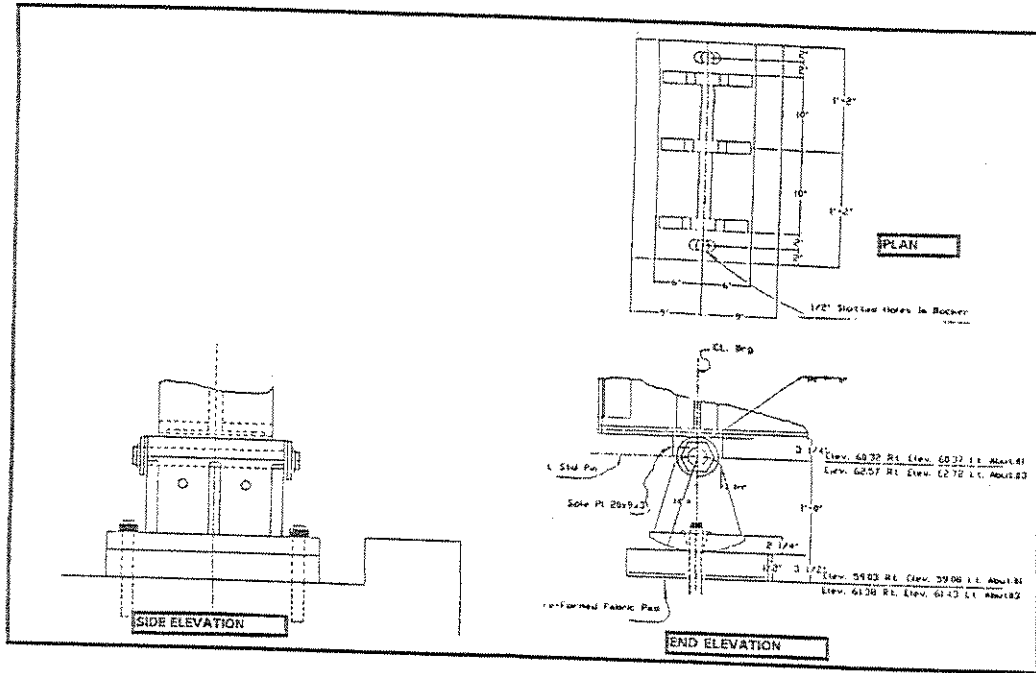


Fig 1.3: Abutment Bearings.

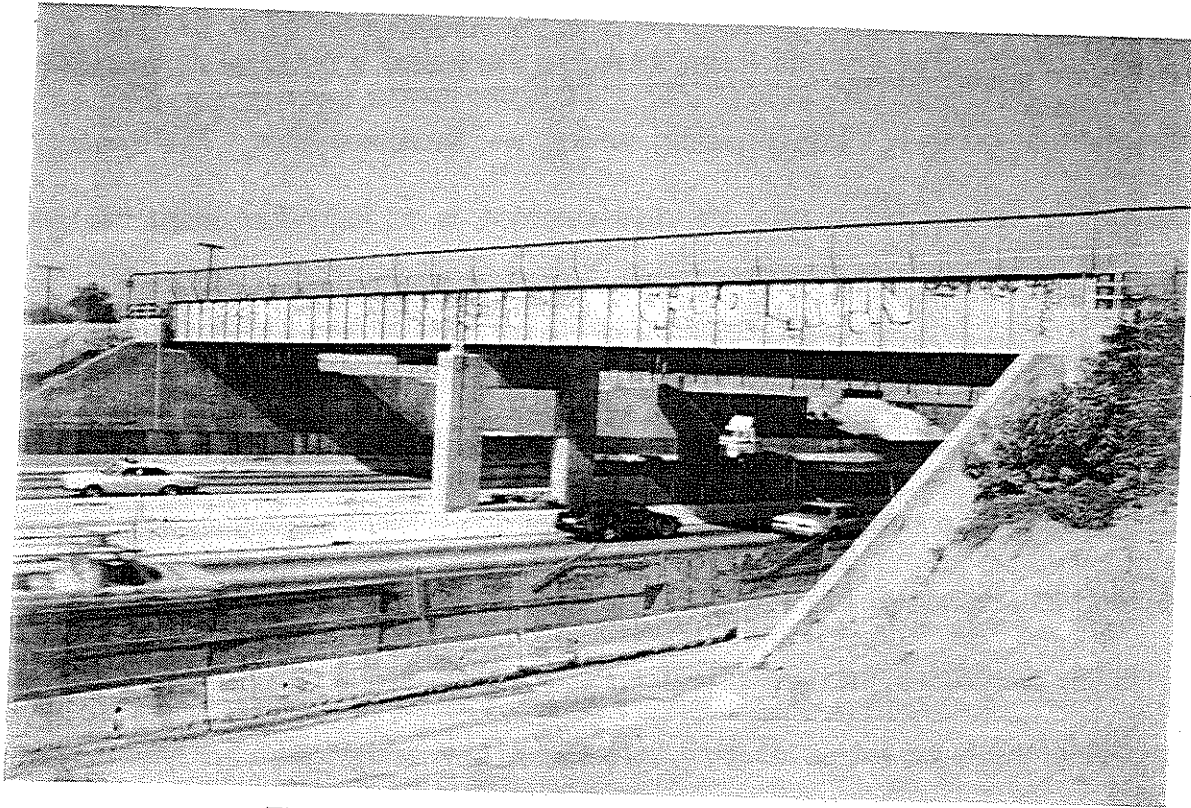


Fig 1.4: Side View of the Strawberry Bridge

CHAPTER 2

EXPERIMENTAL SETUPS AND PROCEDURES

2.1 INTRODUCTION

The dynamic tests of the bridge required the installation of the shaker on the bridge, setting of its eccentricity and the placement of the accelerometers on the bridge. The detailed description of the installation of the shaker, and setting up of its eccentricity are discussed in the following sections.

2.2 GENERAL SYSTEM DESCRIPTION

The MK-12.8A-4600 Eccentric Mass Shaker System was used to excite the bridge. This shaker was installed in the middle of the east span at the north girder as shown in Fig 2.1. The system consists of an eccentric mass shaker, a drive motor, a frequency inverter with a remote operator's station, interconnecting cabling, and flexible shafting. The system is portable in the sense that it may be disassembled into individual elements and transported.

The eccentric mass shaker consists of matched sets of eccentric weights, which rotate in opposite directions about parallel vertical shafts. The shaker contained two sets of weights, a 4600 lb-in. eccentricity set and a 980 lb-in. eccentricity set. To achieve higher forces at low frequencies, the large weight set is used. The small weight set must be used if the system is operated in the 10-20 Hz range.

The direction of the force vector resulting from shaker operation can be adjusted to any direction in a horizontal plane, however, shaker output force in the direction of the short

axis of the shaker is preferred. The shaker is powered by a 10-hp(1200 rpm) induction motor. The speed of the motor is established by the frequency of the output current from a frequency inverter.

The running speed of the shaker is controlled by test personnel, either by rotation of a 10-turn potentiometer or by application of an external 0-9.0 vdc signal. The shaker can either be operated from the inverter or from a remote operator's station. Cabling, permitting a 100-ft separation between the inverter and the remote operator's station, has been provided. More details about the shaker can be found in the shaker's manual [1].

2.3 MOUNTING OF THE SHAKER TO THE TEST STRUCTURE

Extreme care had to be taken to ensure that the shaker was secured to the mounting surface. Thru-bolting is recommended to mount the shaker to the test structure. A total of 12 mount-bolt holes have been provided through the shaker's base plate. During this test a steel plate welded strongly to the north main girder of the bridge, having the same number of bolt holes and size as the base plate of the shaker, was used to mount the shaker in the middle of east span of the bridge. Periodical checkings of the bolt tightness were performed during the test.

According to the shaker manual guidelines, the shaker drive motor should be located in the rear of the shaker at an angle of about 30 degrees off the long surface. Motor location should be established by a smooth curve formed by the flexible shaft. The motor need not be anchored but should be held in place to prevent overturning. The set screws, holding

the flexible shaft to the shaker input shaft and motor output shaft, should be checked periodically for snugness. The motor was located and periodically inspected according to these guidelines.

2.4 INSTALLING WEIGHTS AND SETTING ECCENTRICITY

The limits of safe shaker operation are illustrated in the shaker manual. If testing is to be done between 10 and 20 Hz, the small set of weights must be used. Below 10 Hz operation, either the small set (980lb-in) or the large set (4,600lb-in) may be used. In either case, output force must be limited to 10,000 lbf continuously or 20,000lbf on an intermittent basis.

In this test, the small weight set was used in all the cases. There are three levels of weights in each stack of the shaker. Eccentricity was established by rotating the top and bottom weights relative to the middle weights in each stack.

The following factors were considered in establishing the shaker eccentricity.

1. The limits of safe operation.
2. Maximum test frequency.
3. Desired applied force at a specific frequency.

The eccentricities of the weights used for this test were 0.2,0.5 and 1.0 respectively. A detailed explanation of the eccentricity values related to each set up and response curves obtained from these tests will be explained in the subsequent chapters. The excitation direction can be established by rotating the left set of weights relative to the right set. In

this case the shaker did not need to be rotated.

The configuration of the weights and the directions of their rotations are shown in Fig 2.2. In the first configuration the weights produce a net force in the Y direction, while in the second configuration they produce a force in the X direction. Detailed information about the drive and control system of the shaker ,as well as other safety procedures can be found in the shaker manual [1].

2.5 HARDWARE SYSTEM USED IN THE TEST

The complete hardware system used in this test consisted of three cabinets containing the analog amplifiers/filters, the digital Dataseis II data acquisition system, twenty four FBA-11 accelerometers, three junction boxes, three large spools of cables and several other interconnecting cables. The data acquisition system was manufactured by Kinometrics. The accelerometers were connected by cables to the junction boxes first and then the junction boxes were connected to the data acquisition system.

2.6 INSTALLATION OF THE ACCELEROMETERS ON THE BRIDGE

Twenty four FBA-11 accelerometers were used to record the accelerations of the bridge caused by the eccentric mass shaker. Prefabricated metal mounting plates were bolted on the ties at 6 feet intervals. The accelerometers were then mounted on the plates. Accelerometers were mounted on bridge and approach ties as well as on the main girders of the bridge. Metal plates clamped on the girders were used to mount the accelerometers to the girders. Two main setups were used in the tests; one in the transverse direction and the other in the longitudinal direction. In the transverse setup, all the accelerometers were

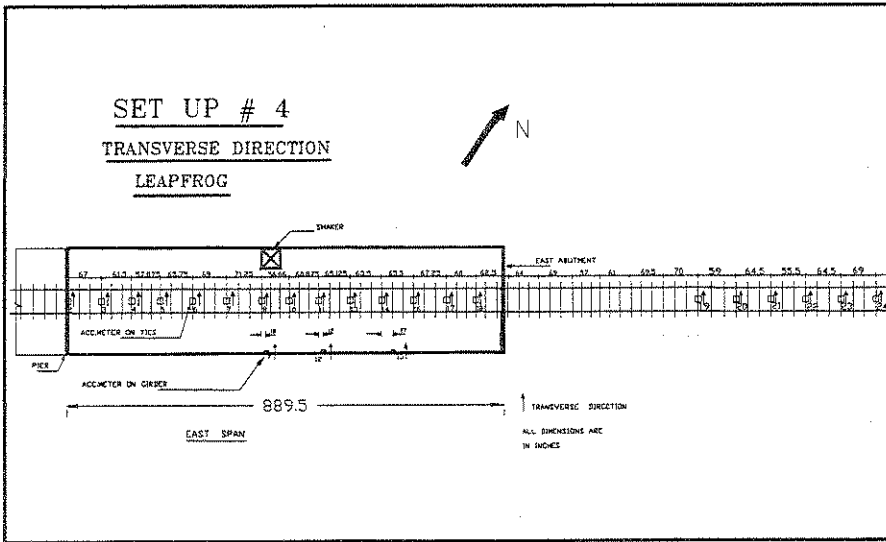


Fig 2.5: Setup#4 in the Transverse Direction.

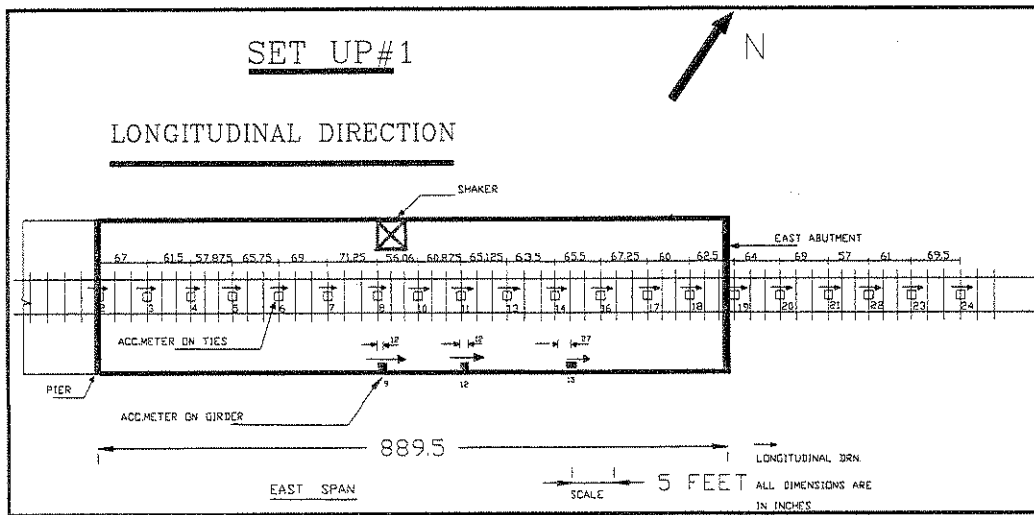


Fig 2.6: Set Up#1 in the Longitudinal Direction.

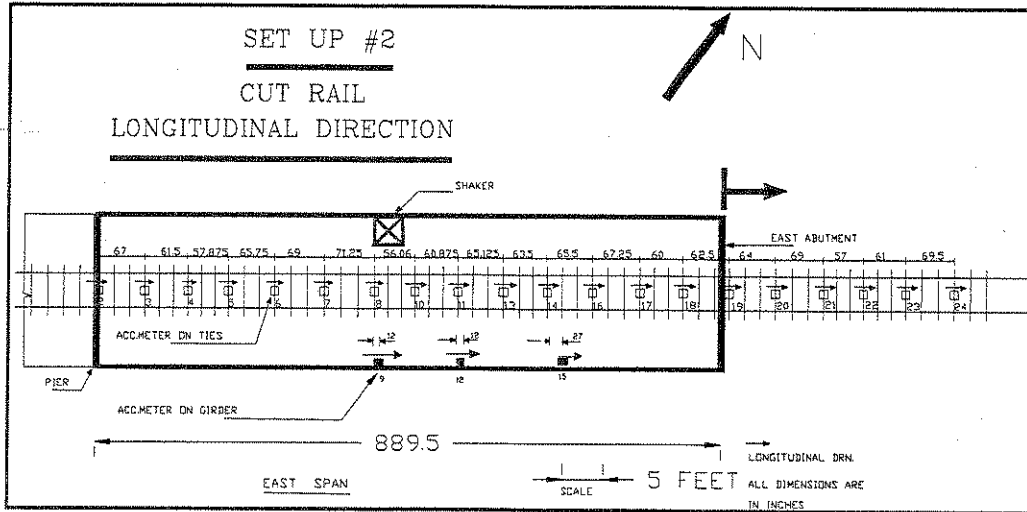


Fig 2.7: Setup#2 in the Longitudinal Direction.

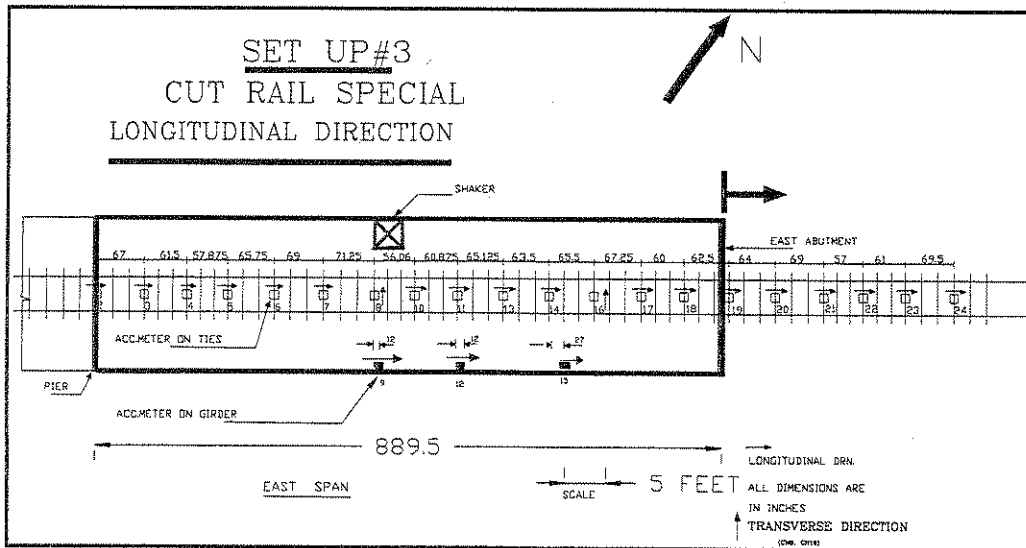


Fig 2.8: Setup#3 in the Longitudinal Direction.

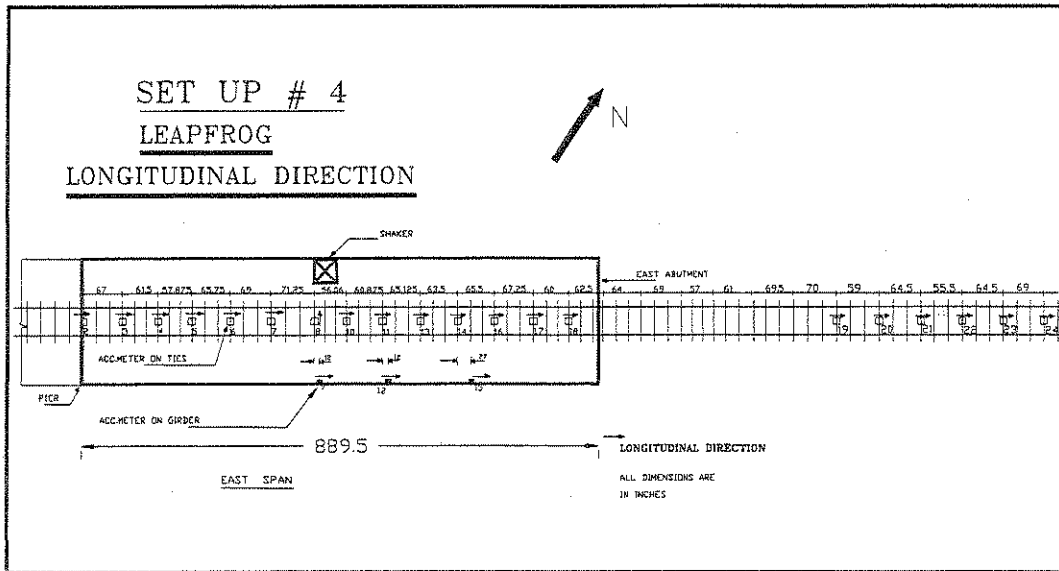


Fig 2.9: Setup#4 in the Longitudinal Direction.

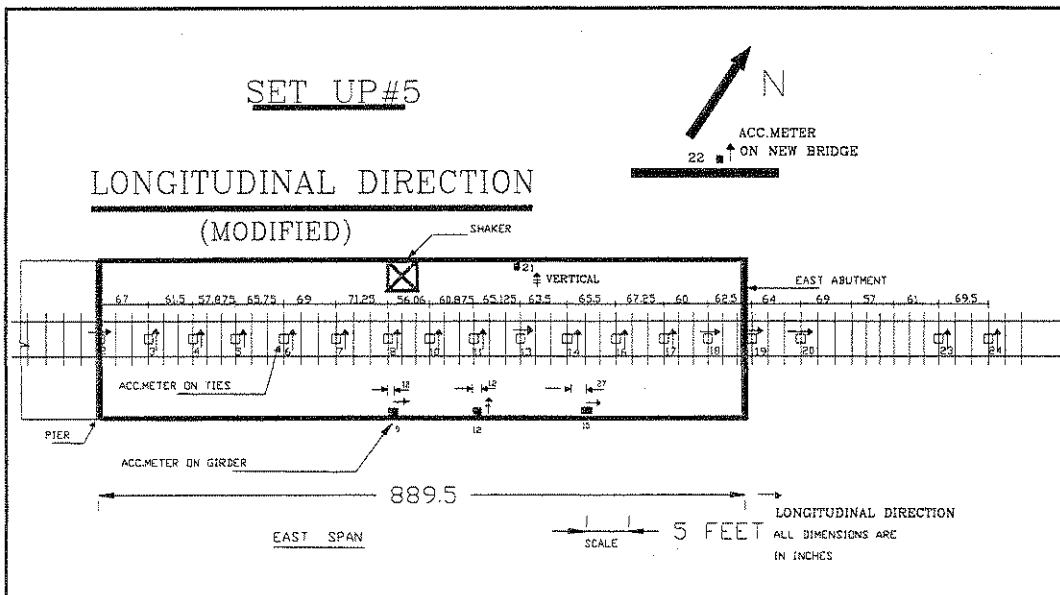


Fig 2.10 : Setup#5 in the Longitudinal Direction.

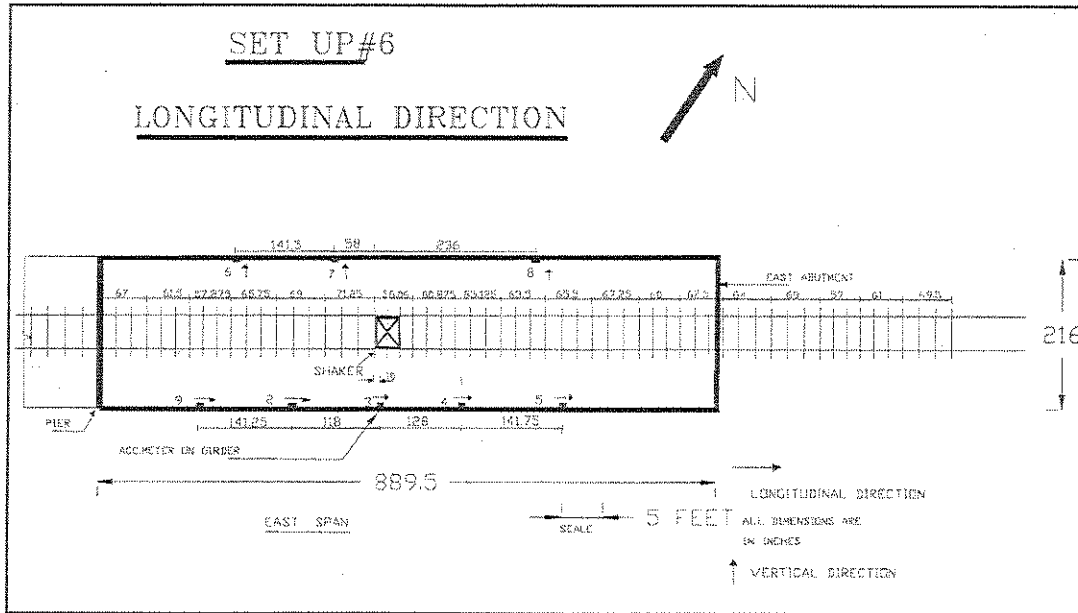


Fig 2.11 : Setup#6 in the Longitudinal Direction.

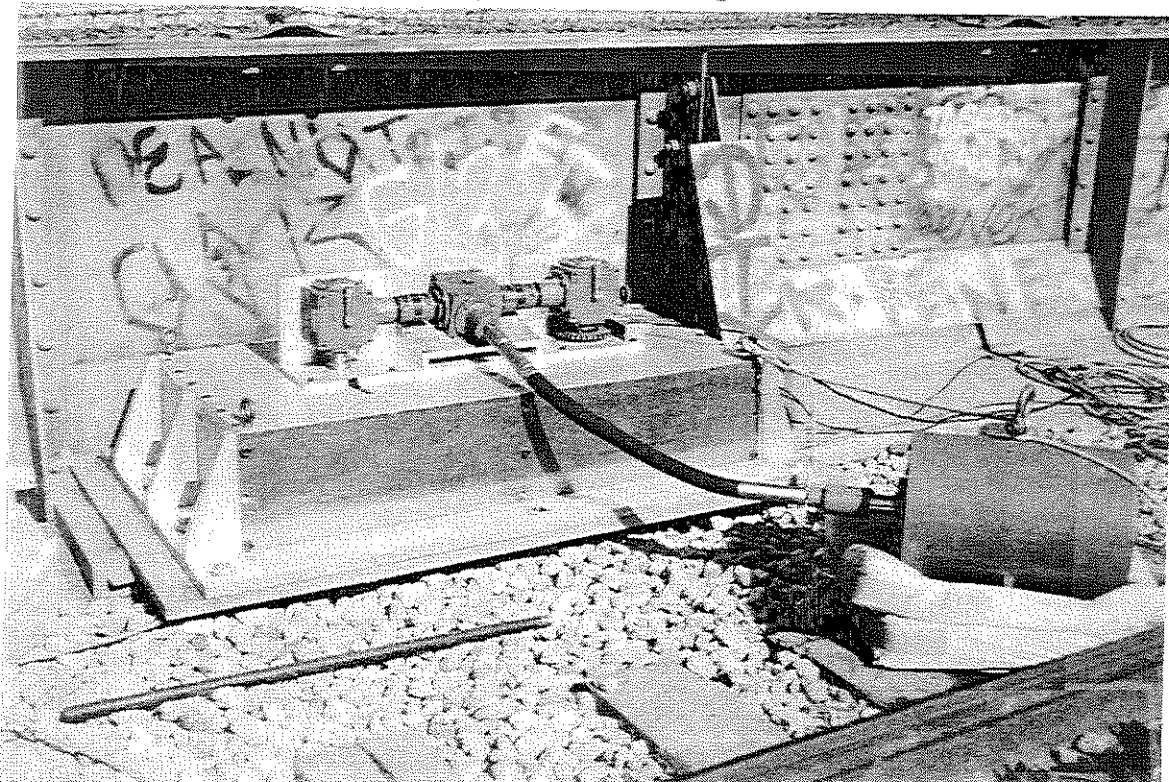


Fig 2.12 View of the Shaker Mounted on the Girder

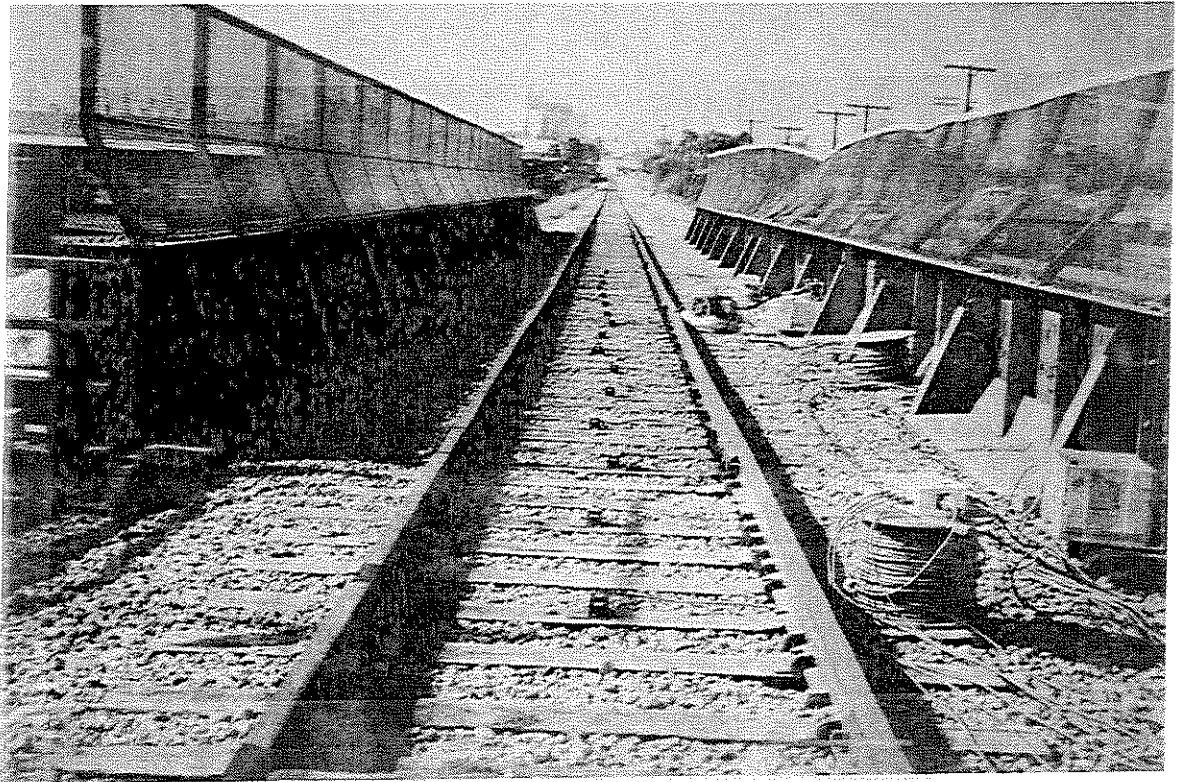


Fig 2.13 Accelerometers Setups on Ties

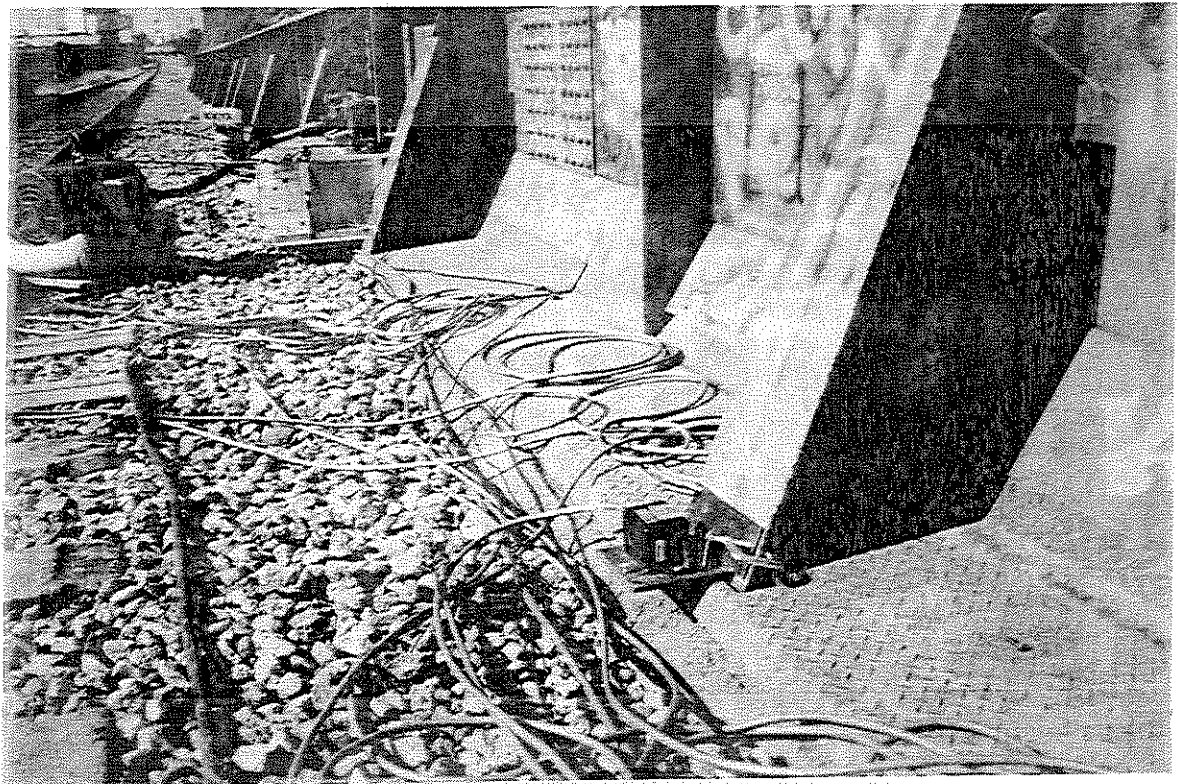


Fig 2.14 Accelerometer Setup on Girder

CHAPTER 3

PROCEDURE FOR THE ANALYSIS OF FIELD DATA

3.1 RESPONSE CURVES

During the test, many frequency sweeps were conducted in the range of 0-20Hz. The acceleration of the bridge was recorded at every accelerometer location for every exciting frequency. Thus, an extensive collection of acceleration response data was recorded. The purpose of the data analysis was to determine natural frequencies and the corresponding mode shapes and modal damping values. Initially, the response curves around the natural frequencies were plotted for many accelerometers. To do this, the peak acceleration values were determined for various values of the excitation frequency bordering the observed natural frequency. At a given frequency, a maximum voltage reading, V_{max} , and a minimum voltage reading, V_{min} , were obtained. Having these two values and the value of the gain, G , of the data acquisition system, the acceleration values in terms of gravity acceleration are obtained by the following formula:

$$a = \frac{[V_{max} + V_{min}]}{[5000 * G]} \quad (1.0)$$

Knowing the acceleration, the maximum displacement value, d , was calculated in terms of the exciting frequency, f , from the following formula:

$$d = \frac{[a * 386]}{[2\pi f]^2} \quad (2.0)$$

In the above equation the 386 term is the acceleration due to gravity in units of in/sec². The maximum force applied by the shaker, can be found in terms of the exciting frequency, f , and the weight setting, W , as follows [1]:

$$F = 0.102 * 980 * W * f^2 \quad (3.0)$$

Finally, having the maximum displacement and force values, the normalized amplitude is defined as :

$$y_i = \frac{\text{Displacement}}{\text{Force}} \quad (4.0)$$

By plotting the normalized amplitude versus the frequency, the response curve was obtained for a particular channel on the bridge. The response curves were used for the evaluation of the modal parameters of their corresponding modes. These parameters are primarily the natural frequencies and the modal damping values. Scatter in the response amplitudes measured during the test, makes the accurate determination of resonant frequencies and modal dampings from the direct examination of the response curves difficult. Because of this, each response curve was used to fit an equivalent single degree of freedom (SDOF) or multi degree of freedom (MDOF) oscillator, from which the natural frequencies and damping values were determined. The idea behind this concept is shown in Fig.3.1. In the case of a response curve with a clear single peak, a single degree of freedom system (SDOF) needs to be fitted in order to calculate the modal frequency and damping values. Referring to the SDOF system shown in Fig.3.1, the response function for a sinusoidal load with exciting frequency, f , is given by :

$$Y = \frac{[P_0 / K]}{\sqrt{[1 - (f / f_n)^2]^2 + [2\zeta f / f_n]^2}} \quad (5.0)$$

where:

$$f_n = \frac{1}{2\pi} \sqrt{[K / m]} \quad (6.0)$$

$$\zeta = \frac{c}{2\sqrt{km}} \quad (7.0)$$

To fit the response of this system to the experimental response curve, the following quantity has to be minimized:

$$J = \sum [y_i - \frac{A f_n^2}{\sqrt{(f_n^2 - f_i^2)^2 + (2\zeta f_n f_i)^2}}]^2 \quad (8.0)$$

In the above expression, the unknown parameters are the natural frequency of the oscillator, f_n , its damping, ζ_n , and the amplitude of its response, A , to achieve the best fit. The subscript i corresponds to the available experimental points. If there are two closely spaced peaks in a response curve, then a two degree of freedom system needs to be fitted to the response curve. In this case there are six unknown parameters: two natural frequencies, two damping values and two response amplitudes. In these tests, response curves with two closely spaced peak appeared when the rails were disconnected in both the transverse and the longitudinal excitation. For a six parameters response curve, the following quantity has to be minimized.

$$J = \sum [Y_i - Y_{th}]^2 \quad (9.0)$$

where the theoretical value Y_{th} is given by:

$$Y_{th} = \frac{A_1 f_1^2}{\sqrt{[f_1^2 - f_i^2]^2 + [2\zeta_1 f_1 f_i]^2}} + \frac{A_2 f_2^2}{\sqrt{[f_2^2 - f_i^2]^2 + [2\zeta_2 f_2 f_i]^2}} \quad (10.0)$$

Where: f_1 -Frequency of first peak , ζ_1 -Damping of first peak, A_1 -Arbitrary amplitude of first peak, f_2 -Frequency Of second peak, ζ_2 -Damping of second peak, A_2 -Arbitrary amplitude of second peak.

If there are three closely spaced peaks in a response curve, then a three degree of freedom system needs to be applied to the experimental response curve. In this case there were nine unknown parameters : three natural frequencies, three damping values and three response amplitudes. The response curves , obtained for the transverse direction with disconnected rails, were used to fit the three degree of freedom system. The parameters in the third degree of freedom system, were used to represent the effect of noise in the response. In this case, the corresponding equation for Y_{th} is given by:

$$Y_{th} = \frac{A_1 f_1^2}{\sqrt{[f_1^2 - f_i^2]^2 + [2\zeta_1 f_1 f_i]^2}} + \frac{A_2 f_2^2}{\sqrt{[f_2^2 - f_i^2]^2 + [2\zeta_2 f_2 f_i]^2}} + \frac{A_3 f_3^2}{\sqrt{[f_3^2 - f_i^2]^2 + [2\zeta_3 f_3 f_i]^2}} \quad (11.0)$$

The quantity J, used in equation 8.0 , has to be minimized to achieve the best fit. By using a simple system identification procedure based on the Hooks and Jeeves method [11], programs were written in FORTRAN to calculate these parameters. The programs, for fitting three , six and nine parameters are given in the appendix A.1, A.2 and A.3 respectively.

3.2 PLOTTING MODE SHAPES

The mode shape of the bridge at a particular natural frequency can be found by plotting the raw acceleration values of all the channels as a function of their locations along the bridge. The mode shape can also be plotted by using the

Fourier Amplitude values of the channels on the bridge at a particular frequency. A Fast Fourier Transform program, available in the Data Seis software, was used to calculate the amplitude values. Then by plotting the Fourier amplitude values of every channel against their locations along the bridge, the mode shape was obtained.

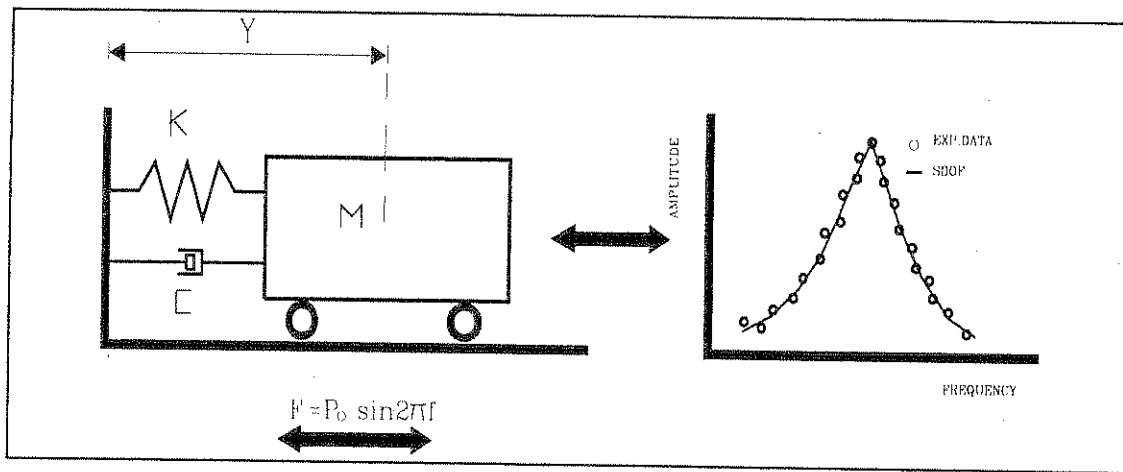


Fig.3.1: Equivalent SDOF system.

CHAPTER 4

RESPONSE OF THE BRIDGE IN THE TRANSVERSE DIRECTION

4.1 FIRST MODE- RAILS IN PLACE

Response curves were developed for most of the accelerometers on ties and all three accelerometers on girders as shown in Fig. 2.1, to identify the fundamental mode characteristics of the bridge in the transverse direction. Since all the test response curves in this case showed a single distinguished peak, the three variable fitting program was used to fit the experimental data points with the theoretical values, in order to determine the fundamental frequency, and the corresponding modal damping. This procedure was discussed in Chapter 3.

Figures 4.1-4.9 show the response curves of nine different channels. Six of these channels were placed on ties and three on the girder. Table 4.1 summarizes the results of the three variable fitting program for each channel, by showing the corresponding calculated values of the natural frequencies, critical damping and amplitudes (not an important parameter for this problem).

Table 4.1 Dynamic properties of the bridge in the First Transverse Mode.

PARAMETER	CHANNEL ON TIES						CHANNEL ON GIRDER		
	CH2	CH3	CH7	CH8	CH11	CH14	CH9	CH12	CH15
FREQUE(Hz)	4.96	4.96	4.94	4.93	4.92	4.92	4.93	4.93	4.92
DAMPING(%)	2.06	2.19	2.2	2.24	2.29	2.27	2.24	2.22	2.31
AMPLITUDE	60.8	65.2	64.6	61.5	55.4	38.8	62.7	52.5	36.5

Note that the values of the parameters do not vary significantly among the channels. The fundamental frequency in the transverse direction is

approximately 4.93Hz and the corresponding modal damping is approximately 2.15%. The experimental response curves were then used to develop an "average" experimental curve, by using the three variable fitting program. The results are shown in Fig .4.10. The values of the fundamental frequency and the corresponding critical damping are 4.93Hz and 2.15% respectively.

The mode shape of the fundamental mode is shown in Fig.4.11. To plot this mode shape, the acceleration amplitude values were calculated for all the accelerometers at 4.93Hz, which is the fundamental frequency. Then, these values were plotted as a function of the distance along the bridge for the east span, which was the only span instrumented. The modal amplitudes for the west span were plotted symmetrically with respect to the center of the bridge. In Fig. 4.11, the distance values along the bridge are shown in inches and they are measured from the center of the bridge. Positive signs correspond to the instrumented span of the bridge (east) while negative signs represent the west span. The dotted vertical line shows the end of the bridge and the beginning of the road bed. The figure illustrates that the mode shape at the middle of the bridge is pulled in , due to the stiffness of the middle pier. It is also obvious from Fig.4.11, that the maximum acceleration response in the first mode was approximately 0.1g.

4.2 SECOND MODE-RAILS IN PLACE

The normalized response curve for channel 7 was developed for the whole frequency spectrum between 0-20Hz, when the bridge was subjected to transverse excitations. This curve is shown in Fig.4.12. The raw acceleration response curve for the same channel and in the same frequency range is shown in Fig .4.13. Similar curves for channel 8 are shown in Figs 4.14, 4.15. It is clear from these curves that there are two predominant peaks between 0-20Hz. One is at 4.9Hz and corresponds to the fundamental mode while the other is approximately at 6.6Hz and indicates the second natural frequency in the transverse direction.

Response curves were developed to identify the second natural frequency in the transverse direction. Since the response curves in this case showed a single distinguished peak, the three variable fitting program was used to fit the experimental data points with the theoretical values in order to determine the natural frequency and the corresponding modal damping. Figures 4.16 and 4.17 show the response curves for two different channels. For both figures the second natural frequency is approximately 6.75Hz and the corresponding modal damping is 4.5%. A summary of the results of both channels is also shown in table 4.2.

Table 4.2: Dynamic properties of the bridge in the Second Transverse Mode.

PARAMETER	CH7	CH8
FREQUENCY (Hz)	6.76	6.75
DAMPING (%)	4.65	4.48
AMPLITUDE	75.56	79.61

As mentioned in Chapter 2, two accelerometers (channels 12 and 21) were oriented in the vertical direction as shown in setup#3 (Fig.2.4), in order to identify any vertical motions of the bridge deck during the transverse excitation. The response curves of these channels are shown in Figures 4.18 and 4.19 . The modal parameters are similar to the ones obtained from channels 7 and 8. A summary of these modal parameters is given in Table 4.3.

Table 4.3: Vertical response of the bridge in the Second transverse Mode.

PARAMETER	CH12	CH21
FREQUENCY(Hz)	6.68	6.71
DAMPING(%)	4.50	4.57
AMPLITUDE	31.00	25.32

Figures 4.18 and 4.19 illustrate that there is a significant presence of vertical motion when the bridge was excited in the Transverse Direction. However, comparison among Figs 4.16-4.19 shows that the amplitude values of the response curves in the transverse direction are much higher than the amplitude values of the response curves in the vertical direction. This indicates that the second mode is a transverse mode rather than a vertical or a torsional mode.

Furthermore, examination of the acceleration records obtained from channels 12 and 21 which were placed across the bridge as shown in Fig .2.4, indicated a 90° out of phase response, which made it clear that the bridge deck was subjected to torsional vibration. The deformed shape of the cross section , which was obtained based on the amplitude values of the vertical and transverse accelerations, is shown in Fig 4.20. It is obvious that there is a strong coupling between transverse and torsional vibrations.

The mode shape of the Second Transverse mode is shown in Fig.4.21. To plot this mode shape, the acceleration amplitude values were calculated for all the accelerometers at 6.6 Hz, which is close to the Second Transverse frequency (6.75Hz). Then, they were plotted as a function of the distance along the bridge for the east span, which was the only span instrumented. The modal amplitudes for the west span were plotted antisymmetrically with respect to the center of the bridge. In Fig.4.21, the distance values along the bridge are shown in inches and they are measured from the center of the bridge. Positive signs correspond to the

instrumented span of the bridge (east), while negative signs represent the west span. It should be noted that, although extensive analysis was performed on the data obtained from the accelerometers placed on the road bed, it was observed that in most of the cases a leapfrog movement of the road bed accelerometers was necessary before the vibration became insignificant. This indicates that vibration was transmitted to approximately 60.0 feet on the road bed, which shows a strong interaction between the bridge deck and the adjacent road bed. It should be mentioned here, that the transmitted vibrations through the soil, were enough to drive in to vibration the adjacent new bridge, which was under construction at that time.

4.3 FIRST MODE -RAILS CUT

When the rails were disconnected at the east and west abutments, frequency sweeps were performed for the identification of the fundamental transverse mode. Initially, the response curves for the accelerometers in the disconnected rail case, were developed by using the three variable fitting program to fit the experimental data points with the theoretical values. This allowed for the determination of the fundamental frequency and the corresponding modal damping. Figures 4.22-4.31 show the response curves for ten different channels. Based on these figures, the following remarks can be made.

(1). The correlation between the experimental and theoretical values is not as close as in the case of uncut rails. This indicates that the three variable program is not adequate to fit the data in this case, perhaps due to the existence of another closely

spaced mode. As discussed in Chapter 3, two closely spaced modes require a six variable fitting program.

There is a strong indication that after disconnecting the rails, another "localized" mode appears, which is closely spaced with the primary transverse mode of the structure. This mode can be viewed as a variation of the primary first mode, generated by the non linearity introduced by a mechanism which could not be explicitly identified in this test.

(2). The three variable fitting program indicates a frequency of approximately 4.78-4.85 Hz and a damping of approximately 5.5% which is almost double the damping calculated in the uncut rail case. The cutting of the rails results in a slightly softer system, which explains the lower value of the natural frequency. However, the larger value of damping is probably due to the closely spaced "localized" mode. The fact that a three variable program is used to approximate an experimental response curve with two closely spaced peaks, results in a wider theoretical response curve with a bigger value of damping that approximates the damping of both the primary transverse and the localized modes.

The fact that there are two peaks, is clearly demonstrated in Figs .4.32-4.37. In these figures, the raw acceleration response curves in the uncut and cut rail cases are compared for different accelerometers. It is clear that in all the cases, the acceleration levels are reduced to almost half in the cut rail case, which is consistent with the double overall damping reported above, while the response curves show one peak around 4.7Hz and the other in the range of 5.0-5.2 Hz.

The response curves were redeveloped using a six variable fitting program. The results are shown in Figs. 4.38-4.45 and in Table 4.4, which shows the results for all the accelerometers inside the bridge. The figures indicate that the first frequency is approximately 4.7Hz, which is the primary fundamental frequency of the structure in the cut rail case. This frequency, as expected, is slightly lower than the uncut rail case, which is due to the softening of the structure resulting from disconnecting the rails. The corresponding damping varies from 1.2% to 3.9% and, on the average, is similar to the damping observed in the uncut rail case. The second frequency is close to 5.05Hz and, probably is the frequency of the local mode (probably due to the sliding of the deck on the bearings). The damping of this mode varies from 2.7%- 5.2%.

To allow for the presence of noise in the data, the experimental response curves were fitted by theoretical curves resulting from a nine variable program. A nine variable program can fit a response curve with three closely spaced peaks by a theoretical curve. The results are shown in Figs 4.46-4.53 and in Table 4.5, which shows the results for all the accelerometers on the bridge. It is clear that the frequency and damping values for the first two peaks are similar to the values predicted by the six variable program. This indicates that the six variable program was adequate for the prediction of the parameters. The "fine tuning", introduced by the nine variable program resulted in minor changes of the results.

The mode shape of the fundamental transverse mode in the cut rail case is shown in Fig .4.54. This mode shape has been plotted along with the corresponding mode

shape of the uncut rail case for the purpose of comparison. To plot this mode shape, the acceleration amplitude values were calculated for all the accelerometers at 4.7Hz. These values were then plotted as a function of the distance along the bridge for the east span, which was the only span instrumented. The modal amplitudes for the west span were plotted symmetrically with respect to the center of the bridge. In Fig. 4.54, the distance values along the bridge are shown in inches and they are measured from the center of the bridge. Positive signs correspond to the instrumented span of the bridge (east) while negative signs represent the west span. The mode shapes are similar, except that in the cut rail case, the acceleration levels have been reduced by almost half.

Based on the remarks made above, when the rails were cut, a "localized" mode was triggered, which allowed for a greater dissipation of energy and significant reduction of the structural acceleration response levels (Refer to Figs. 4.32-4.37). The exact nature of this mode which is a variation of the primary fundamental structural mode could not be identified from the instrumentation scheme and the procedure used in this test. However, in an event of an earthquake, the presence of this mode close to the primary transverse fundamental mode of the bridge, will probably contribute to higher energy dissipation and reduction of the acceleration response. The structure will probably have an "equivalent" damping of 5.5%, which was the value predicted by the three variable program.

Table 4.4 : Response Parameters of the Bridge for the Cut Rail Transverse case

(Six variable).

CHANNEL	FREQ1(Hz)	DAMP1(%)	AMPLI1	FREQ2(Hz)	DAMP2(%)	AMPLI2
CH2	4.72	1.23	7.51	5.05	5.22	65.64
CH3	4.72	1.53	10.58	5.03	4.92	62.98
CH4	4.71	1.86	15.62	5.03	4.49	55.93
CH5	4.71	2.61	25.53	5.04	3.91	43.87
CH6	4.70	2.58	28.48	5.04	3.77	40.20
CH7	4.71	3.24	37.11	5.04	3.54	31.61
CH8	4.71	3.36	41.00	5.03	3.36	25.43
CH10	4.71	3.65	45.26	5.05	3.17	20.28
CH11	4.71	3.69	43.44	5.04	2.65	15.60
CH13	4.72	3.94	41.46	5.04	2.88	14.53
CH14	4.70	2.54	20.40	5.03	3.03	14.60
CH16	4.71	2.44	18.18	5.04	2.69	15.81
CH17	4.71	2.44	18.00	5.03	2.71	15.87
CH18	4.70	2.97	5.95	5.01	2.97	4.49

Table 4.5: Response Parameters of the Bridge for Rail Cut Transverse case

(Nine variable).

CHA-	F1	D1	A1	F2	D2	A2	F3	D3	A3
CH2	4.70	1.29	7.87	4.96	3.58	25.9	5.12	5.59	35.70
CH3	4.71	2.15	19.9	5.02	3.05	28.6	5.28	3.88	14.50
CH4	4.71	2.38	25.1	5.02	3.06	30.4	5.27	2.76	7.52
CH5	4.71	3.02	34.9	5.04	2.72	26.2	5.29	1.60	3.19
CH6	4.70	2.83	37.4	5.00	3.02	24.0	5.18	2.19	7.50
CH7	4.72	3.43	42.9	5.03	2.72	21.5	5.26	1.18	1.74
CH8	4.72	3.58	47.3	5.03	2.56	17.2	5.26	0.48	0.66
CH10	4.71	3.54	45.7	5.06	2.15	16.6	4.94	3.40	19.20
CH11	4.71	3.72	44.7	5.01	2.28	15.6	5.15	2.01	3.08
CH13	4.72	3.53	34.3	5.04	2.49	13.4	4.50	3.80	28.30
CH14	4.70	3.29	29.1	5.05	2.78	12.4	4.50	3.48	25.40
CH16	4.70	3.40	25.3	5.05	2.20	12.4	4.50	2.80	11.50
CH17	4.70	3.31	25.5	5.03	2.51	12.3	4.50	2.90	11.60
CH18	4.72	2.95	9.36	5.03	2.89	9.62	4.97	2.99	10.50

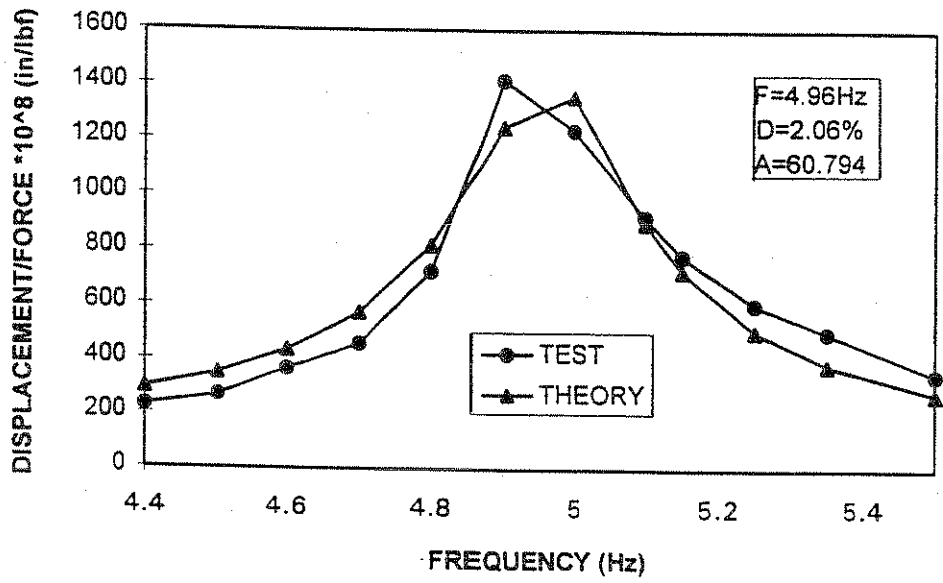


Fig 4.1 : CH2 Response Curve-First Transverse Mode.

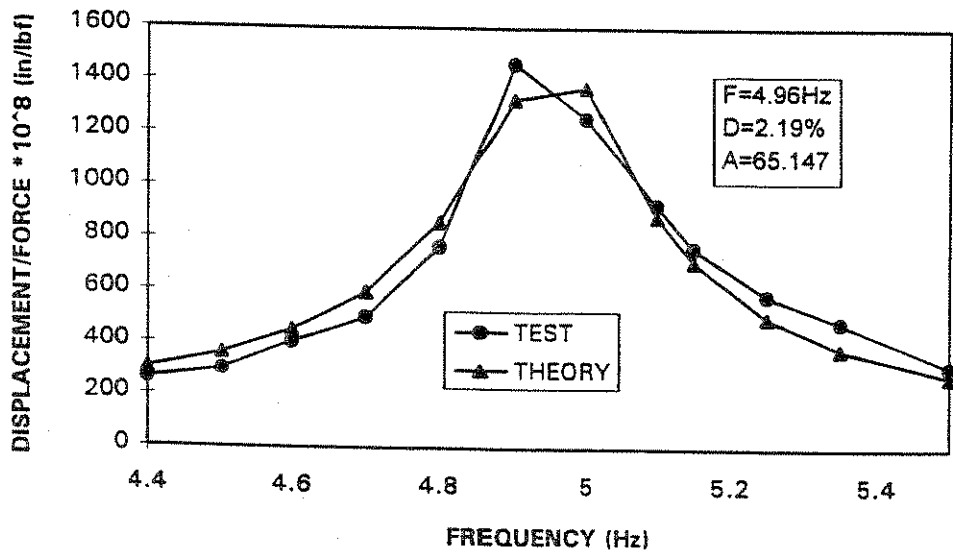


Fig 4.2: CH3 Response Curve -First Transverse Mode.

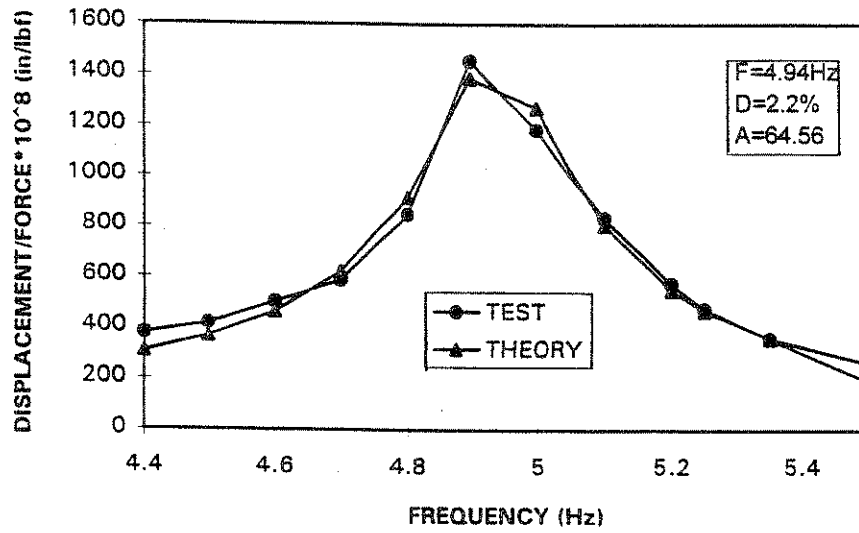


Fig 4.3: CH7 Response Curve-First Transverse Mode.

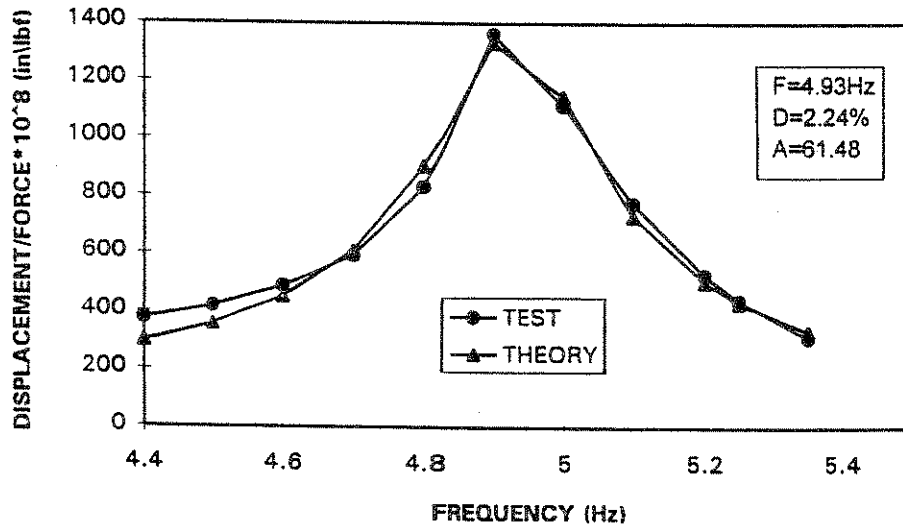


Fig 4.4: CH8 Response Curve-First Transverse Mode.

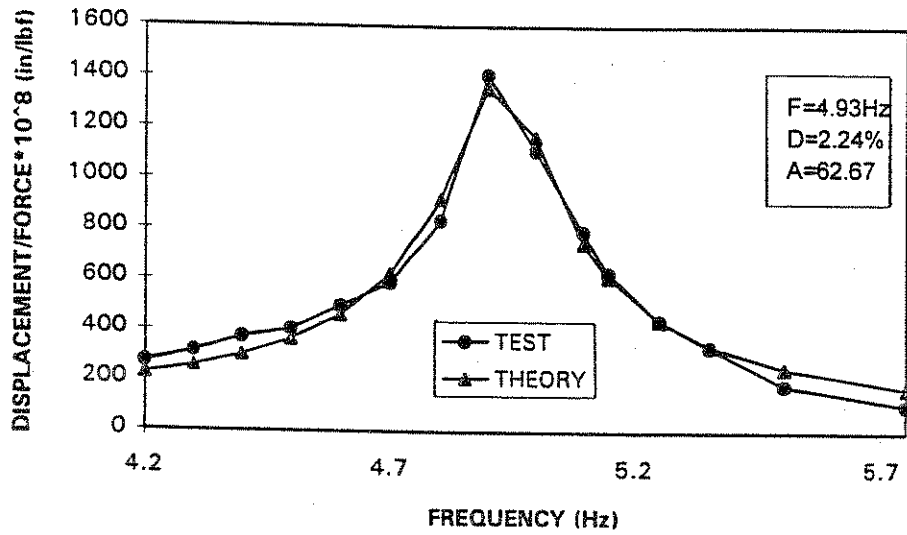


Fig 4.5: CH9 Response Curve-First Transverse Mode.

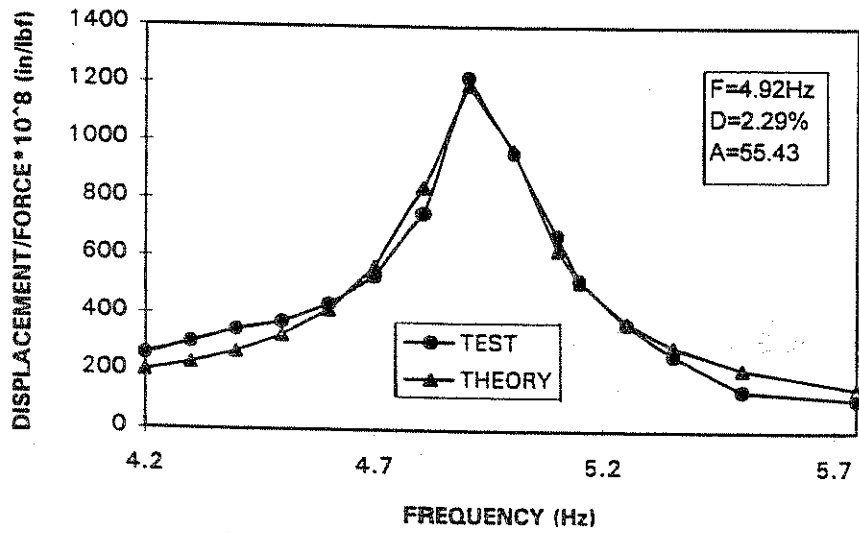


Fig 4.6: CH11 Response Curve -First Transverse Mode.

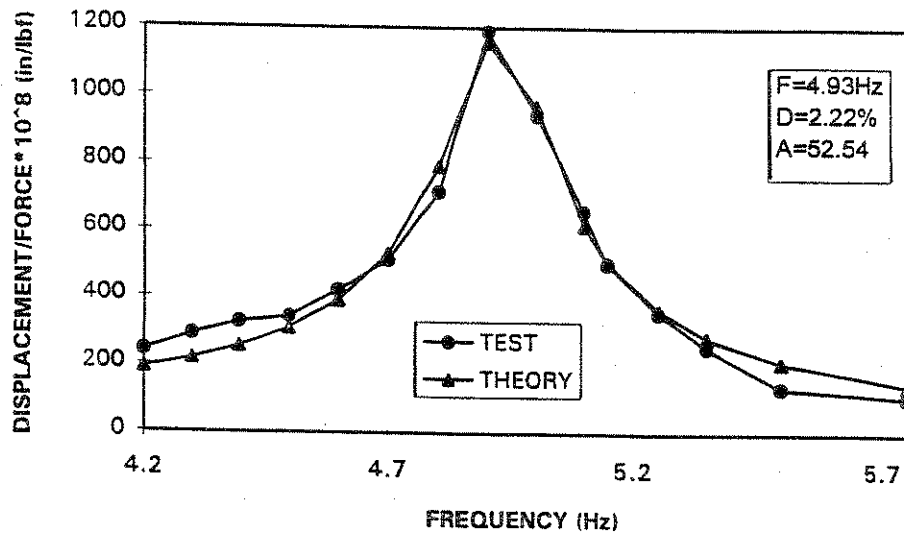


Fig 4.7: CH12 Response Curve -First Transverse Mode.

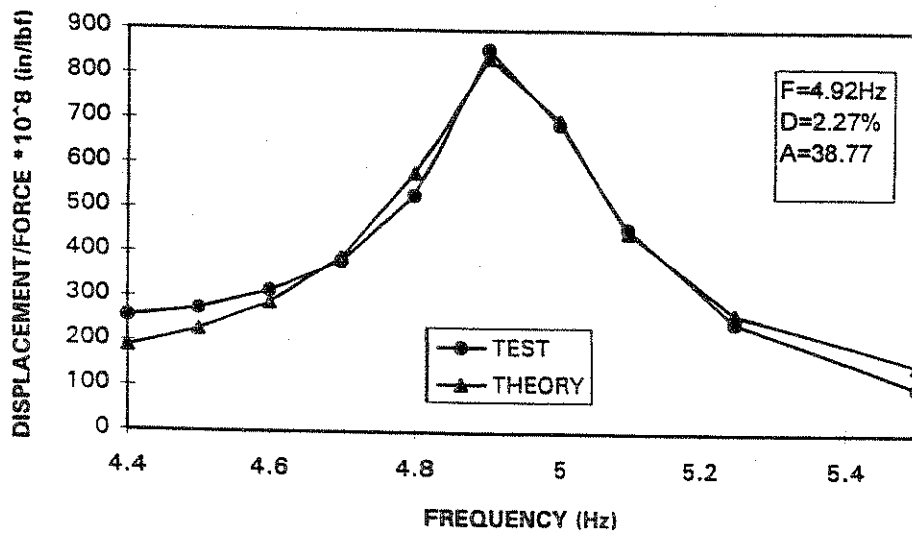


Fig 4.8: CH14 Response Curve -First Transverse Mode.

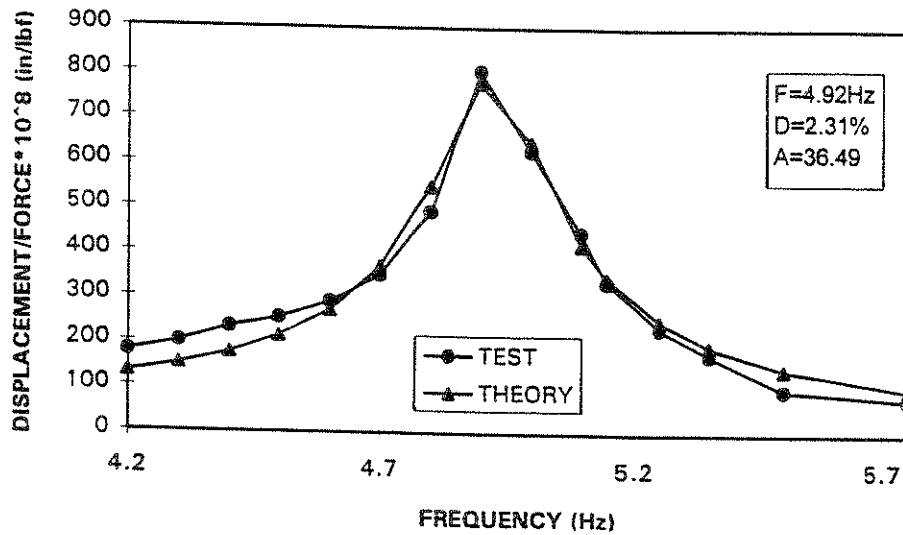


Fig 4.9: CH15 Response Curve-First Transverse Mode.

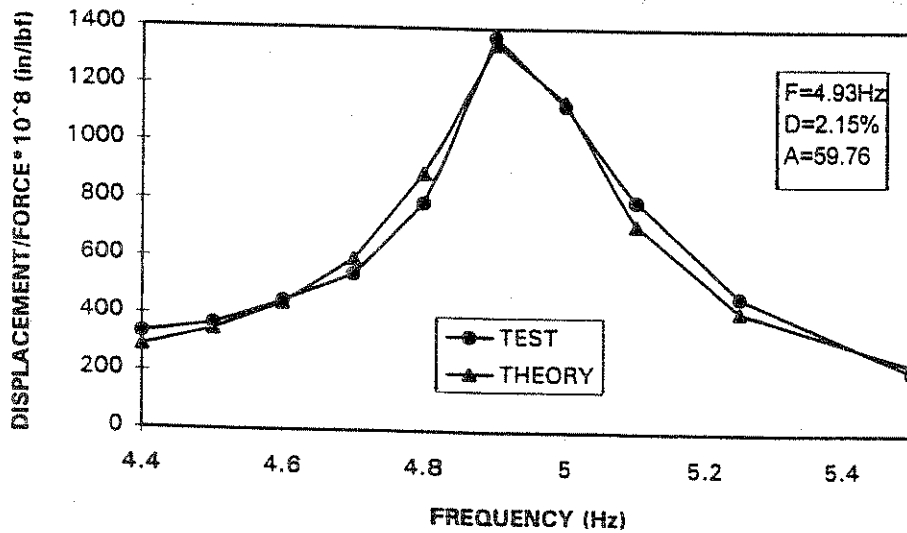


Fig 4.10: Average Response -First Transverse Mode.

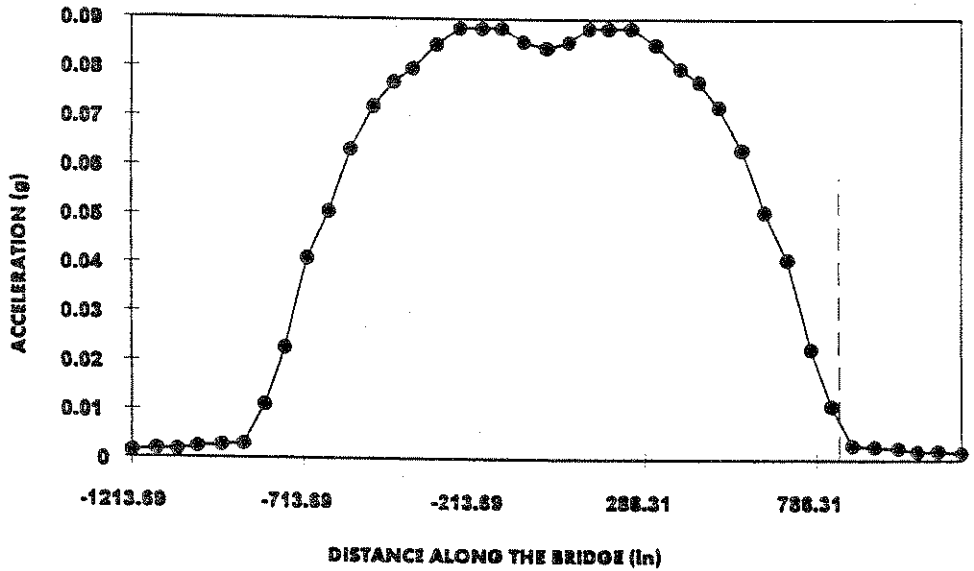


Fig 4.11: First Transverse Mode Shape.

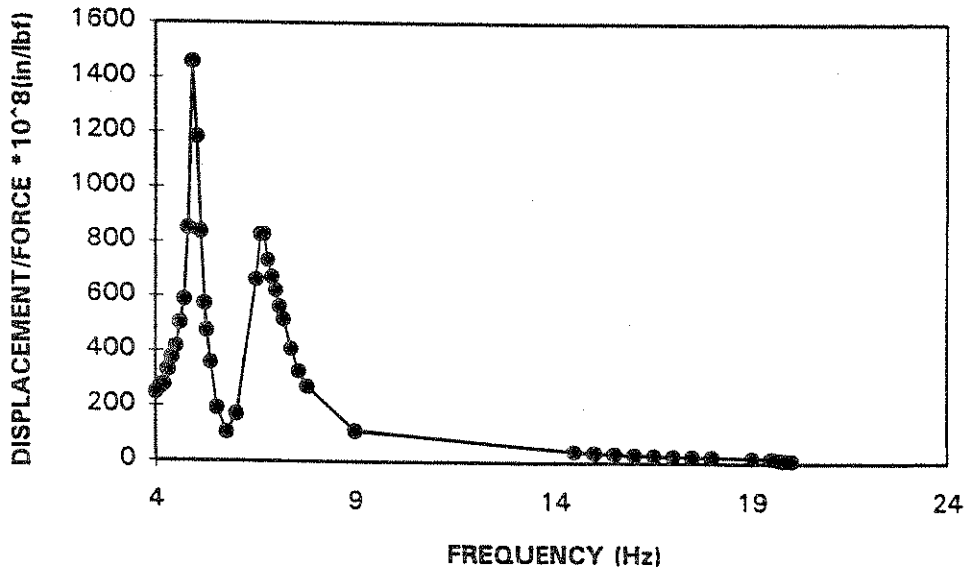


Fig 4.12: CH7 Test Response -Transverse Direction.

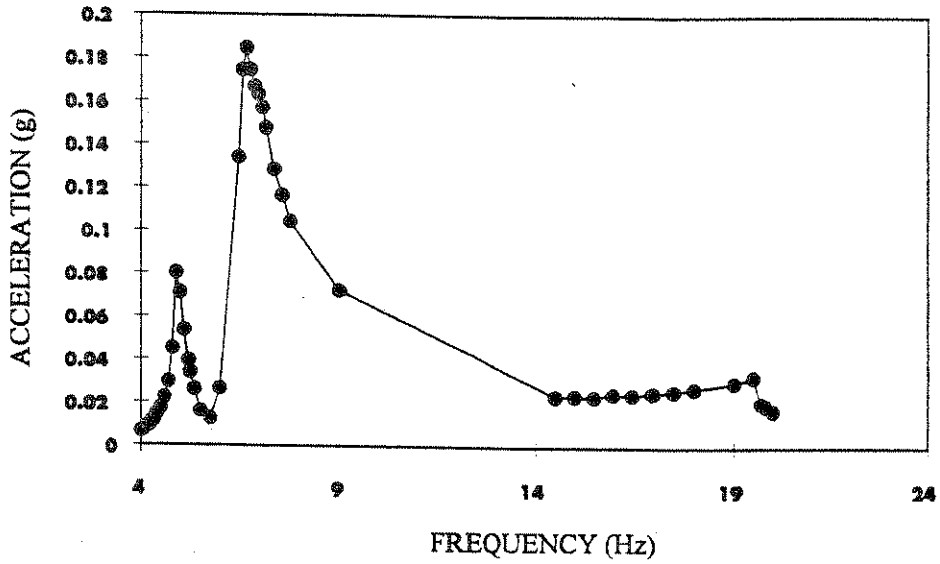


Fig 4.15: CH8 Acceleration Response-Transverse Direction.

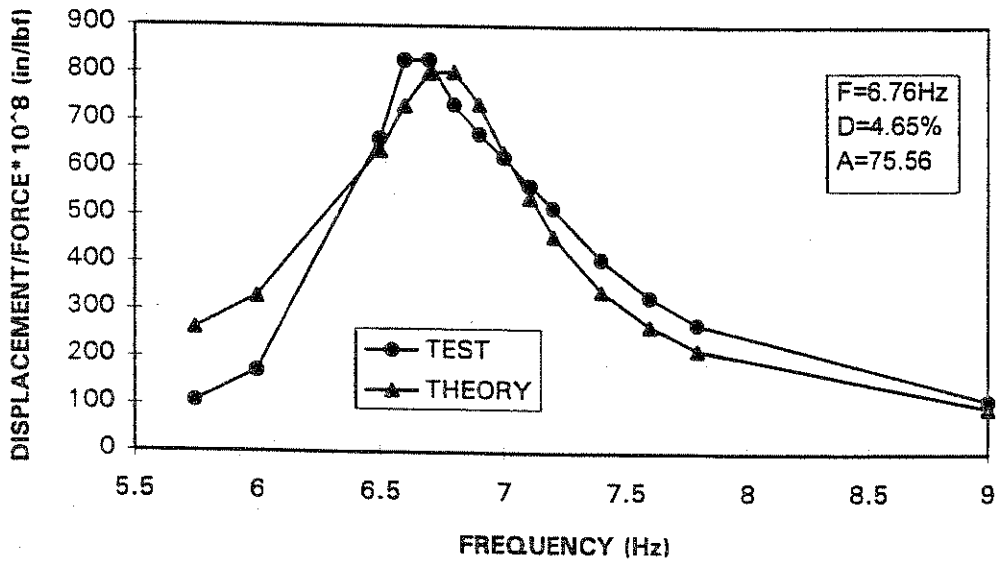


Fig 4.16: CH7 Response Curve-Second Transverse Mode.

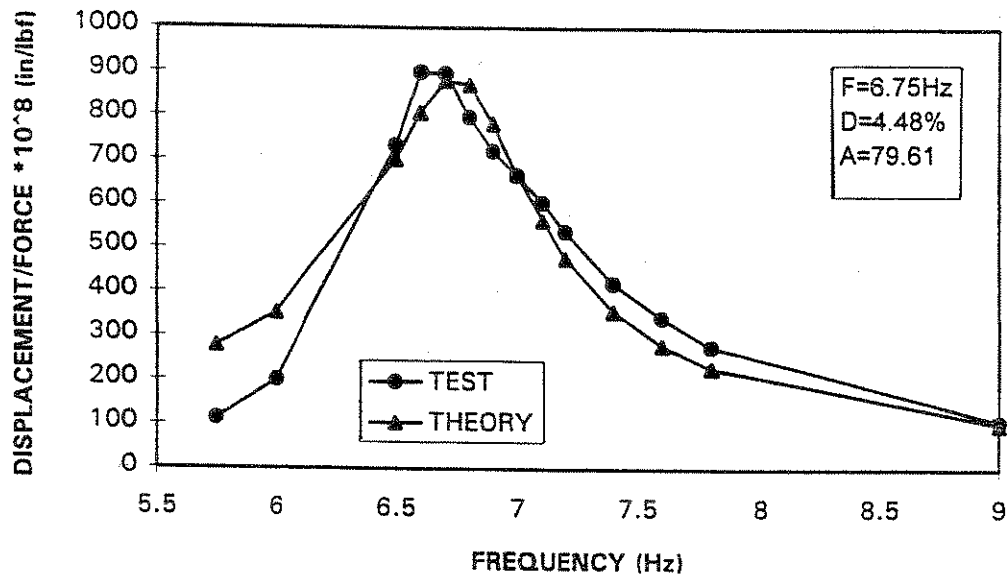


Fig 4.17: CH8 Response Curve-Second Transverse Mode.

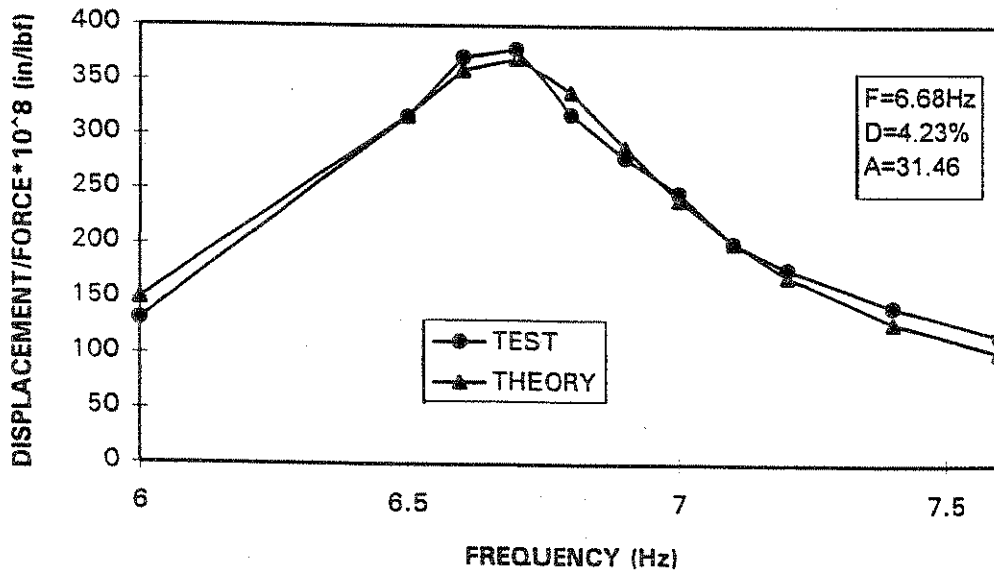


Fig 4.18: CH12 Vertical Response -Second Mode.

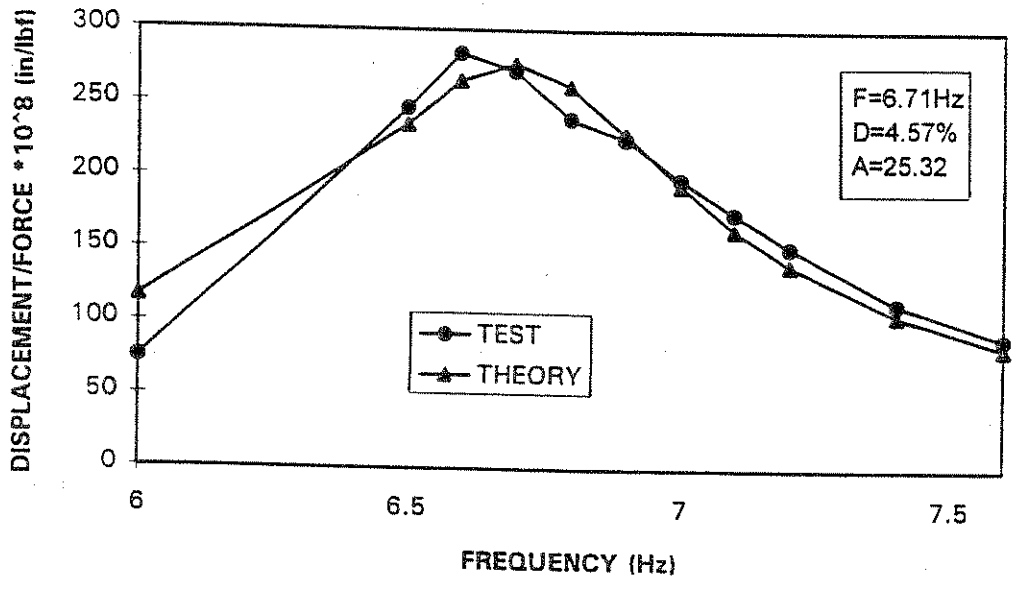


Fig 4.19: CH21 Vertical Response-Second Mode.

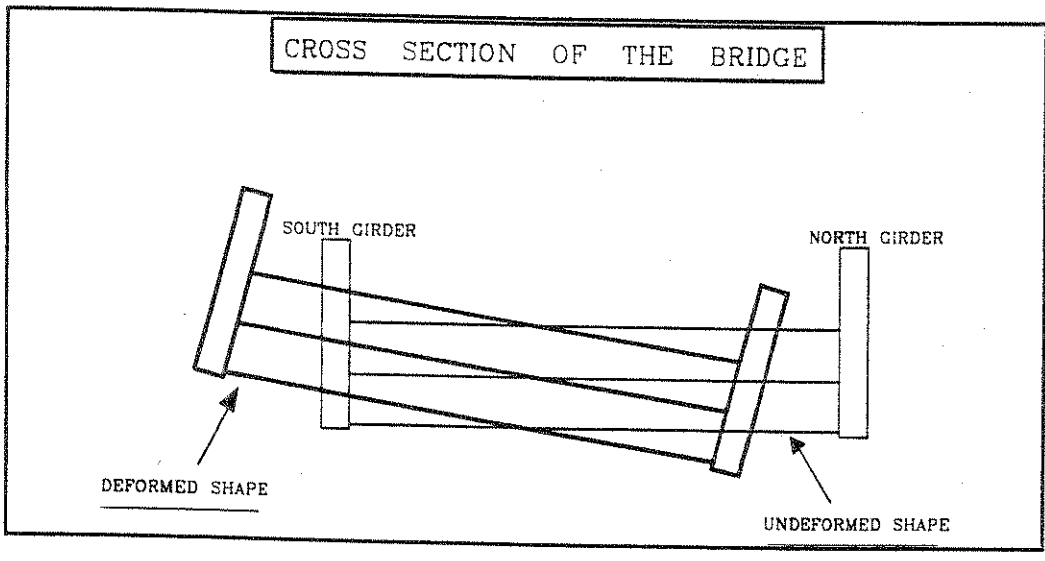


Fig 4.20: Cross Section - Second Transverse Mode.

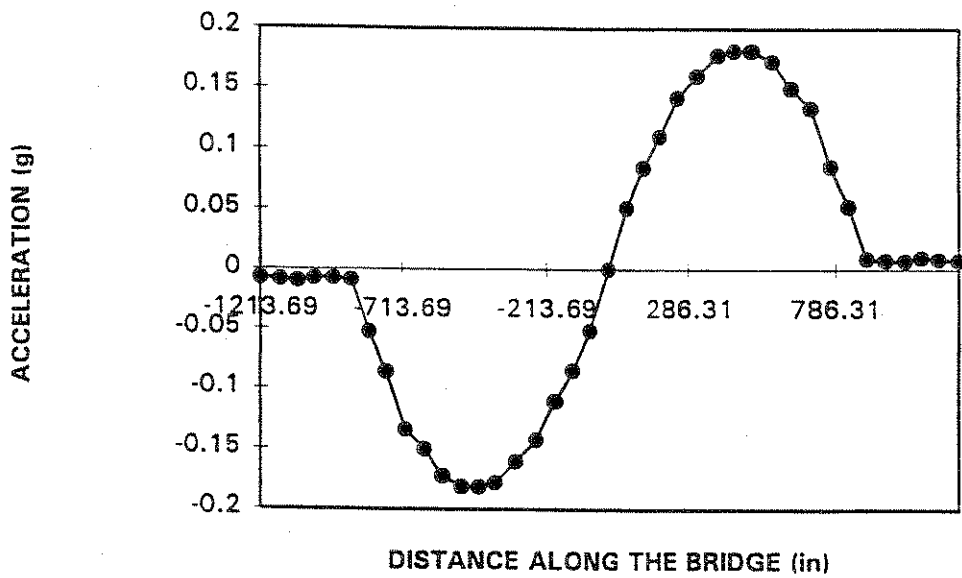


Fig 4.21: Second Transverse Mode shape.

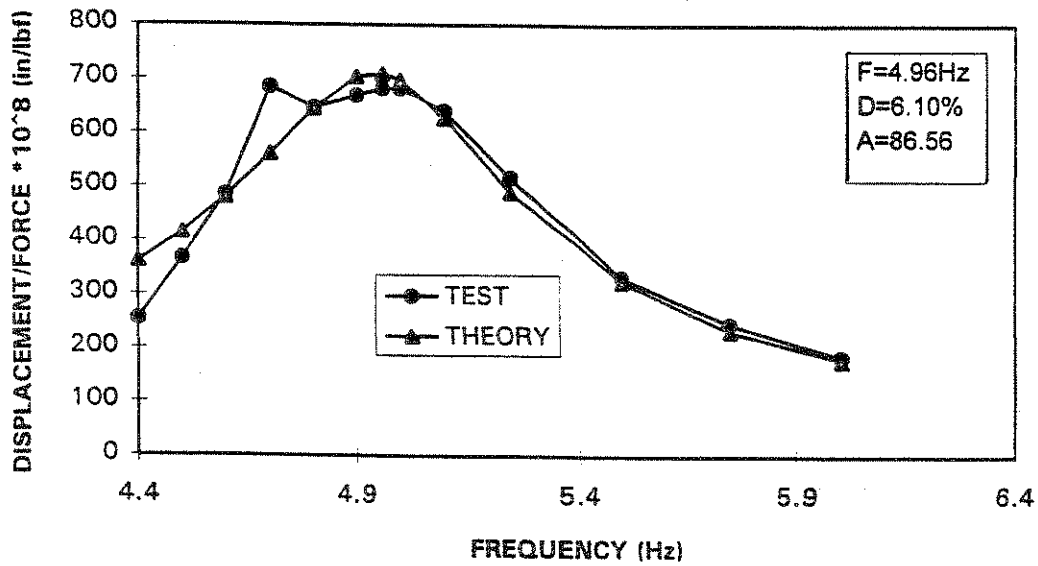


Fig 4.22: CH2 Response Curve-Cut Rail Transverse (3 Variables)

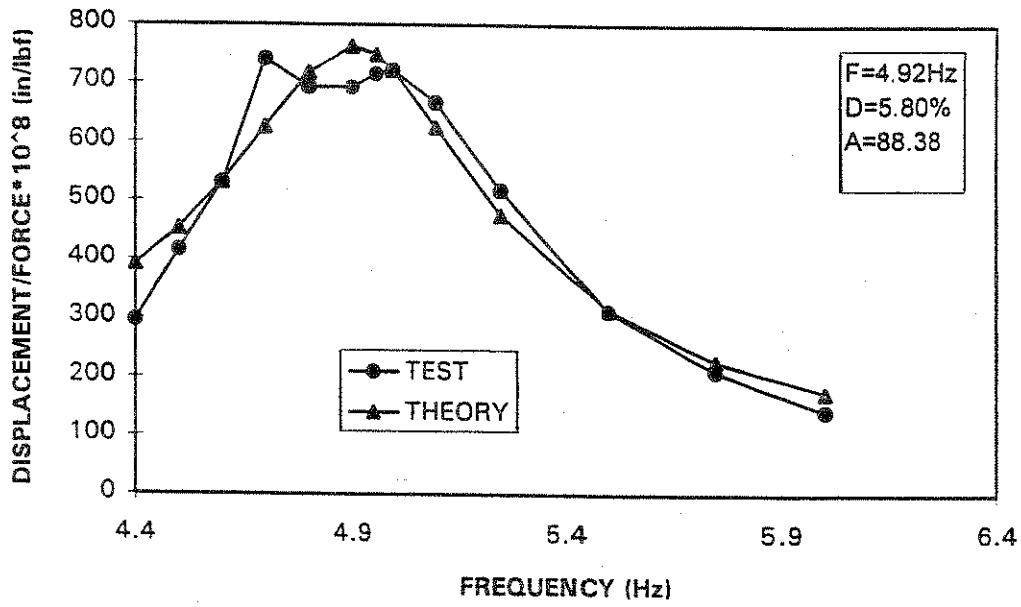


Fig 4.23: CH3 Response Curve-Cut Rail Transverse (3 Variables)

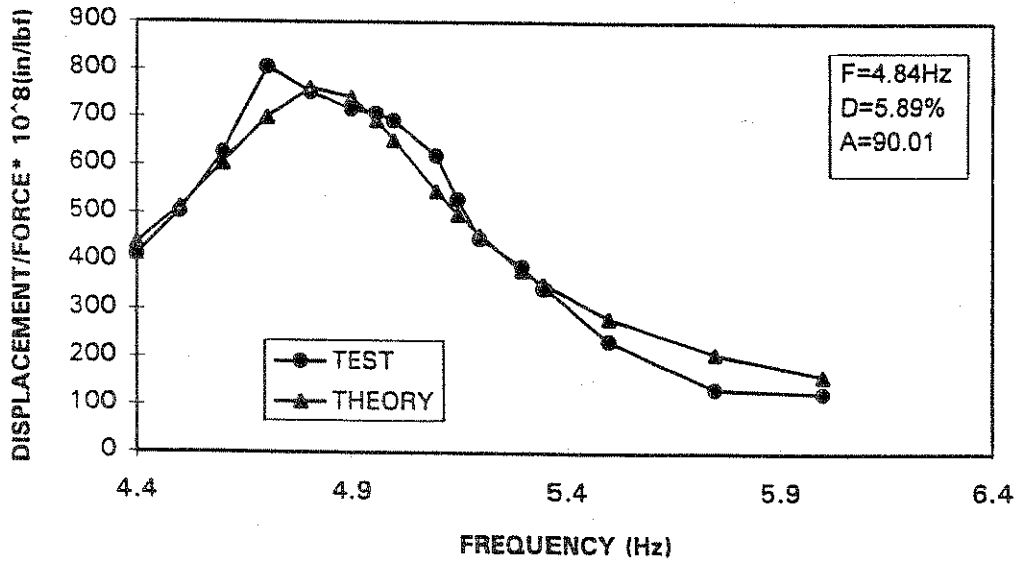


Fig 4.24: CH7 Response Curve-Cut Rail Transverse (3 Variables)

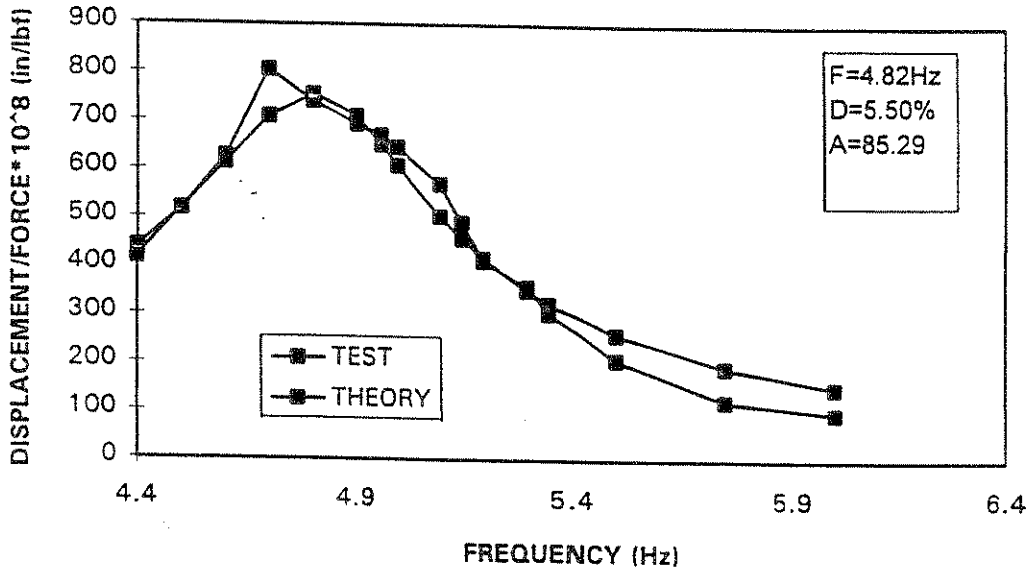


Fig 4.25: CH8 Response Curve-Cut Rail Transverse (3 Variables)

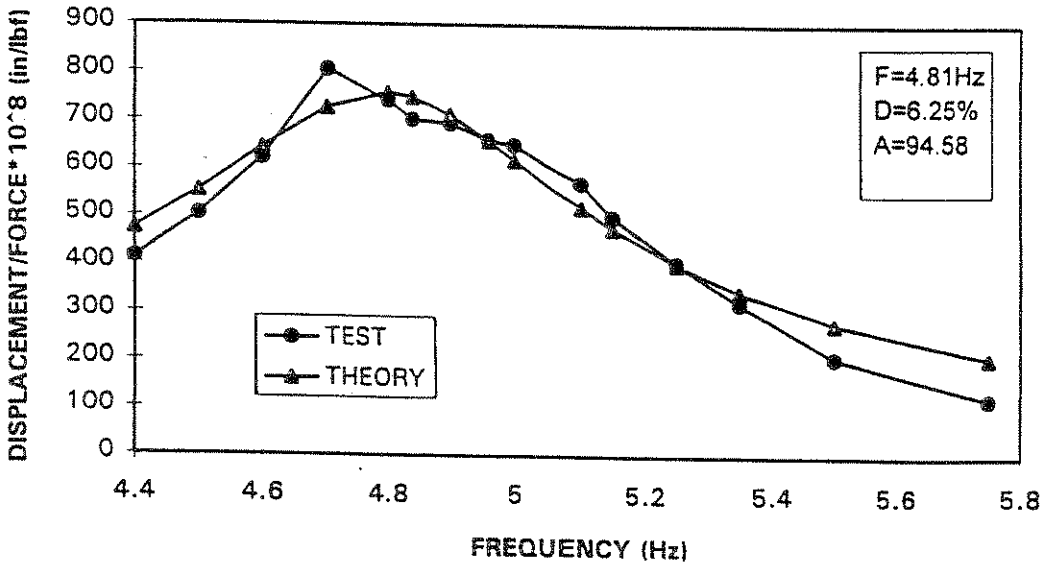


Fig 4.26: CH9 Response Curve-Cut Rail Transverse (3 Variables)

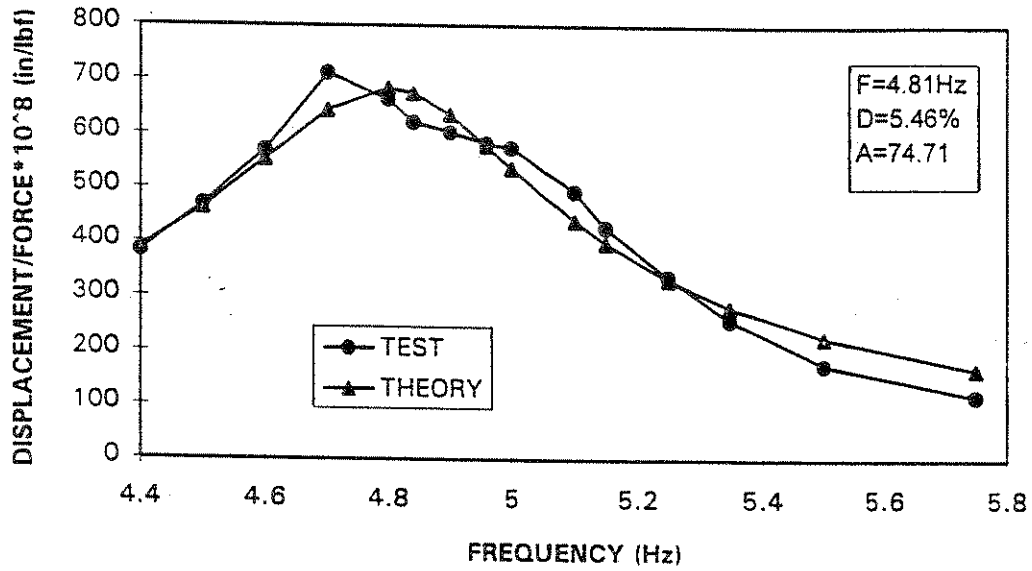


Fig 4.27: CH11 Response Curve-Cut Rail Transverse (3 Variables)

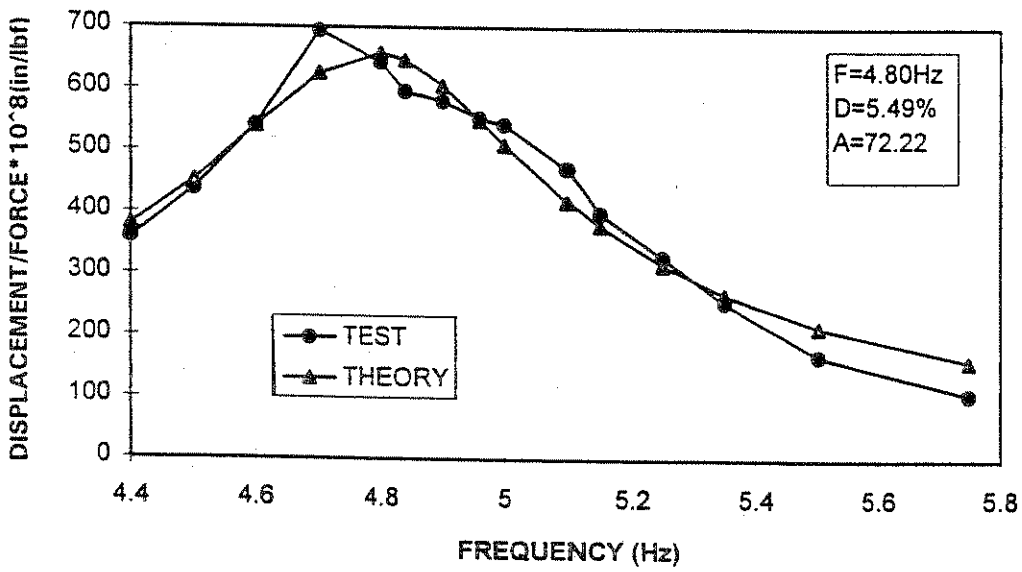


Fig 4.28: CH12 Response curve -Cut Rail Transverse (3 Variables)

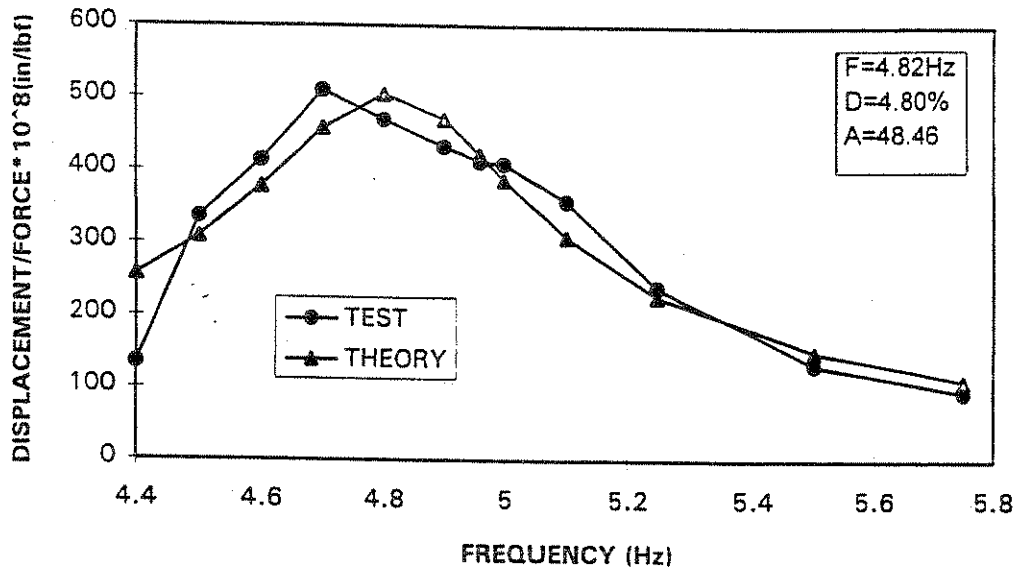


Fig 4.29: CH14 Response Curve -Cut Rail Transverse (3 Variables)

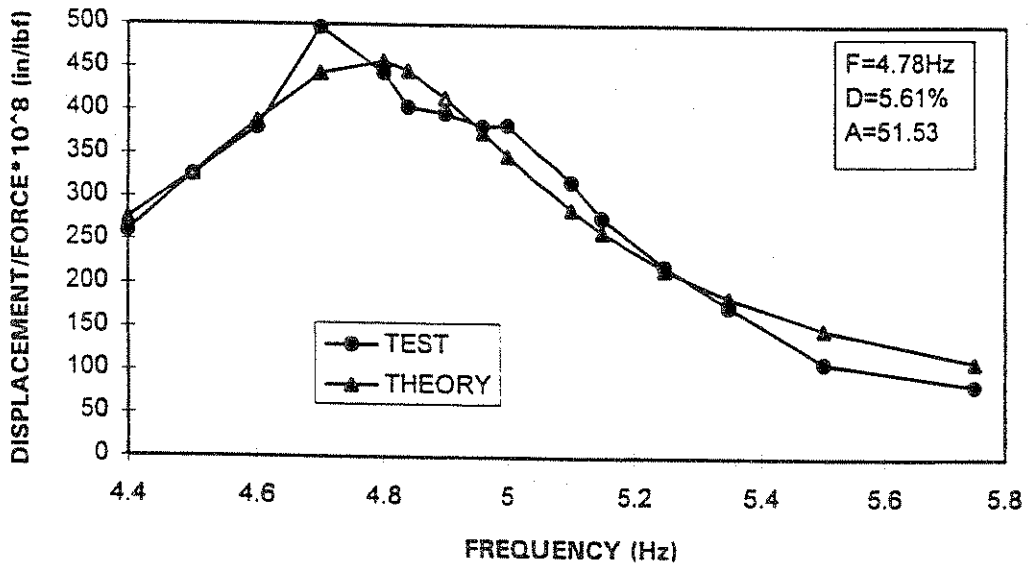


Fig 4.30: CH15 Response Curve -Cut Rail Transverse (3 Variables)

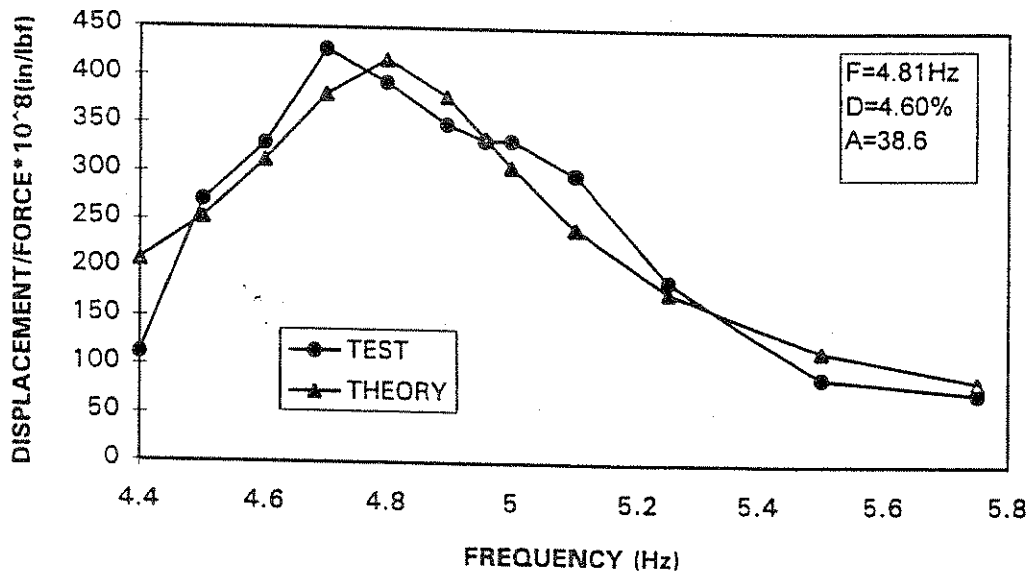


Fig 4.31: CH16 Response Curve-Cut Rail Transverse (3 Variables)

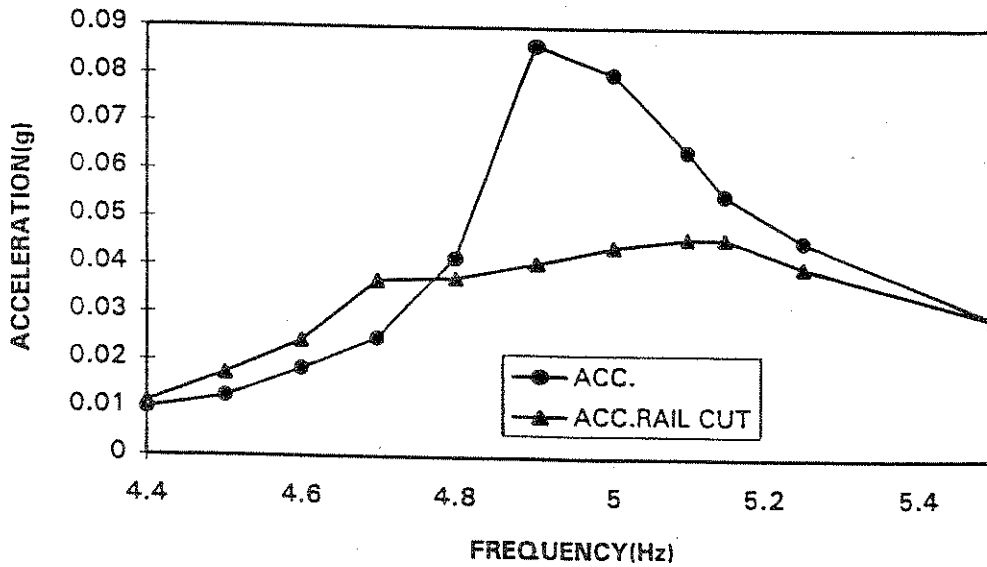


Fig 4.32: CH3 Acceleration Response-Cut Rail Transverse.

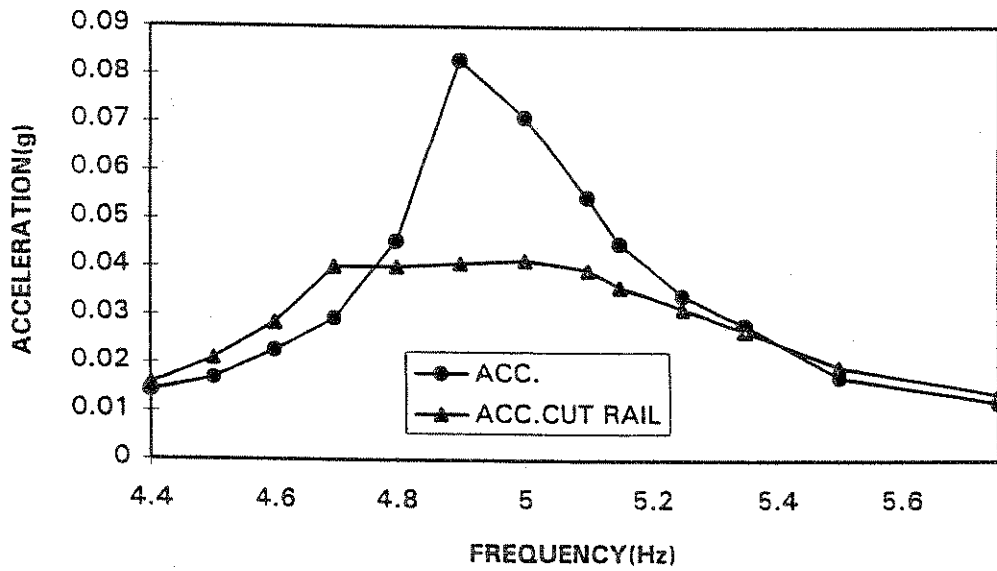


Fig 4.33: CH9 Acceleration Response-Cut Rail Transverse.

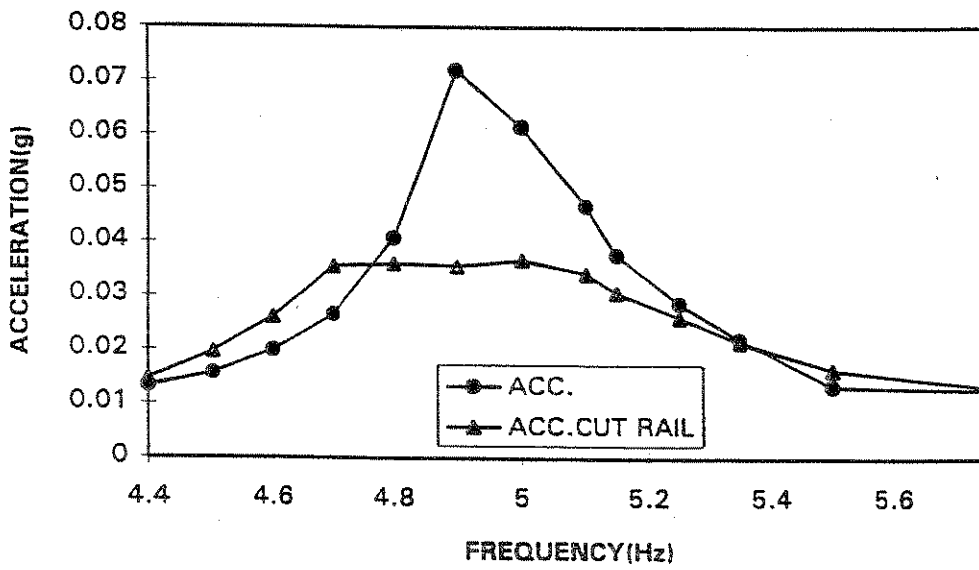


Fig 4.34: CH11 Acceleration Response-Cut Rail Transverse.

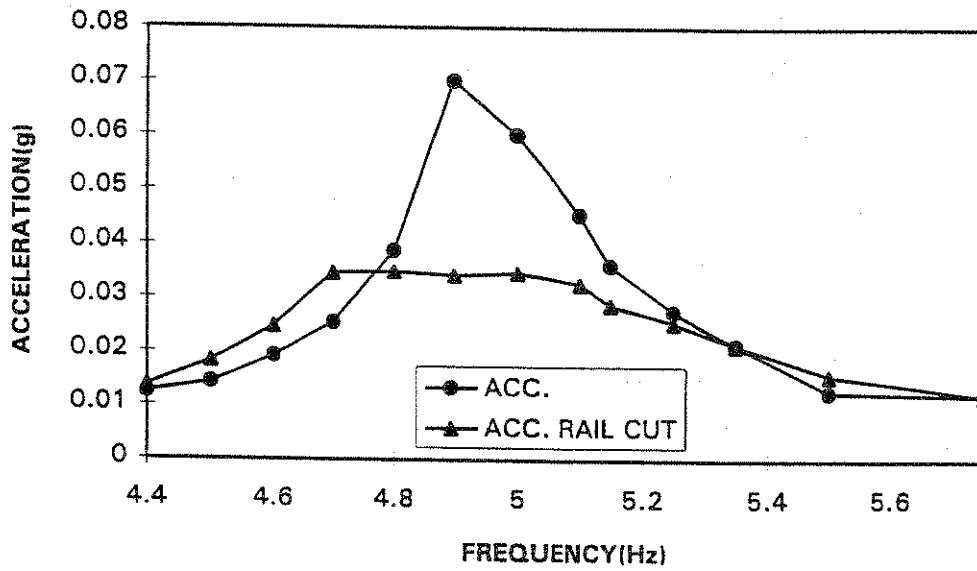


Fig 4.35: CH12 Acceleration Response-Cut Rail Transverse.

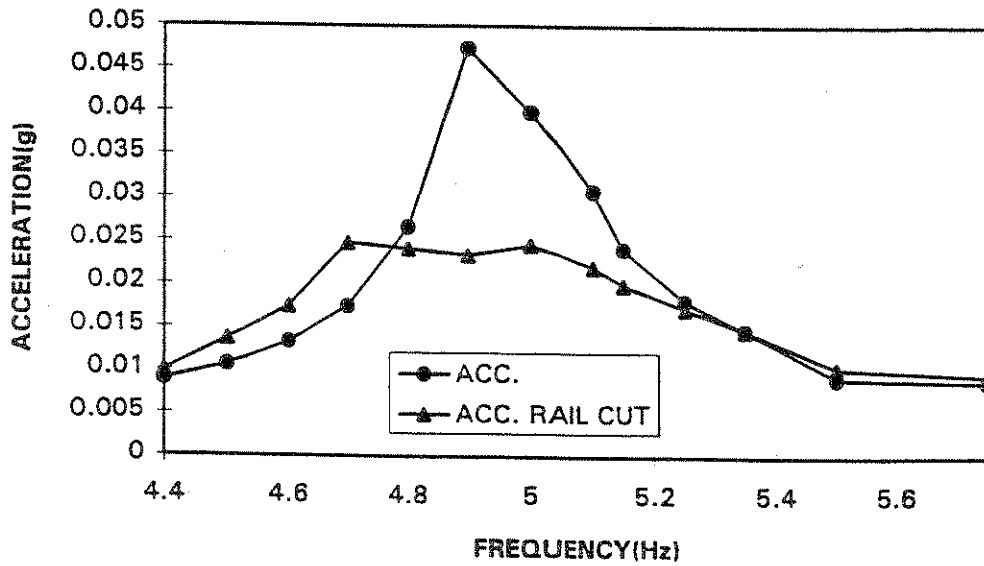


Fig 4.36: CH15 Acceleration Response-Cut Rail Transverse.

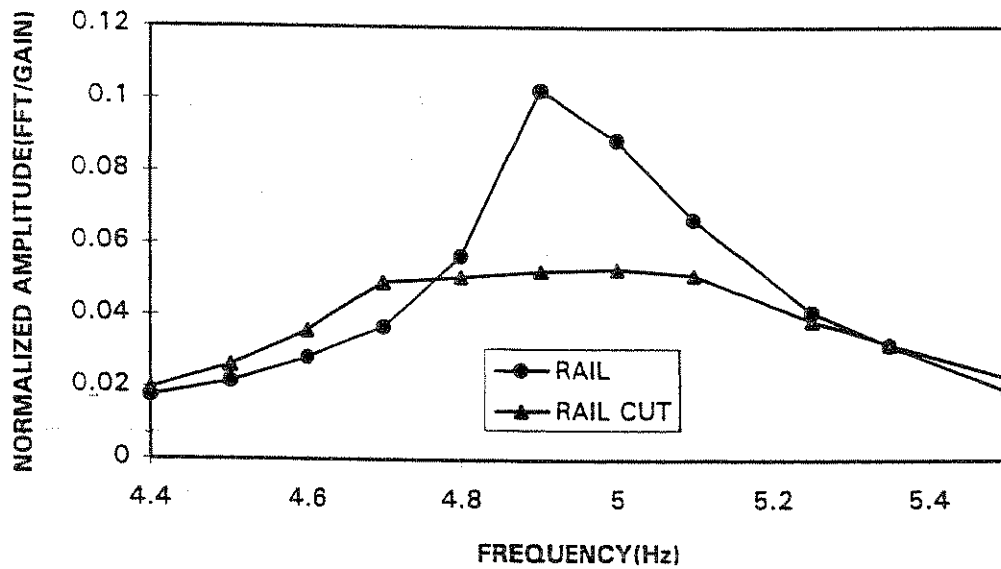


Fig 4.37: CH8 FFT Response-Cut Rail Transverse.

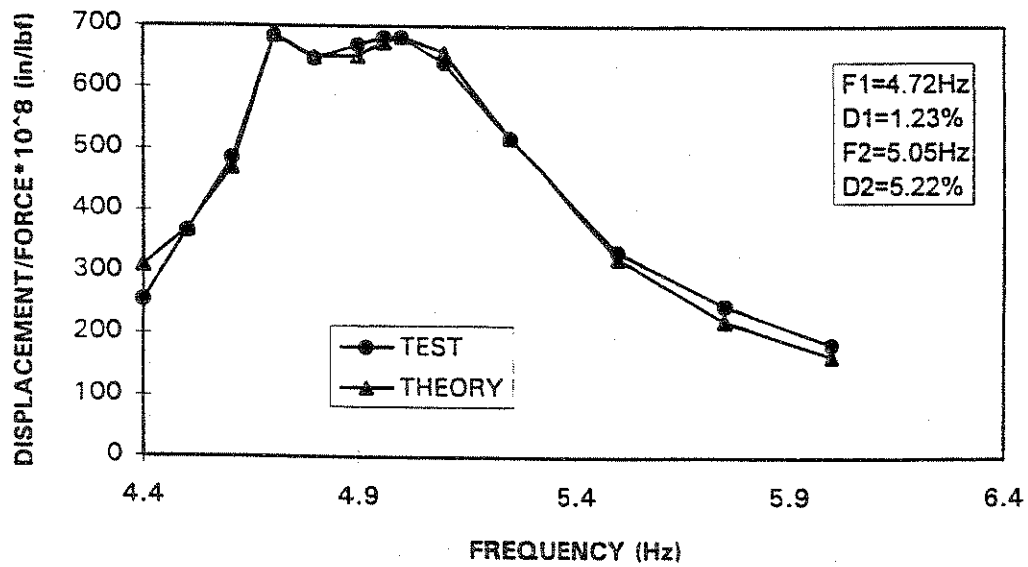


Fig 4.38: CH2 Response Curve-Cut Rail Transverse(6 Variables)

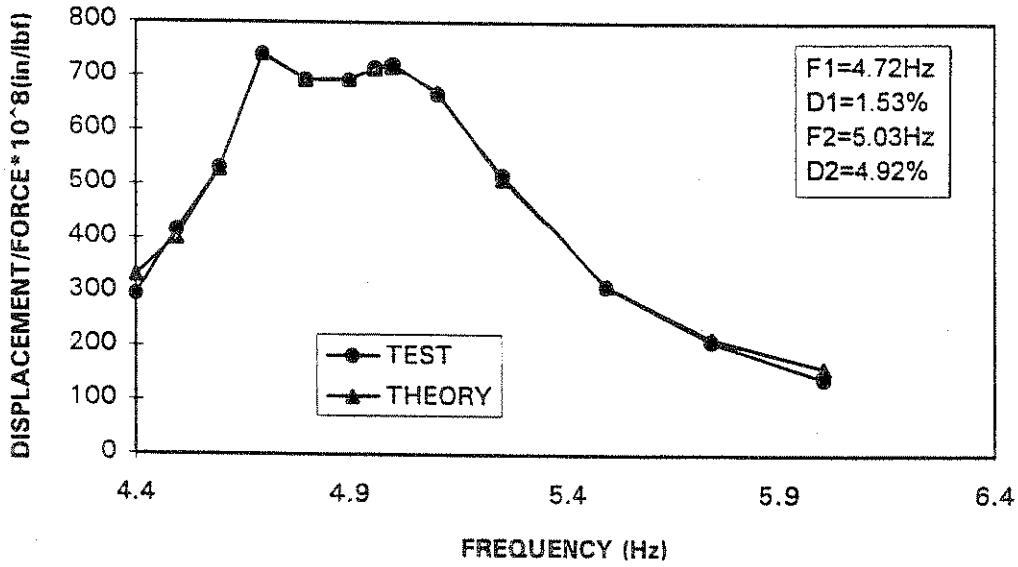


Fig 4.39: CH3 response Curve-Cut Rail Transverse (6 Variables)

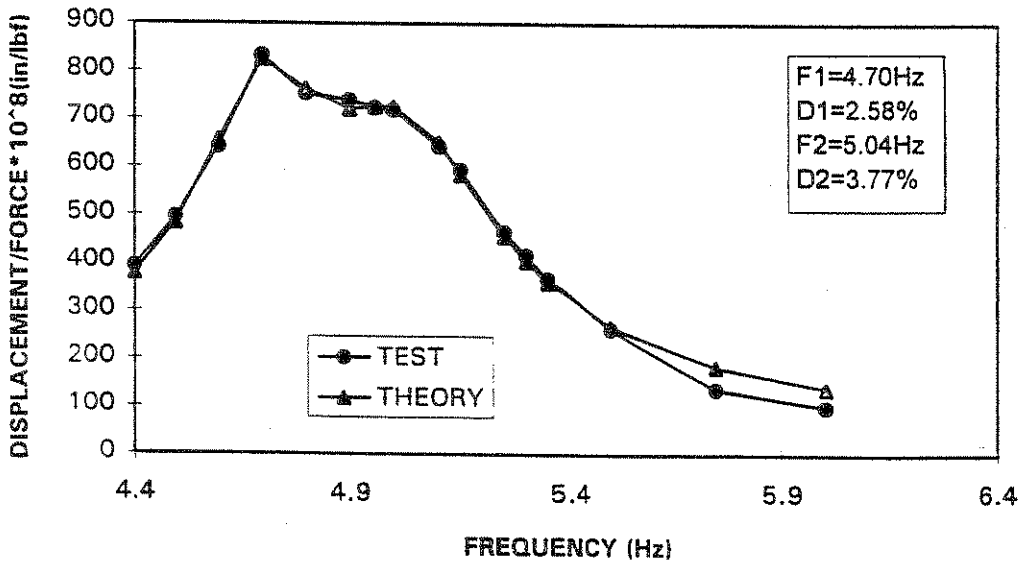


Fig 4.40: CH6 Response Curve-Cut Rail Transverse (6 Variables)

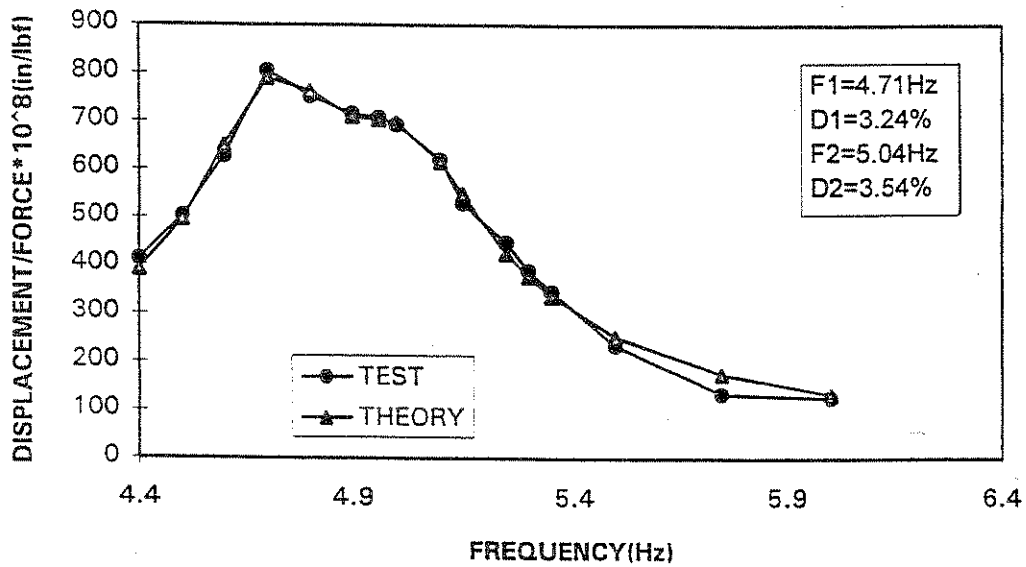


Fig 4.41: CH7 Response Curve-Cut Rail Transverse (6 Variables)

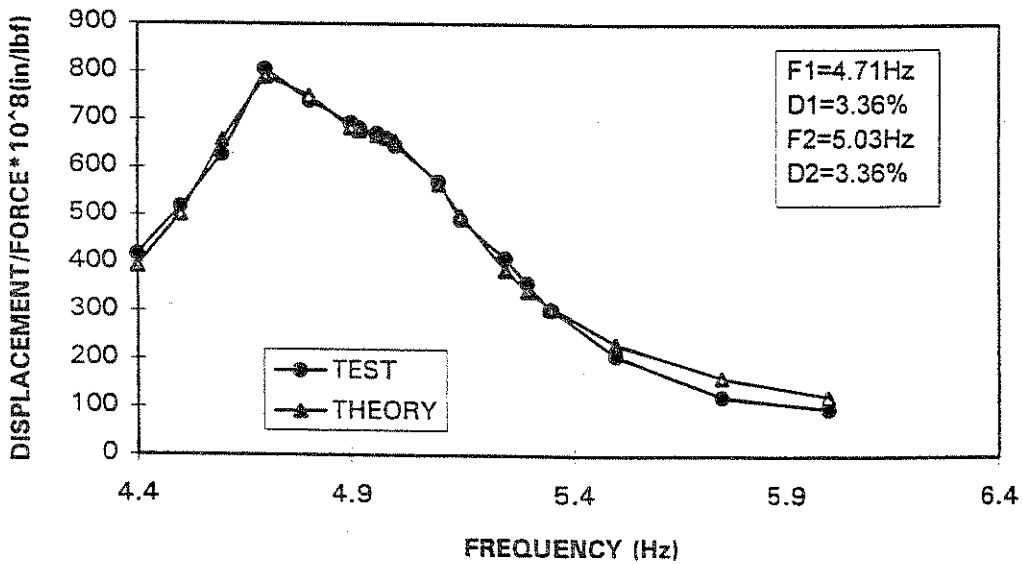


Fig 4.42: CH8 Response Curve-Cut Rail Transverse (6 Variables)

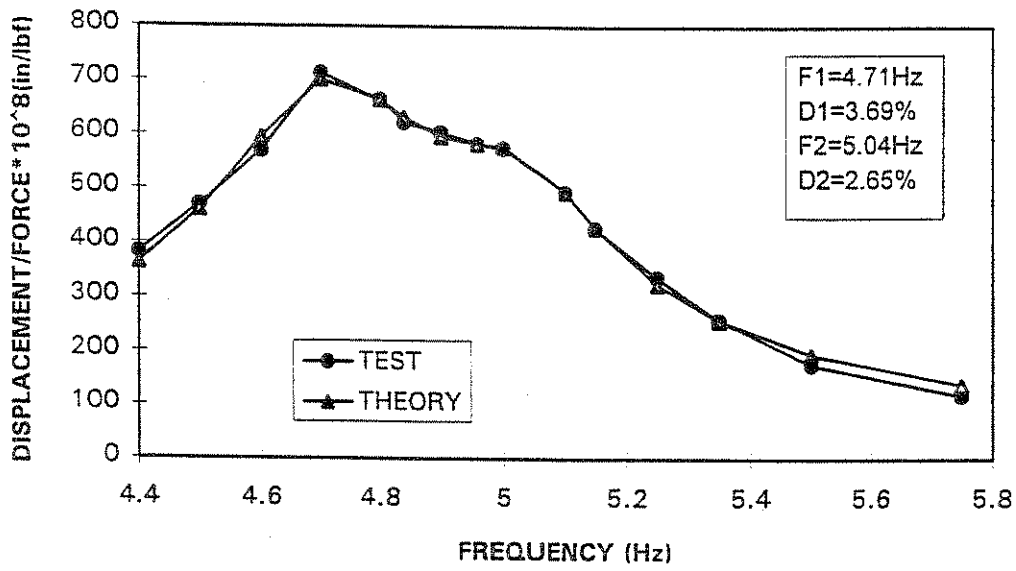


Fig 4.43: CH11 Response Curve-Cut Rail Transverse (6 Variables)

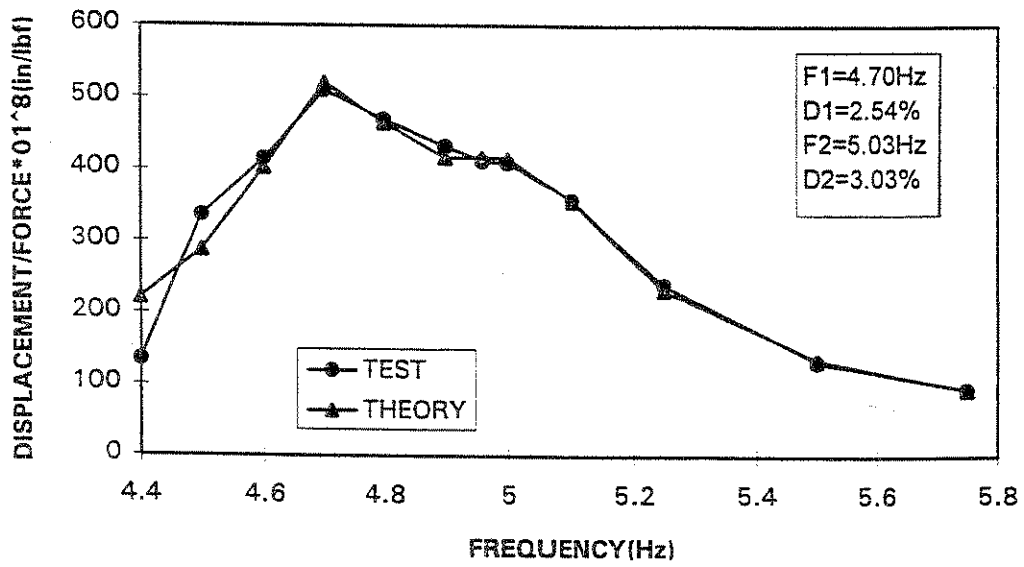


Fig 4.44: CH14 Response Curve-Cut Rail Transverse (6 Variables)

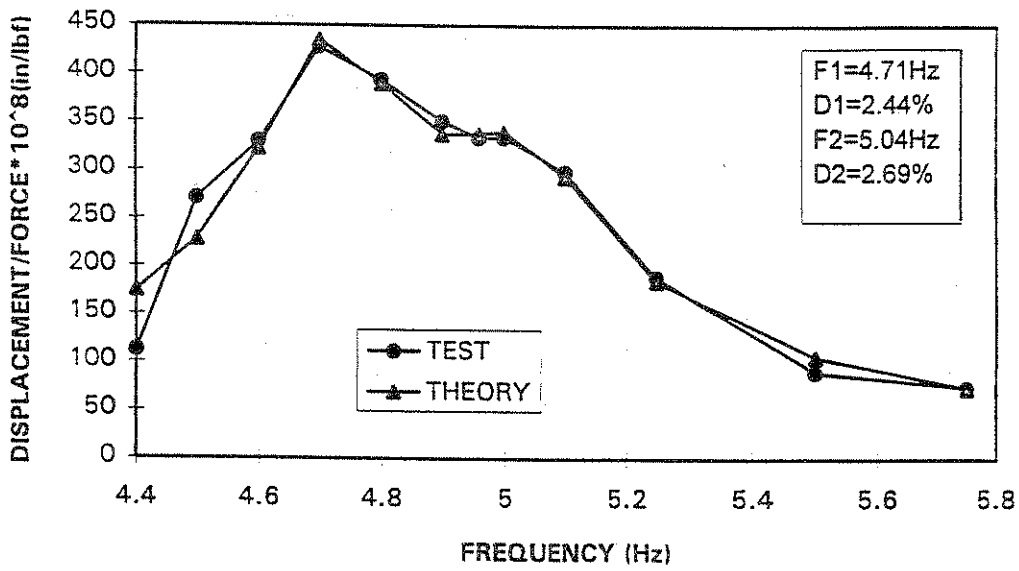


Fig 4.45: CH16 Response Curve-Cut Rail Transverse (6 Variables)

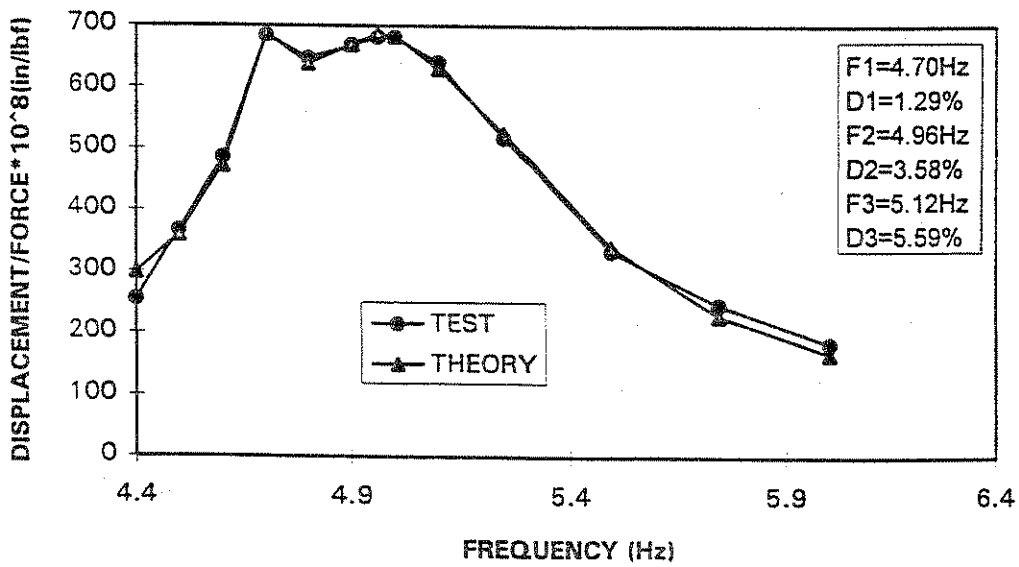


Fig 4.46: CH2 Response Curve-Cut Rail Transverse (9 Variables)

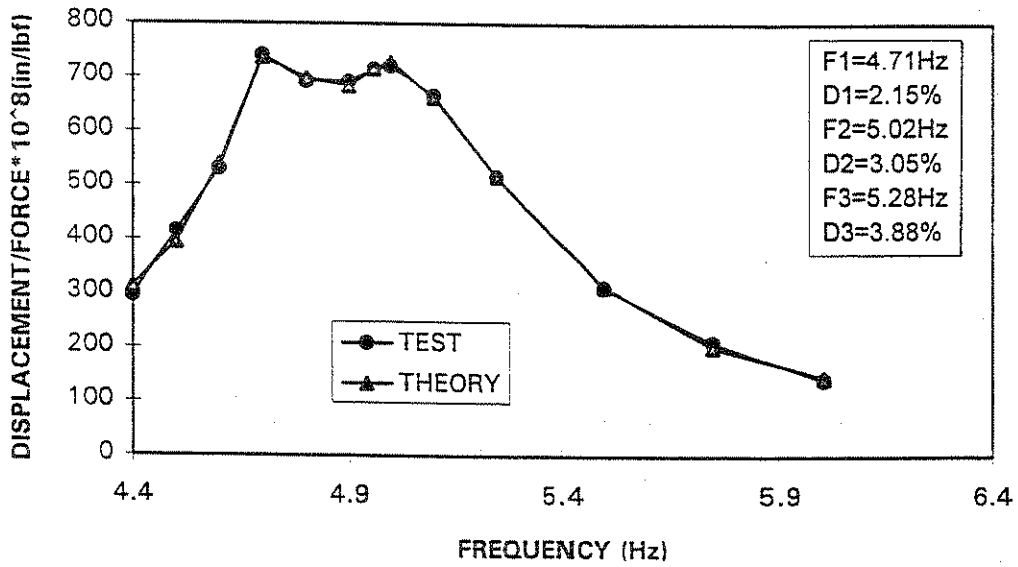


Fig 4.47: CH3 Response Curve-Cut Rail Transverse (9 Variables)

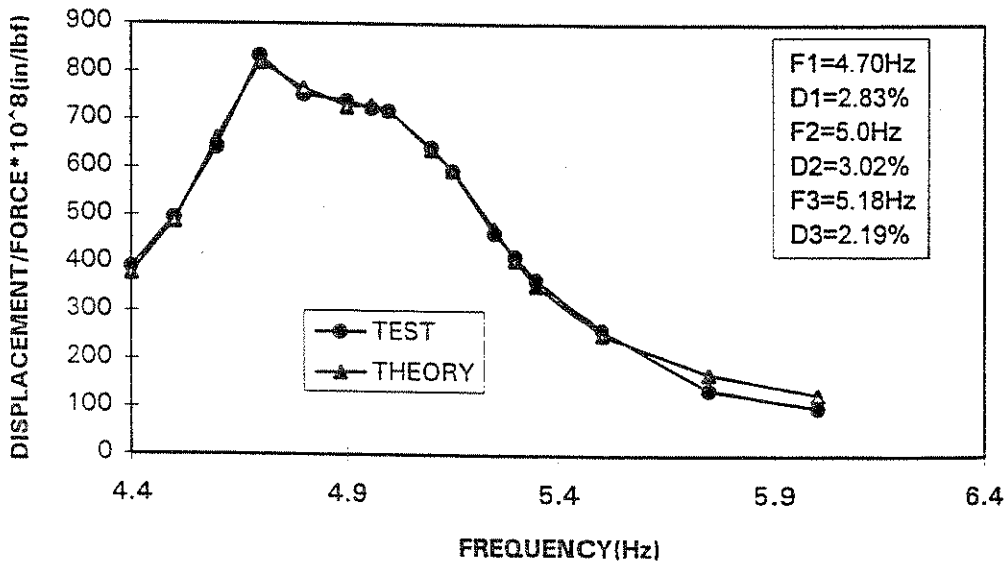


Fig 4.48: CH6 Response Curve-Cut Rail Transverse (9 Variables)

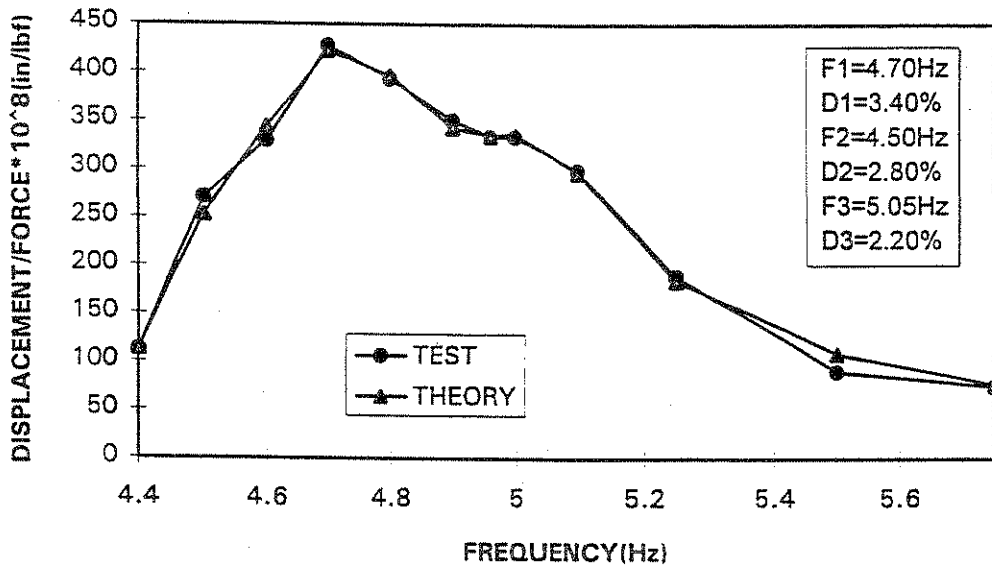


Fig 4.53: CH16 Response Curve-Cut Rail Transverse (9 Variables)

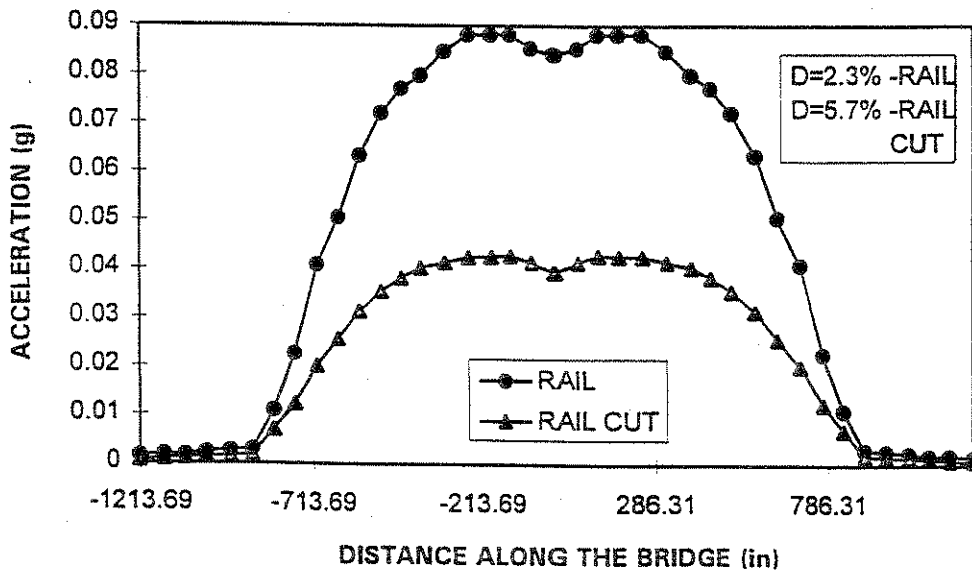


Fig 4.54 : First Transverse Mode shapes For Rail and Cut Rail Cases.

CHAPTER 5

RESPONSE OF THE BRIDGE IN THE LONGITUDINAL DIRECTION

5.1 INTRODUCTION

During the initial five setups in the longitudinal direction (Figs.2.6-2.10), frequency sweeps were performed between 8.0-20.0 Hz. This was done because it was anticipated, based on the results of a preliminary analysis, that the fundamental frequency in the longitudinal direction would be over 10Hz. No clear peaks in the response curves were identified in this range, which indicated that no natural frequencies existed. However, some useful information was obtained regarding the role of the rails in transmitting vibration to the adjacent road bed. Figures 5.1 and 5.2 show the acceleration response of the accelerometers on and off the bridge for the cases of uncut and disconnected rails respectively at 8.0Hz. The dotted vertical lines show the end of the bridge deck. It can be seen that the transmission of vibration outside the bridge is more significant when the rails were in place.

A second test was performed between 4.0- 9.0 Hz in the longitudinal direction. In this test, the shaker was attached to the rails in the middle of the east span. Initially the accelerometers were attached on the ties as in the previous setups. However, significant vertical vibration of the rail track system was observed during the longitudinal excitation of the bridge. The presence of this vibration makes the calculation of the fundamental longitudinal frequency very difficult. As a result, the accelerometers were placed on the bridge girders. Four of them

directed longitudinally, were placed on the south girder, and three, directed vertically, were placed on the north girder as shown in Fig 2.11. The vertical accelerometers allowed for the identification of the fundamental vertical frequency, which was not originally planned.

5.2 FIRST MODE-RAILS IN PLACE

Response curves were developed for all four accelerometers on the south girder, as shown in Fig.2.11, to identify the fundamental mode characteristics of the bridge in the longitudinal direction. Initially, the three variable fitting program was used to fit the experimental data points with the theoretical values, in order to determine the fundamental frequency, and the corresponding modal damping.

Figures 5.3-5.6 show the response curves of all four channels, placed on the bridge in the longitudinal direction. It should be noted that, since there were no clear peaks below 6.0Hz in the response curves, they were plotted from 6.3 - 9.0 Hz. Table 5.1 summarizes the results of the three variable fitting program for each channel, by showing the corresponding calculated values of the natural frequencies, critical damping and amplitudes.

Table 5.1: Response Parameters of the bridge for the Longitudinal excitation.

PARAMETER	CH2	CH3	CH4	CH5
FREQUENCY	6.57Hz	6.54Hz	6.58Hz	6.56Hz
DAMPING	11.11%	11.19%	10.8%	11.72%
AMPLITUDE	15.43	15.08	13.43	13.82

Table 5.1 illustrates that the values of the parameters do not vary significantly among the channels. The fundamental frequency in the longitudinal direction is approximately 6.6Hz and the corresponding modal damping is approximately 11.0%. One can observe from Figs 5.3-5.6 that, the fitting of the experimental data points with the theoretical values was not very close. This indicates the existence of possibly another peak in the response curve. A six variable program was then used to fit the theoretical curves to the obtained experimental curves. The results are shown in Figs 5.7-5.10 and in Table 5.2. The first frequency is close to 6.5Hz and the corresponding damping about 5.0%. The second peak is around 8.3Hz, a value that is not close to 6.5Hz. Comparing these results with the results of the three variable program, one concludes that the fundamental longitudinal frequency is 6.5Hz with a corresponding modal damping of about 5.0%. The three variable program predicts closely the frequency value at 6.5 Hz, because this is the predominant peak in the response curve. However, the theoretical curve is artificially widened by the presence of the other secondary peak. Because of this second peak, the program predicts a higher damping value of 11%. Detailed analytical studies are needed for further clarification of the second peak at 8.3Hz.

Table 5.2: Response parameters for the longitudinal response with noise effect.

PARAMETER	CH2	CH3	CH4	CH5
FREQUE1	6.58Hz	6.56Hz	6.56Hz	6.53Hz
DAMPING1	5.02%	5.17%	5.01%	3.24%
AMPLITUDE1	6.14	6.06	5.32	2.25
FREQUE2	8.34Hz	8.31Hz	8.17Hz	7.09Hz
DAMPING2	18.13%	18.51%	18.44%	16.68%
AMPLITUDE2	6.82	6.53	6.39	16.35

In this test , data from only four accelerometers were available to plot the fundamental mode in the longitudinal direction. The mode shape of the fundamental mode, obtained for the east span is shown in Fig.5.11. To plot this mode shape, the acceleration amplitude values were calculated for all four accelerometers at 6.6 Hz, which is the fundamental frequency. These values were then plotted as a function of the distance along the bridge. In Fig.5.11, the distance values along the bridge are shown in inches and are measured from the center of the bridge. From Fig 5.11, the maximum acceleration response in the first mode was approximately 0.015g.

5.3 FIRST VERTICAL MODE- RAILS IN PLACE

As mentioned earlier in this chapter, there were three channels (6,7 and 8) oriented vertically in this test. Even though it was not intended to analyze the vertical response of the bridge during the longitudinal excitation , strong vertical

vibrations present during these tests, made it possible to identify the fundamental vertical frequency through the response of the vertically oriented accelerometers. Response curves were developed for all three accelerometers placed on the north girder as shown in Fig.2.11, to identify the fundamental vertical modal characteristics of the bridge. Since all the test response curves in this case showed a single distinguished peak, the three variable fitting program was used to fit the experimental data points with the theoretical values. This allowed for the determination of the vertical frequency and the corresponding modal damping. Figures.5.12-5.13 show the response curves of all three channels placed on the bridge in the vertical direction. Table 5.3 summarizes the results of the three variable fitting program for each channel, by showing the corresponding calculated values of the natural frequencies, critical damping and amplitudes.

Table 5.3: Vertical response parameters of the bridge with rails in their as built condition.

PARAMETER	CH6	CH7	CH8
FREQUENCY	6.06Hz	6.07Hz	6.06Hz
DAMPING	1.64%	1.64%	1.65%
AMPLITUDE	5.77	8.67	7.69

Table 5.3 indicates that the values of the parameters do not vary significantly among the channels. The fundamental vertical frequency is approximately 6.0Hz and the corresponding modal damping is approximately 1.65%.

Due to the unavailability of the data points, the vertical mode shape was plotted for three modal amplitude values at 6.0Hz as shown in Fig 5.15. The three data points were then fitted by a sinusoidal curve, which is the theoretical curve for the first vertical mode. This fitting produced excellent results, which are shown in Fig.5.16.

5.4 FIRST LONGITUDINAL AND VERTICAL MODES- RAILS CUT

Response curves for two of the accelerometers placed on the south girder of the bridge oriented in the longitudinal direction, were developed for the case of disconnected rails. These response curves are shown in Figs.5.17-5.18. The six variable fitting program was used for the development of these curves. Examining the curves, it appears that the peaks are closely spaced. The first peak is located near 5.6Hz and has a modal damping value approximately equal to 5.3%. It is likely that the first peak corresponds to the fundamental vertical mode and the second peak corresponds to the fundamental longitudinal mode with disconnected rails. Comparing these results with the results from the uncut rail cases, it appears that disconnecting the rails results in a softer system with lower natural frequencies. No major changes on damping were observed. A detailed analytical model is needed to investigate the exact role of the rails. Based on the results from the transverse, longitudinal and vertical mode, it appears however that the lack of rails results in softer system with lower frequencies. The effects were more significant in the longitudinal mode. It is believed that the effects of rails will be more significant in the case of open deck bridges.

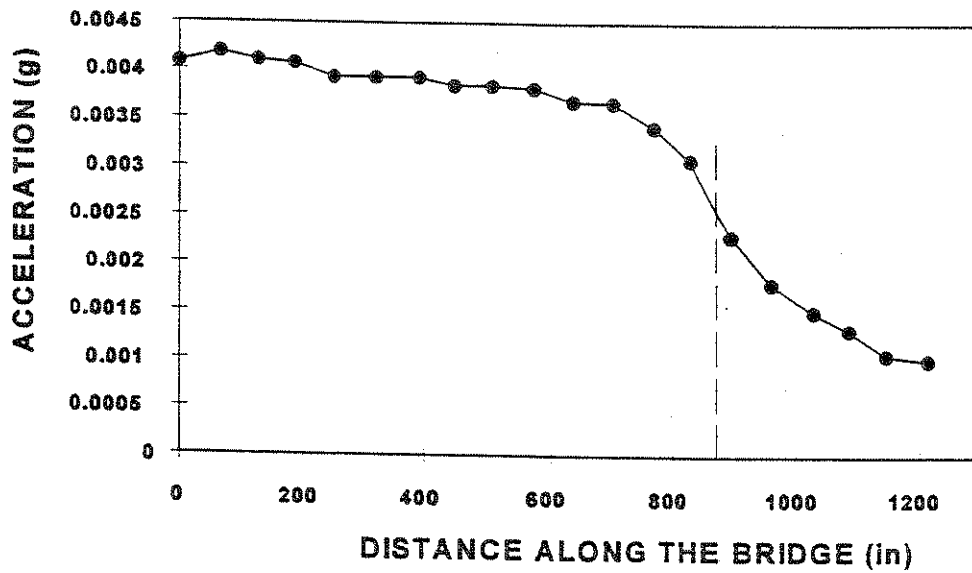


Fig 5.1: Longitudinal Response at 8.0Hz - Uncut Rail.

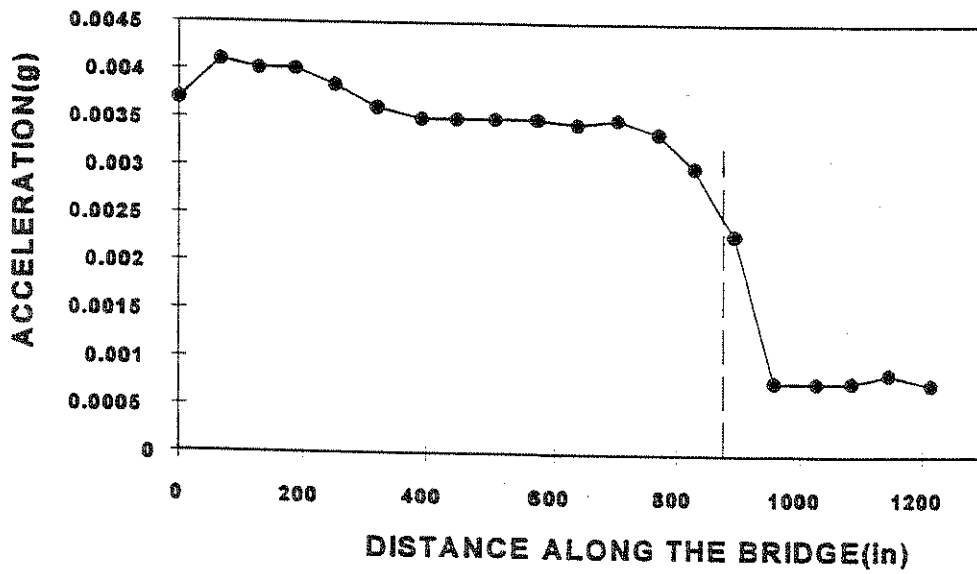


Fig 5.2: Longitudinal Response at 8.0Hz- Cut Rail

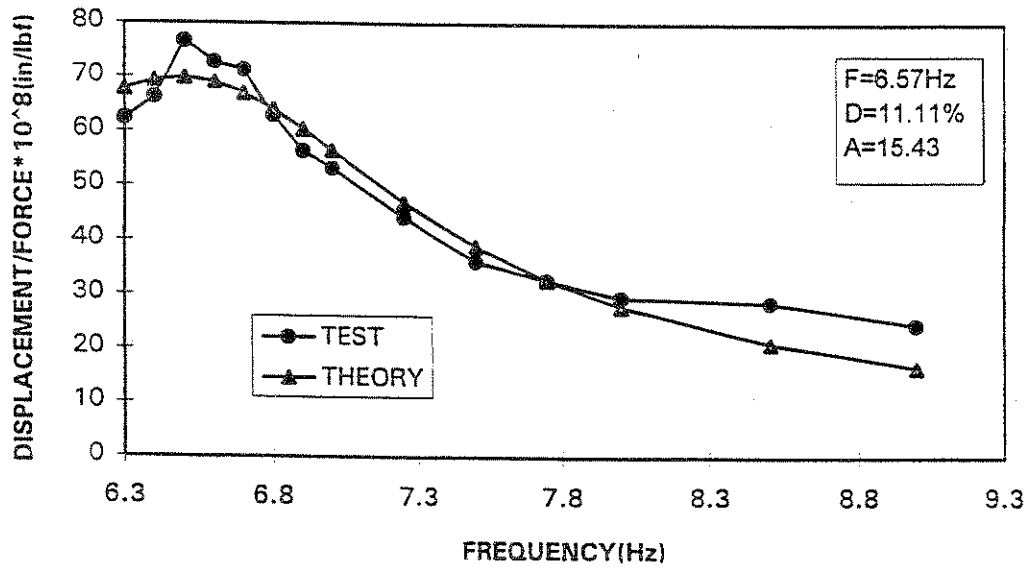


Fig 5.3:CH2 Response Curve First Longitudinal Mode.

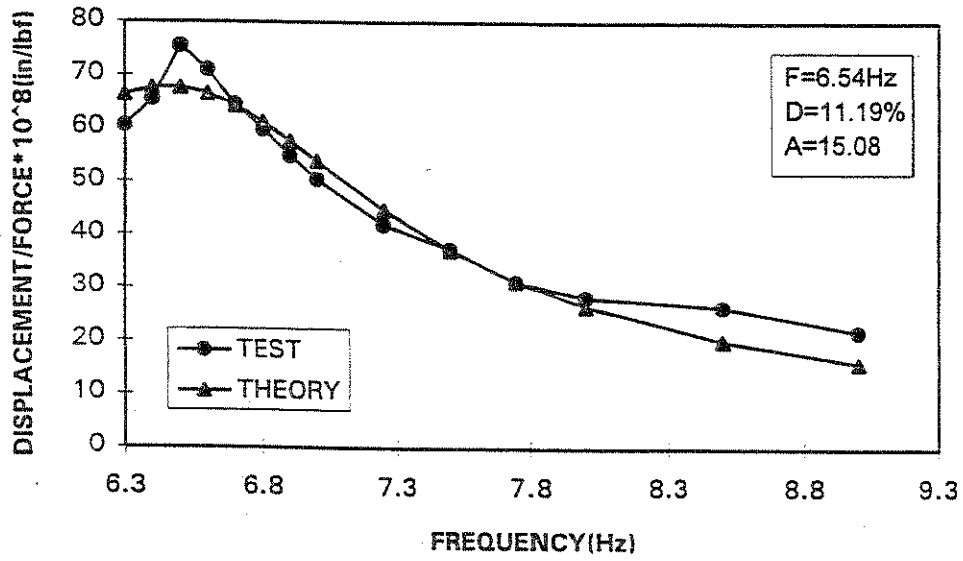


Fig 5.4:CH3 Response Curve-First Longitudinal Mode.

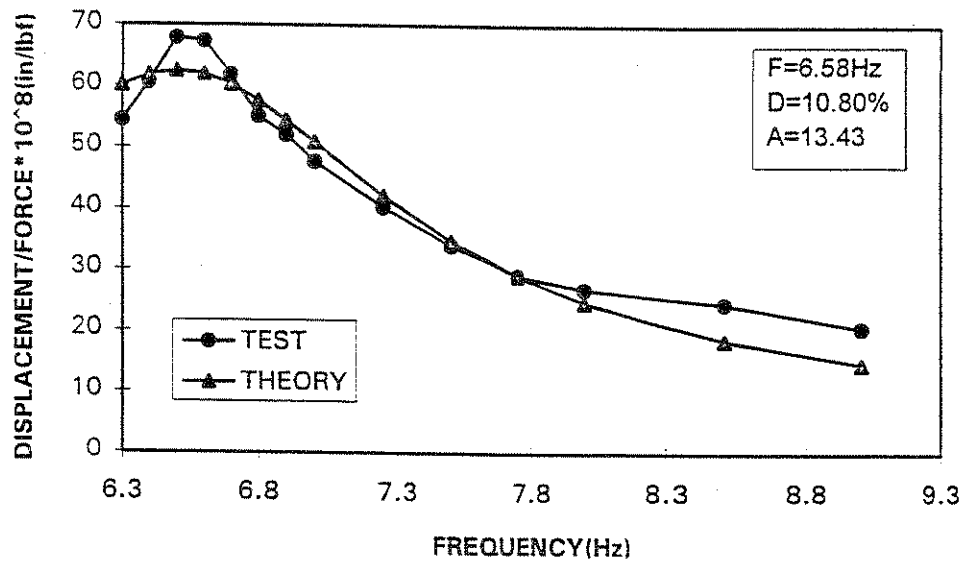


Fig 5.5:CH4 Response Curve-Longitudinal Mode.

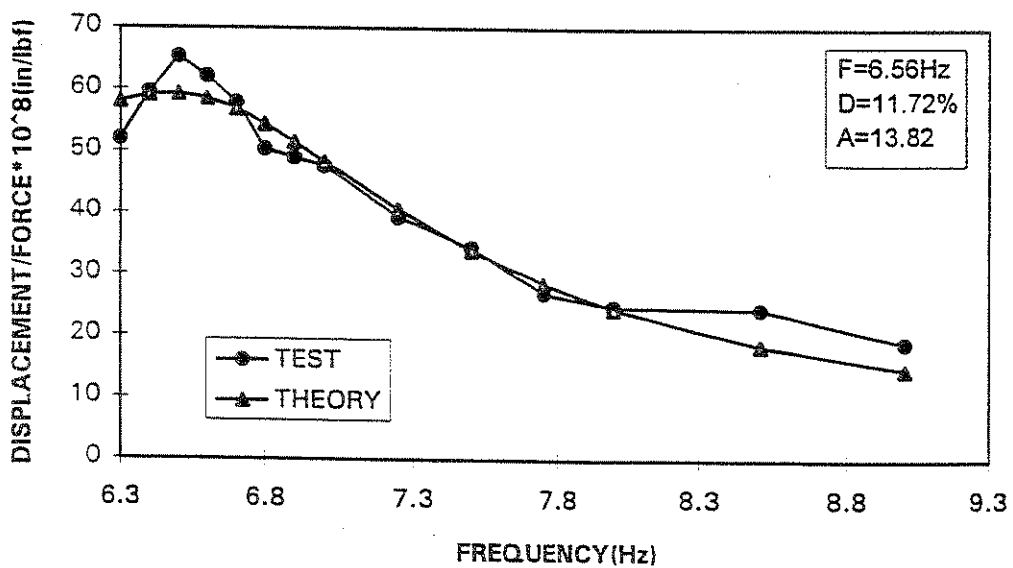


Fig 5.6:CH5 Response Curve-first Longitudinal Mode.

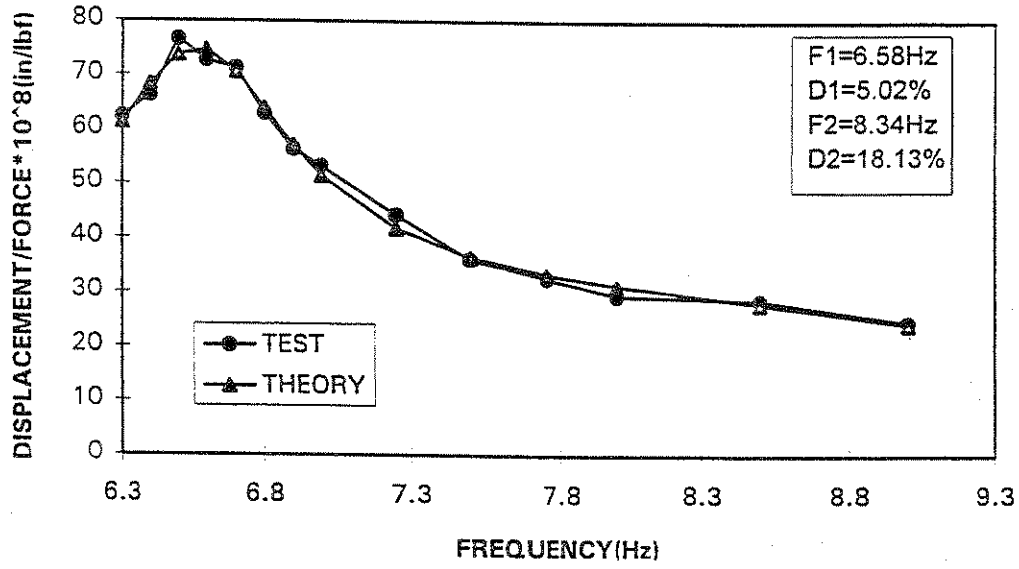


Fig 5.7: CH2 Response Curve-First Longitudinal Mode (6 Variables)

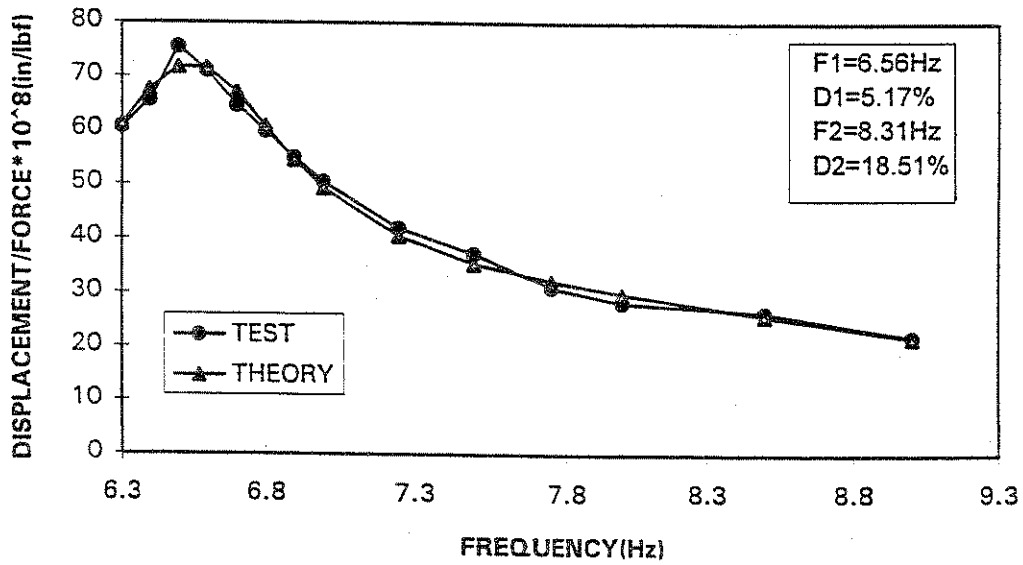


Fig 5.8: CH3 Response Curve-First Longitudinal Mode (6 Variables)

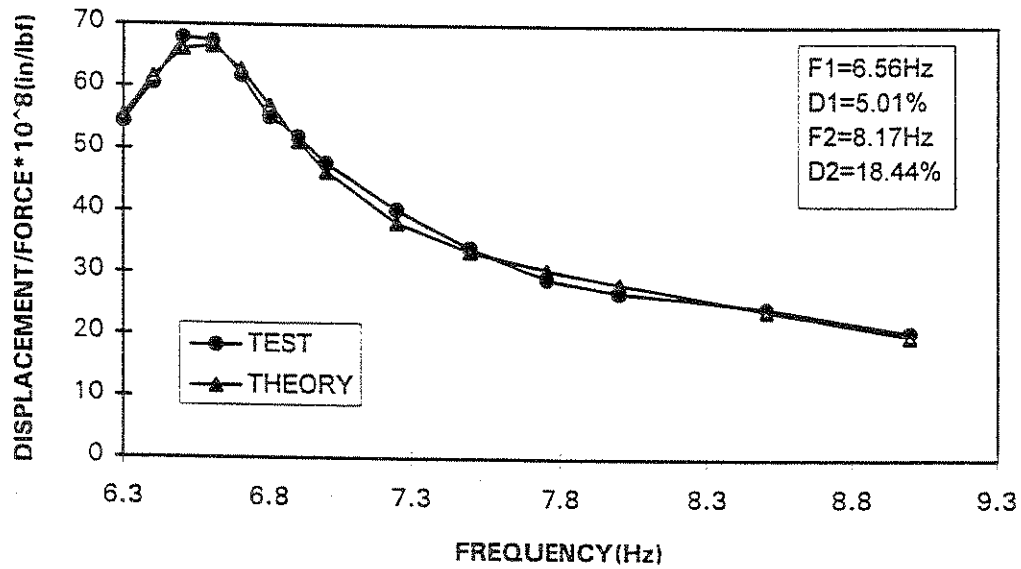


Fig 5.9: CH4 Response Curve-First Longitudinal Mode (6 Variables)

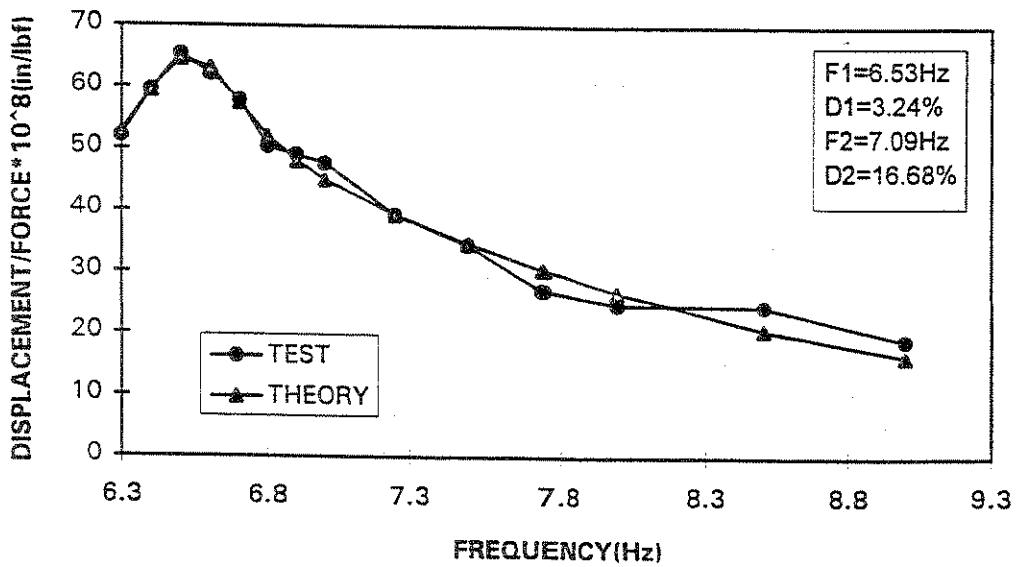


Fig 5.10: CH5 Response Curve-First Longitudinal Mode (6 Variables)

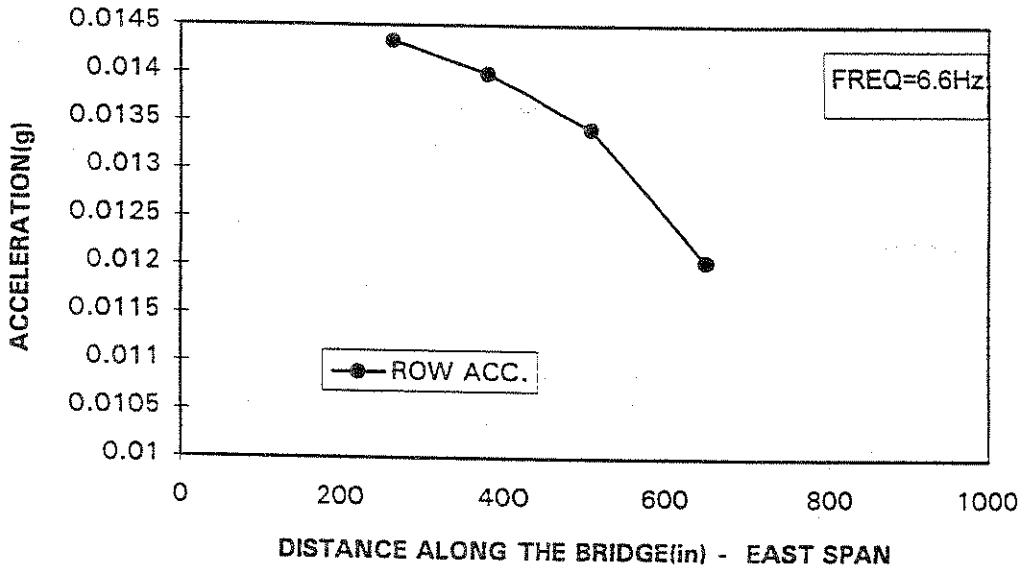


Fig 5.11: Longitudinal Mode Shape At 6.6Hz

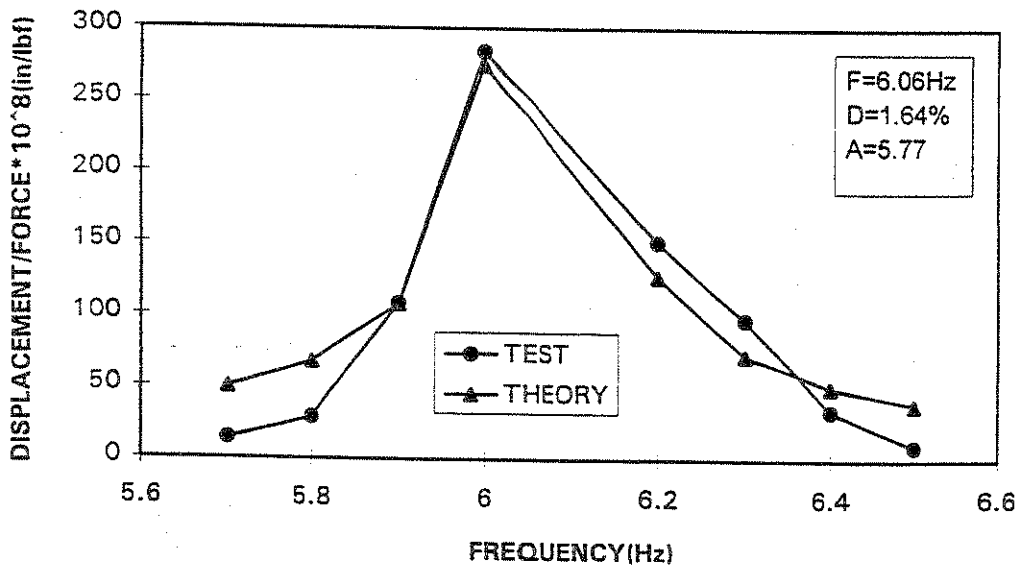


Fig 5.12: CH6 Response Curve-First Vertical Mode(Lon. Set Up).

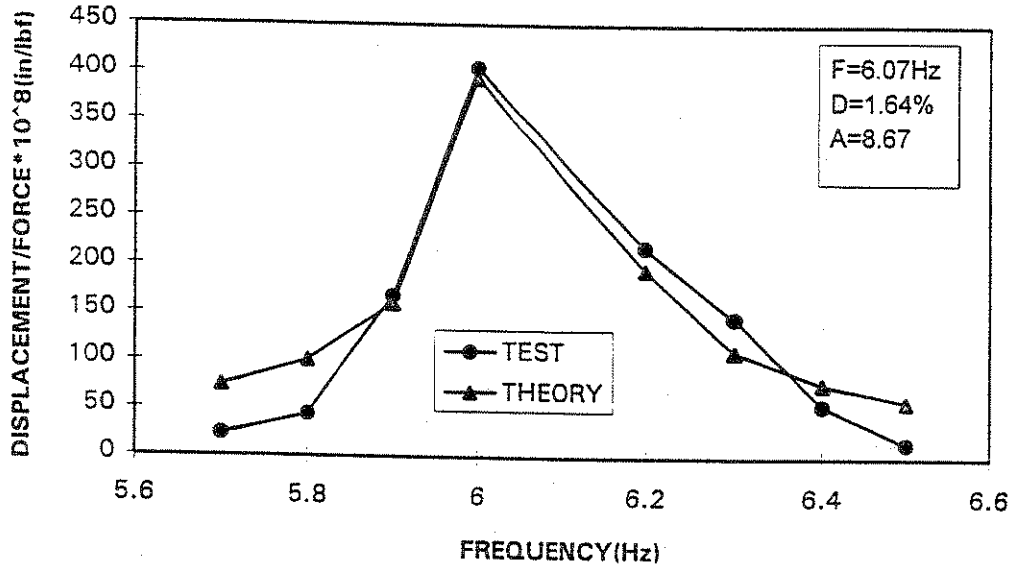


Fig 5.13:CH7 Response Curve-First Vertical Mode(Lon.Set Up).

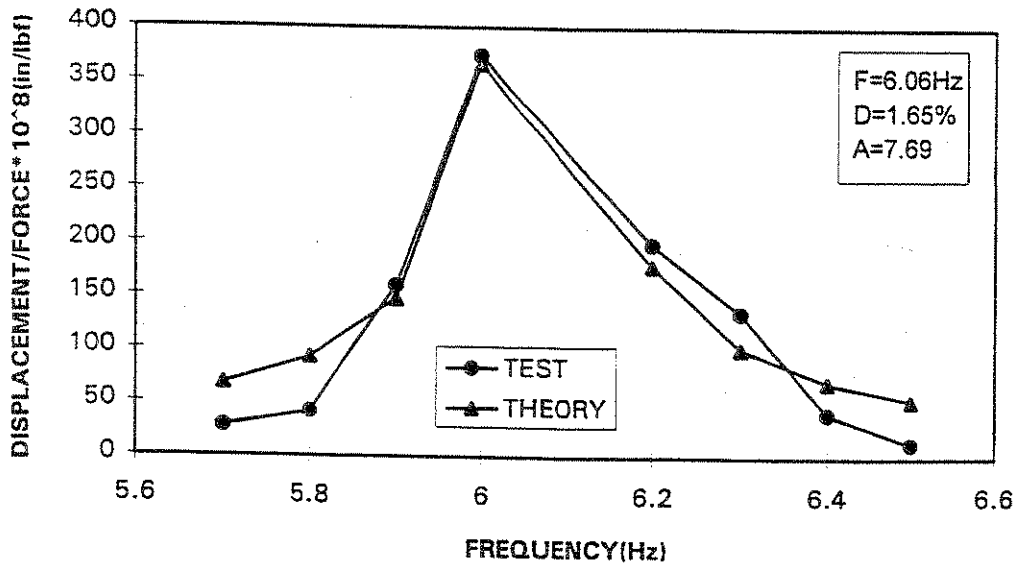


Fig 5.14: CH8 Response Curve-First Vertical Mode(Lon.Set Up).

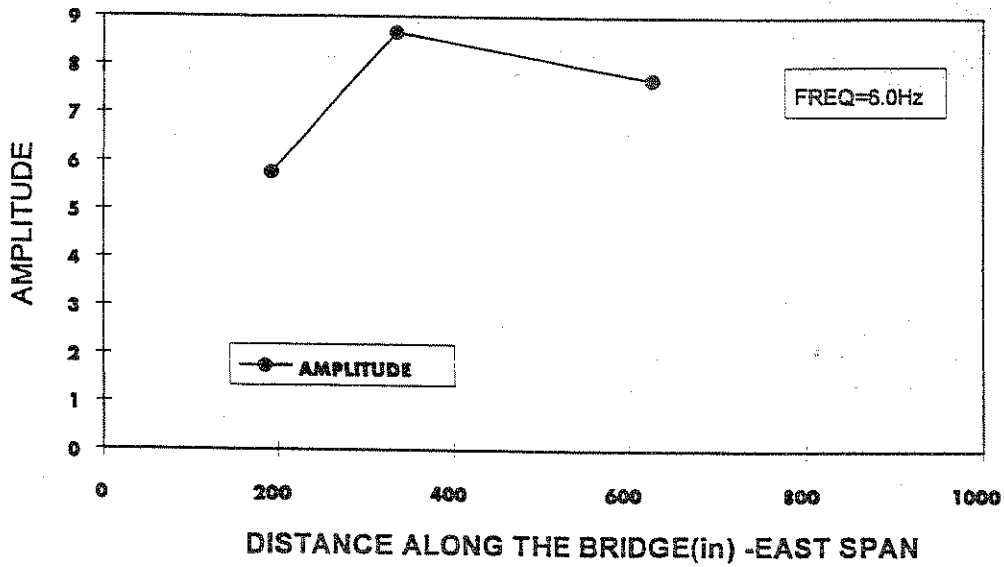


Fig 5.15: Vertical Mode Shape At 6.0Hz

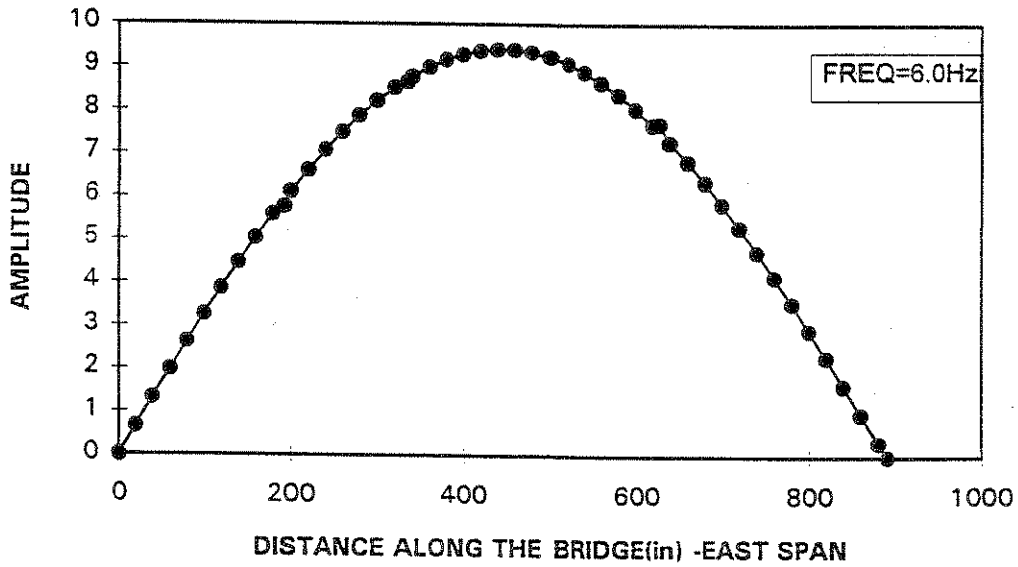


Fig 5.16: Vertical Mode Shape At 6.0Hz
"Sinusoidal Fitting"

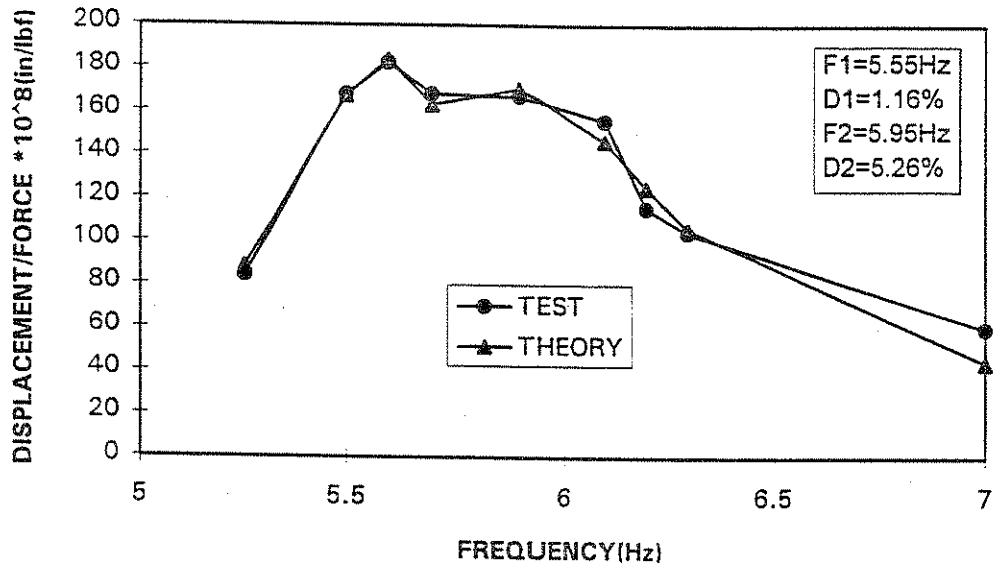


Fig 5.17: CH2 Response Curve-Cut Rail Longitudinal.

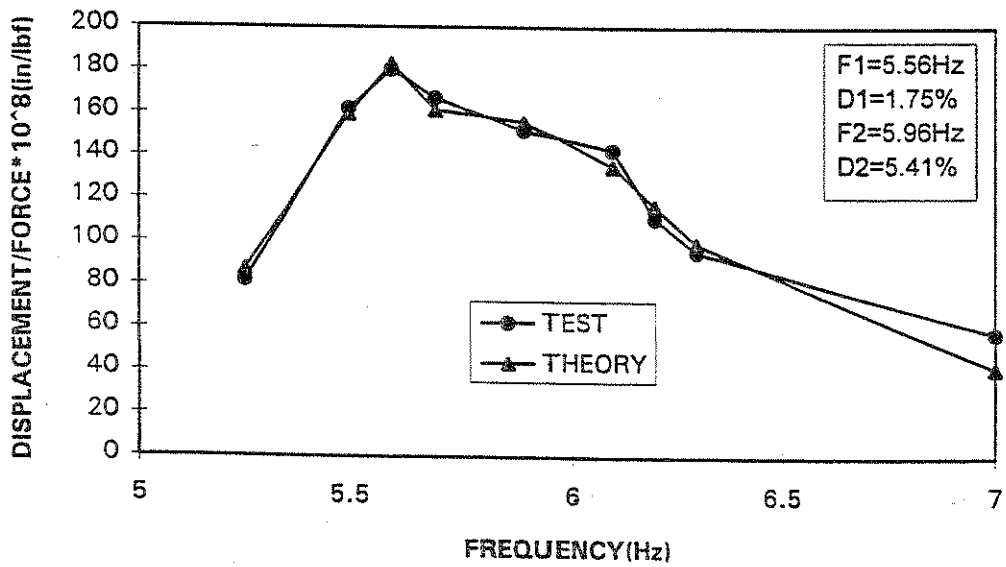


Fig 5.18: CH3 Response Curve-Cut Rail Longitudinal.

CHAPTER 6

ANALYTICAL MODELING OF THE BRIDGE

6.1 INTRODUCTION

In the course of the experimental studies involving vertical excitation, two fairly closely spaced frequencies at 6.06Hz and 6.75Hz were found. These two frequencies were thought to be those of the second global vertical mode and the second transverse global mode having strong torsional coupling. In a first attempt to identify these frequencies, the continuous beam theory on a model of the half bridge was used. The half bridge was used because there is insignificant coupling of the two bridge halves over the central pier in these two modes of vibration. The first vertical mode frequency obtained by using continuous beam theory was 6.25 Hz [12]. In this calculation the combined vertical moment of inertia of the girders and the ballast pan was used for the total vertical moment of inertia, while the mass per unit length was calculated using the construction drawings. The vertical frequency of the first mode for this simplified model was 6.25 Hz, reasonably close to the observed frequency of 6.06 Hz. A second similar calculation was made for the first transverse mode using the transverse moment of inertia of the bridge girders. This calculation yielded a transverse frequency of 18.16 Hz, which was larger than the experimentally determined value as 6.75 Hz. It should be noted that the first transverse mode of the single span FEM model of the half bridge corresponds to the second mode of the actual two span bridge.

This last result is not too surprising if one can consider the bridge to approximate a large open channel section subjected to combined St. Venant and restrained warping torsional effects [13]. To investigate this phenomenon and to attempt to identify the 6.75Hz experimental natural frequency, a full three dimensional finite element model of the bridge was developed.

For this purpose, the finite element program , "COSMOS/M", was used [14]. The two main girders, floor beams, knee brackets, connecting angles, deck plates, fill plates and diaphragms were modeled using "SHELL" elements. The ballast, rails, and ties were considered as lumped mass elements on the nodes of the deck plates.

6.2 MODEL OF THE TWO MAIN GIRDERS:

Each main girder consists of a 78"x 7/16" web plate , a continuous 18"x5/8" cover plate at top and the bottom of the web, and a second cover plate of the same size centered midway in the span for a length of 46.0' at the top and the bottom of the web plate. The cover plates and the web are connected by 8"x6"x3/4" double angles at the top and the bottom as shown in the left half of Fig .6.1. To model this girder, plates with different thickness as shown on the right half of Fig.6.1, were used. For the double cover plate and the long leg of the angles at top and bottom, a single plate with the total thickness of the cover plates and the angles was used. At the web, where the angles thicken it , a plate with the actual total thickness was used. The middle of the web plate was

modeled with a plate of the same thickness. All the plates were represented by "SHELL" elements in the finite element model. The three dimensional model of the bridge is shown in Fig.6.2.

6.3 MODEL OF THE FLOOR BEAMS

The two main girders of the bridge spaced 18.0' apart, were connected by W18X60 floor beams spaced 2.0' apart longitudinally and covered by a 0.5" thick low alloy plate. The two ends of the floor beam were connected to the bottom of the web plate by 4"X4"X3/8" angles and a 3/4" fill plate. The floor beams were modeled in a manner similar to the main girders by replacing the web and the flanges with plates of same thickness. Then the plates were modeled by "SHELL" elements in the finite element model as shown in Fig.6.3. The nodes of the elements representing the web of the floor beam were connected to the nodes of the web elements in the main girder at the same location. This is shown in Fig.6.3.

6.4: MODEL OF THE BALLAST PAN

The ballast pan, made of 0.5" thick low alloy steel and carrying the ballast, rail, and tracks of the bridge, rests on top of the floor beams and spans between individual floor beams. This pan consists of a bottom plate on top of the floor beams and two side plates supported by the knee brackets attached to the main girders. These three plates were modeled by "SHELL" elements in the finite element model as shown in Fig.6.4. The nodes of the elements of the ballast plate at the top of the floor beams are connected to those nodes of the top

flange elements in the floor beam. The nodes of the elements of the two side plates at the knee bracket supports are connected to the nodes of the knee bracket elements at the same location.

6.5 MODEL OF THE KNEE BRACKET SUPPORTS

The knee brackets, consisting of a trapezoidal steel plate with angle connections, are located on top of the floor beam at both ends as shown in Fig 6.4. This gives support to the ballast pan. The position of these brackets along the two main girders is shown in the drawings of the bridge. The vertical portion of this bracket is connected to the web of the main girder just above the floor beam by 4"x4"x3/8" angles. Angles of the same size are used to connect the bottom part of the bracket to the floor beam. The portion of the bracket supporting the two side plates of the ballast pan is also connected by the angles mentioned above.

The steel plate and the angle connection of the bracket are considered to be plates of same thickness and modeled by "SHELL" elements. The nodes of the elements representing the bracket at the edges are connected to the corresponding nodes of the floor beams, ballast pan, side plates, and web of the main girders.

6.6 MODEL OF THE TRACK STRUCTURE

The mass of the ballast was represented by lumped mass elements, located at the nodes of the plates representing the ballast pan in the model. The mass of the rail tracks and the ties was also considered to be lumped mass elements on the pan.

6.7 MODEL OF THE MAIN GIRDER STIFFENERS

Stiffeners are provided along the length of the main girder on both sides as shown in Fig 6.4, to prevent buckling of the girder. An angle section of 4"X4"X7/16" is used for these stiffeners. The stiffeners are considered as plates of same thickness and modeled by "SHELL" elements. The nodes at the edges of the stiffener touching the web and the flanges of the main girder were connected to those corresponding nodes of web and flanges elements.

6.8 FIRST VERTICAL MODE SHAPE OF THE MODEL

The frequency of the first vertical mode of the bridge from the model is 5.944Hz as shown in Fig 6.5. To confirm that this was a vertical mode, the modal amplitude values in the vertical direction and in the transverse direction along the center line of the span were obtained at 5.944Hz and then plotted as shown in Figs 6.11 and 6.12 respectively. A comparison of these amplitude values was plotted in Fig.6.13. One can see that the vertical amplitudes are much larger than the transverse amplitudes in this mode. Therefore, the mode at 5.944Hz is a vertical mode. The cross section of the bridge illustrating the modal deformations at 5.944Hz is shown in Fig.6.6. Finally, the calculated vertical frequency of 5.944Hz is in good agreement with the experimental natural frequency of 6.06Hz.

6.9 TRANSVERSE MODE SHAPE OF THE MODEL

A transverse mode shape at 7.091 Hz was obtained from the model as shown in Fig.6.7. To make sure that the mode was a primarily transverse mode, modal amplitude values in both the transverse and the vertical directions were obtained and then plotted as shown in Figs 6.14 and 6.15. A comparison of these plots is shown in Fig 6.16. From these figures, one can conclude that the mode at 7.091Hz is a transverse mode. The cross section of the bridge at 7.091Hz, illustrating the modal distortions, is shown in Fig.6.8. The calculated frequency of 7.091Hz for this mode is in reasonable agreement with the experimentally determined frequency of 6.75Hz. This indicates that applying a simple beam theory, which gave a natural frequency of 18.16Hz compared to 6.75Hz, is unacceptable. A modified simple theory will have to be developed, which will give better results.

The third mode shape of the bridge at 9.2Hz is shown in Fig.6.9. Figure 6.10 shows the cross section of the bridge in the third mode.

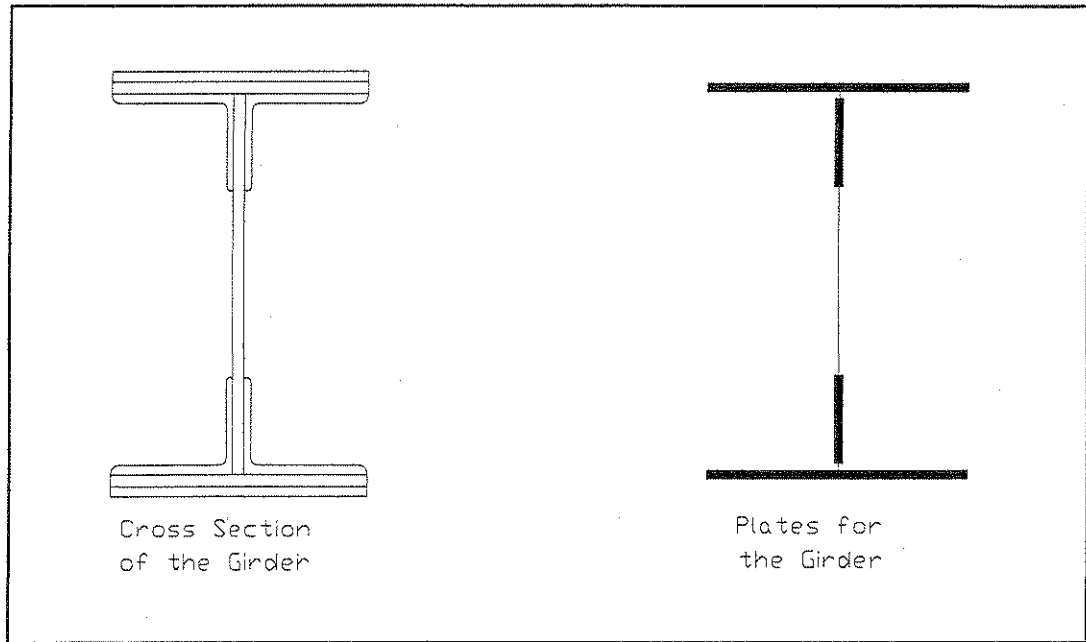


Fig 6.1: Cross Section of Main Girder with a Model of the Plates.

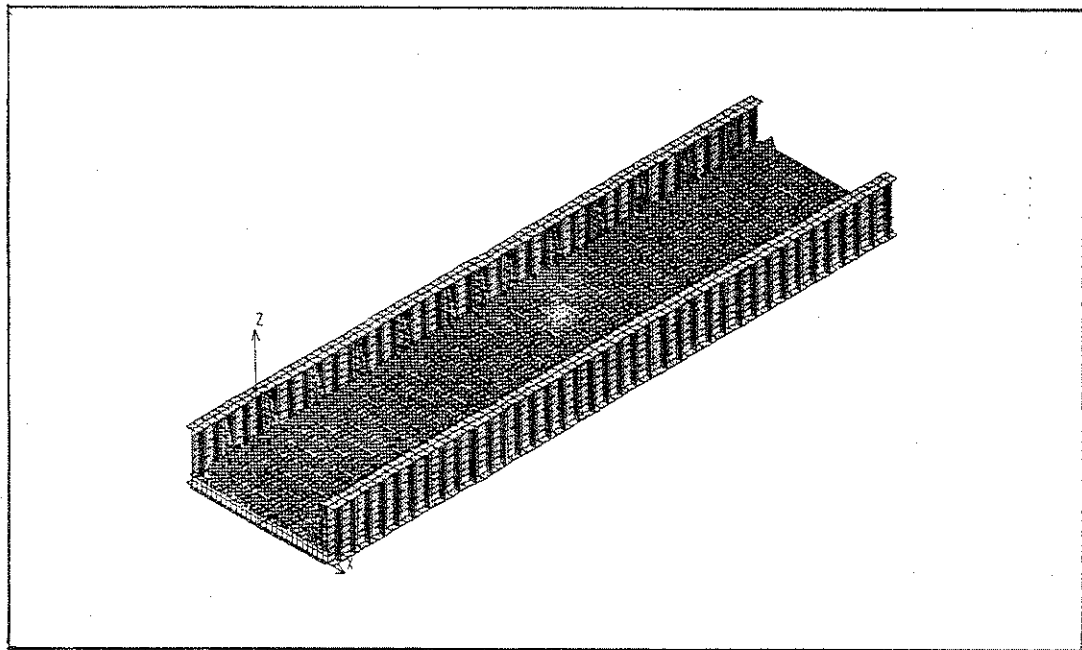


Fig 6.2: Three Dimensional Model of the Bridge.

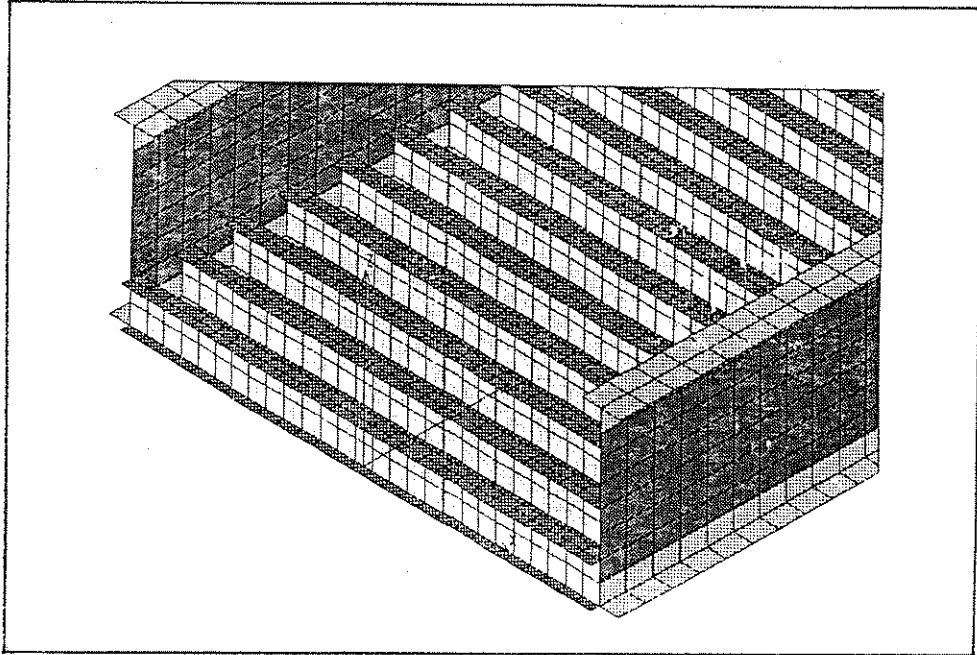


Fig 6.3: Part of the Model Showing Floor Beams Connected to the Main Girders.

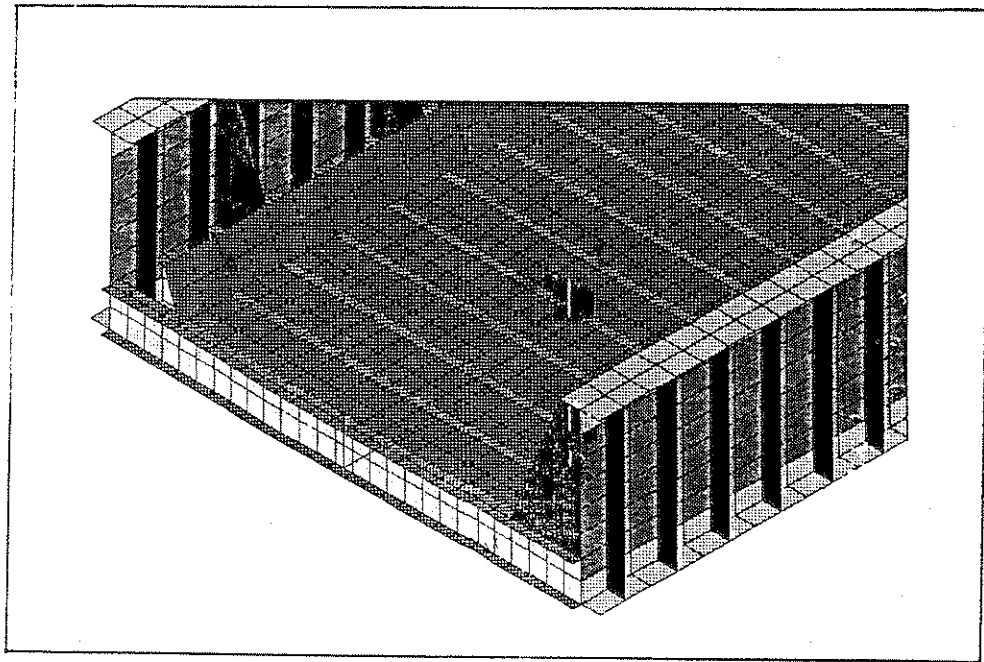


Fig 6.4: Part of the Model Showing the Brackets, Ballast Pan and Stiffeners

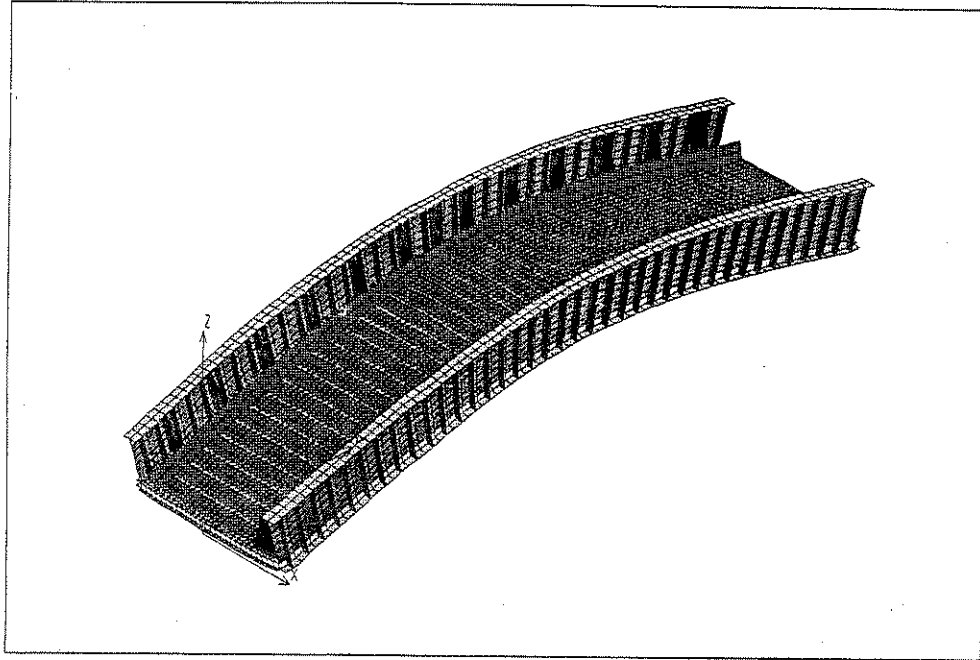


Fig 6.5: First Vertical Mode of the Model at 5.9 Hz.

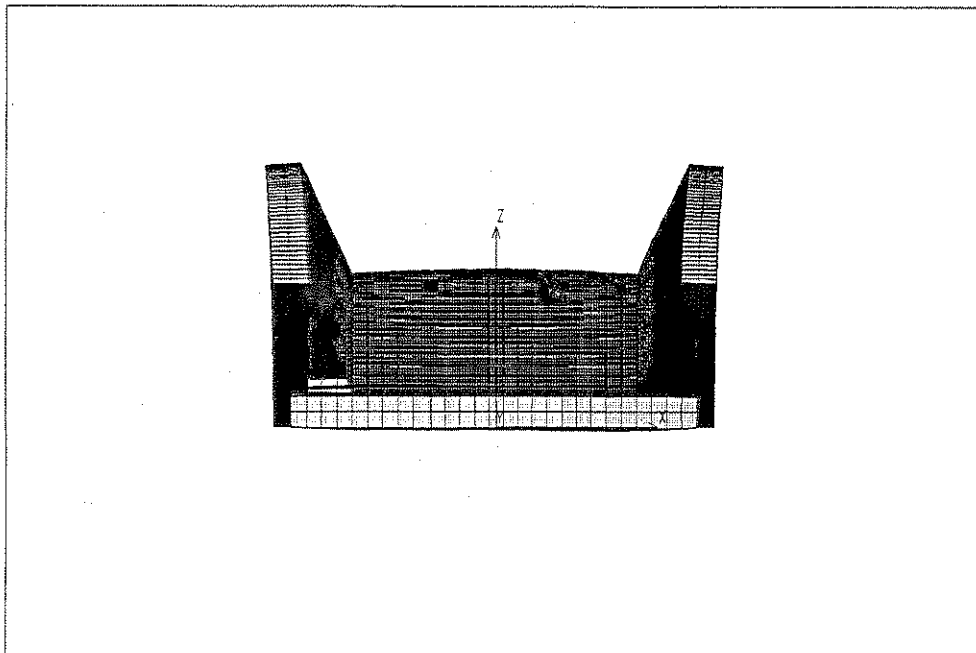


Fig 6.6: Cross Section of the Vertical Mode at 5.9 Hz.

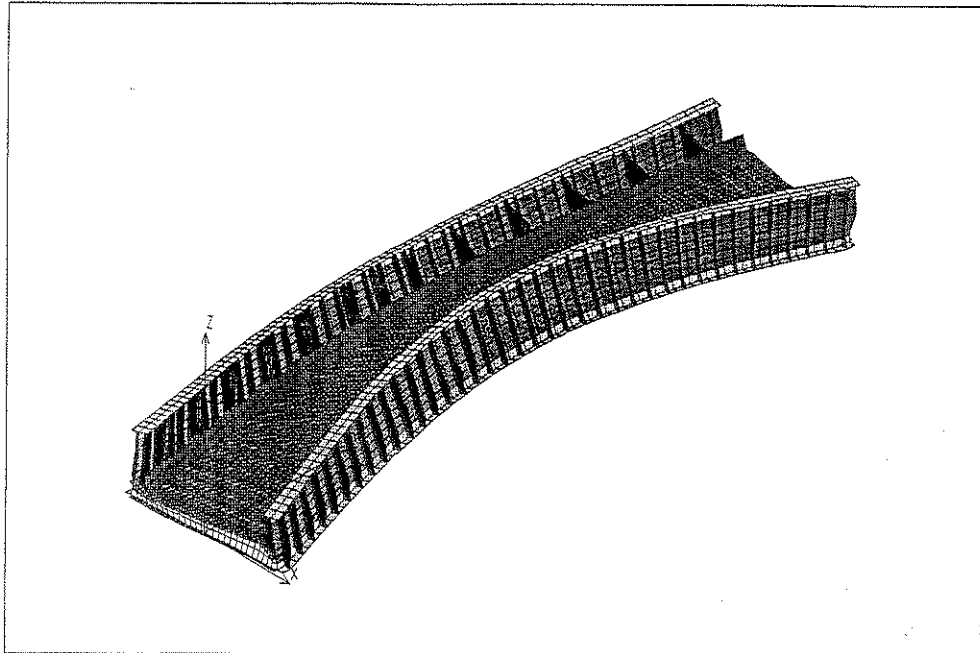


Fig 6.7: First Transverse Mode Shape of the Model at 7.0 Hz.

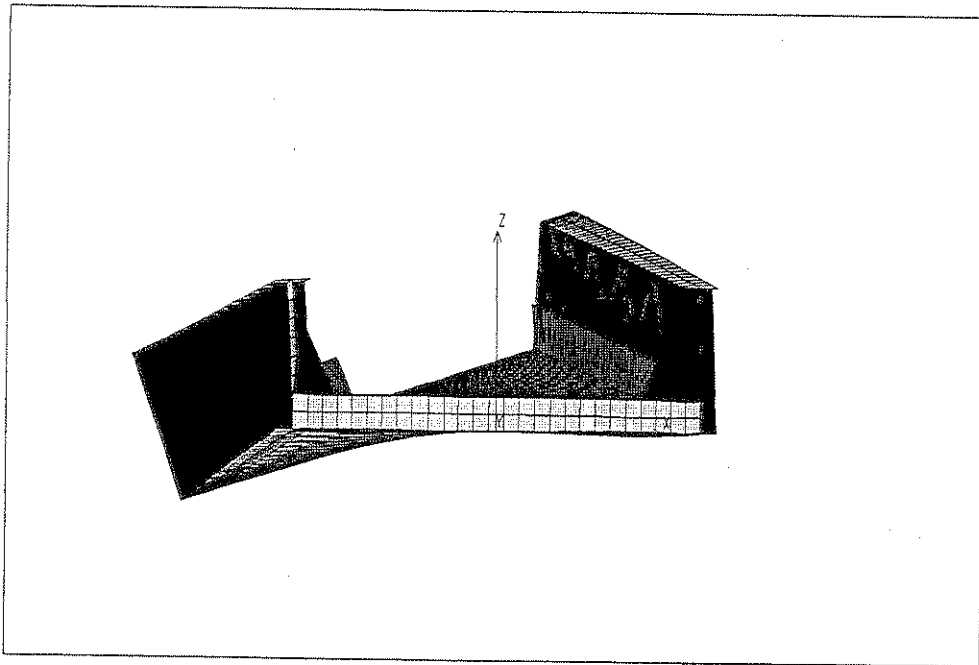


Fig 6.8: Cross Section of the Model at 7.0 Hz.

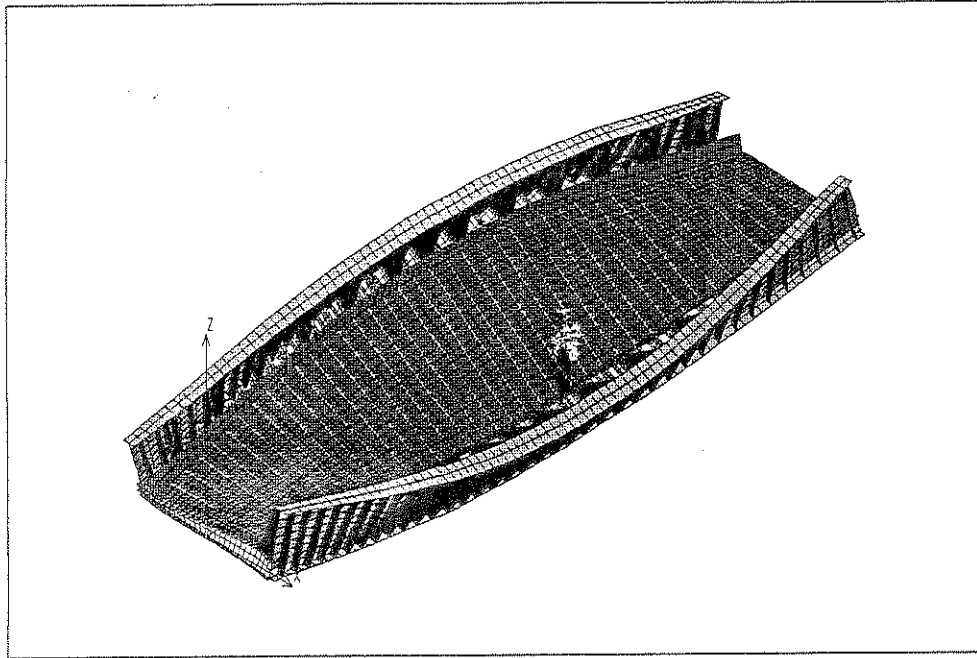


Fig 6.9: Mode Shape of the Model at 9.2 Hz.

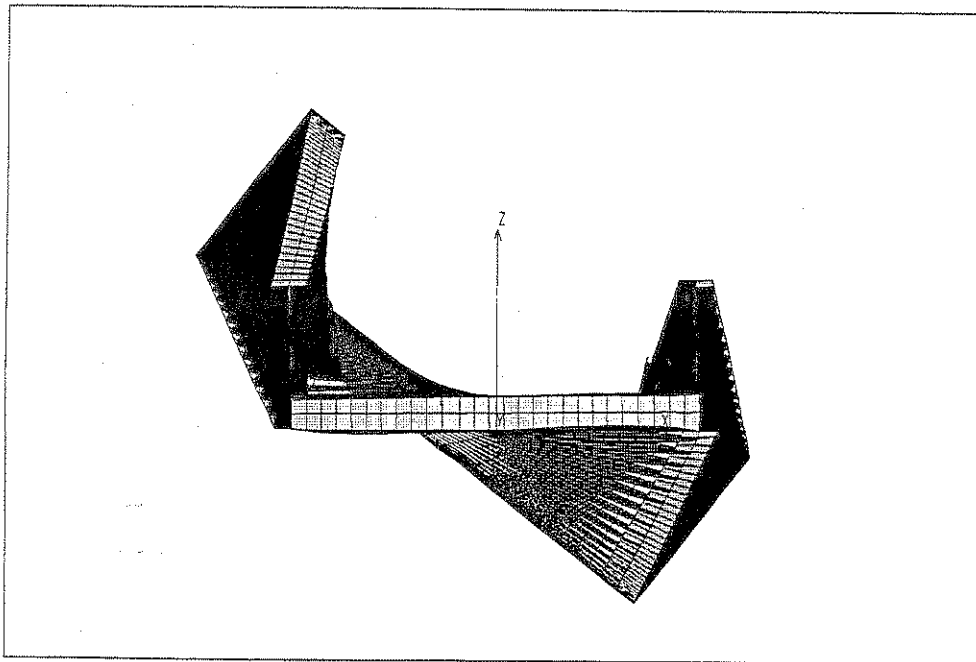


Fig 6.10: Cross Section of the Model at 9.2 Hz.

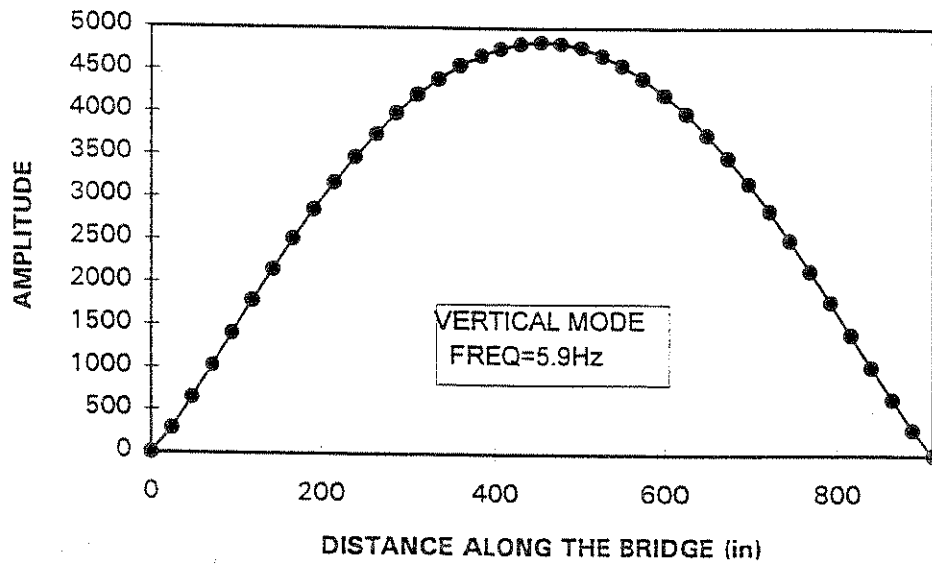


Fig.6.11: Vertical Amplitudes at 5.9 Hz

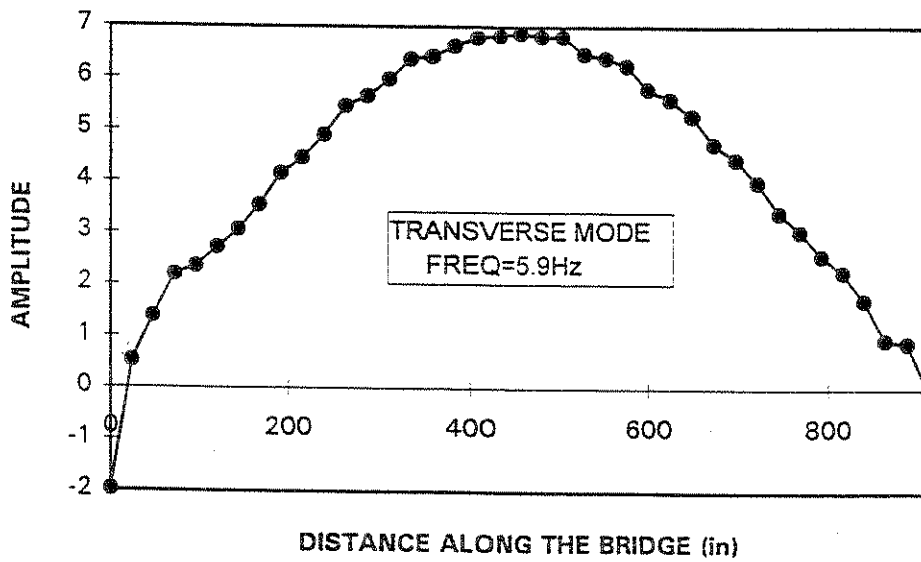


Fig.6.12: Transverse Amplitudes at 5.9 Hz

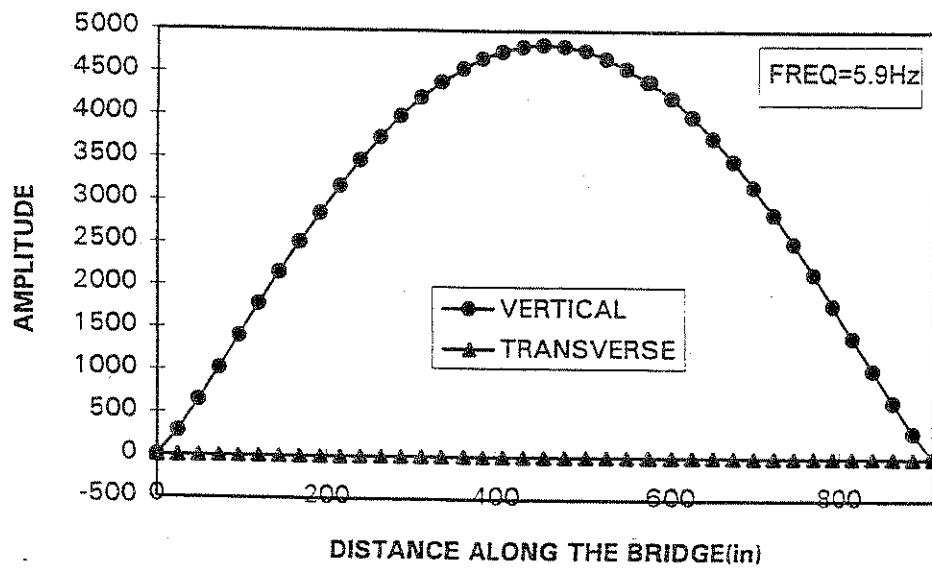


Fig.6.13: Comparison of the Amplitudes at 5.9 Hz

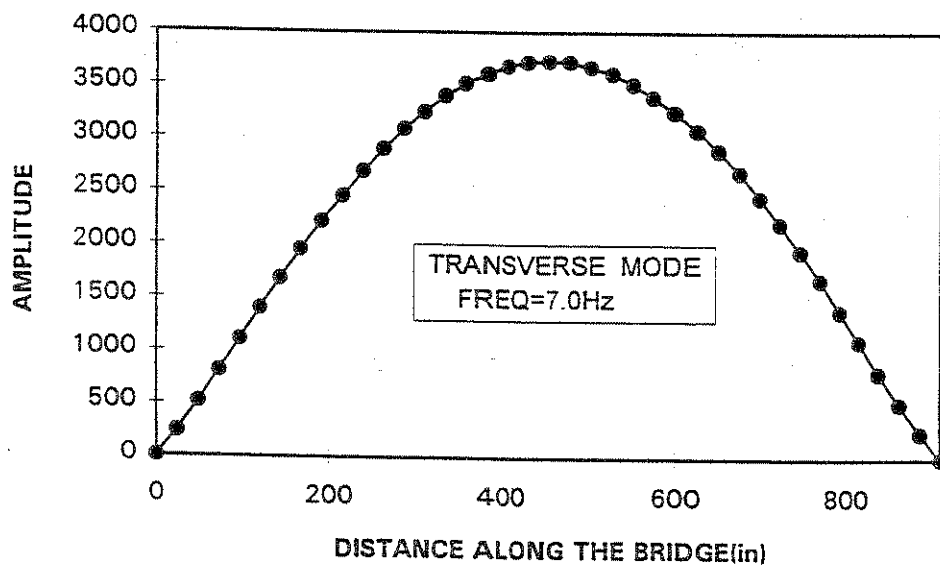


Fig.6.14: Transverse Amplitudes at 7.0 Hz

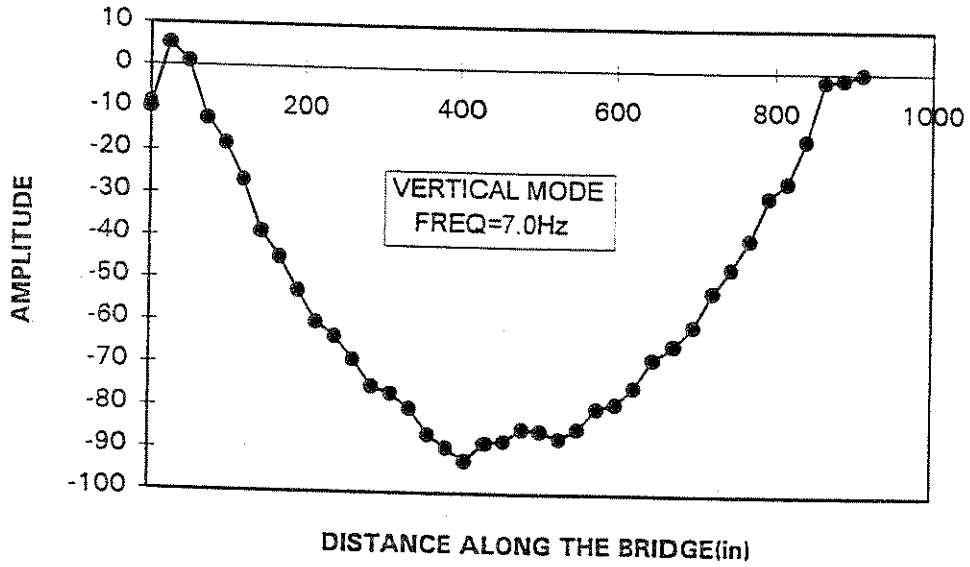


Fig.6.15: Vertical Amplitudes at 7.0 Hz

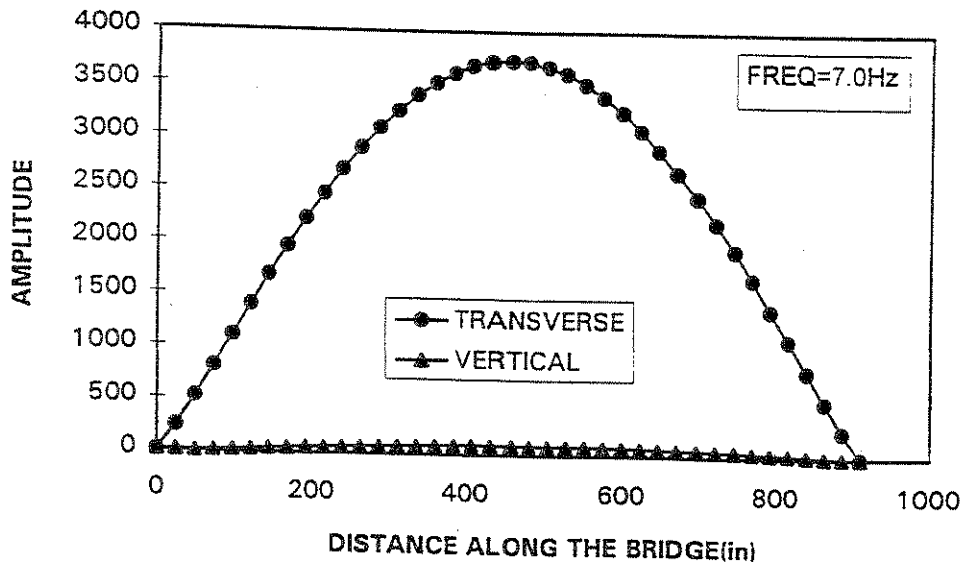


Fig.6.16: Comparison of the Amplitudes at 7.0 Hz.

CHAPTER 7

SUMMARY AND CONCLUSIONS

This report describes the full scale resonance tests and the analysis of the field data from the Strawberry Underpass, a two span, simply supported railway bridge located across the Harbor Freeway in Los Angeles, California.

The bridge measures 143' 3" long by 18' 0" wide and has a ballasted deck steel through plate girder superstructure with a concrete substructure.

The tests were performed in both the transverse and the longitudinal directions. To investigate the influence of the rails, the bridge was initially tested with the rails in place and then with the rails cut at both abutments.

The bridge was shaken using an eccentric mass dynamic shaker, which utilized a matched set of eccentric weights that rotated in opposite directions about parallel vertical shafts, producing an excitation force in a particular direction. For all of the transverse tests, the shaker was installed on the north girder in the middle of the east span. Two series of longitudinal tests were performed. In the first series of longitudinal tests, the shaker was installed on the north girder in the middle of the east span, while in the second series of tests the shaker was installed on the railroad track in the middle of the east span.

The main objective of these tests was to identify the basic dynamic properties of the structure with the rails in place and then with the rails cut.

These properties included natural frequencies, modal damping values and mode shapes in the transverse and longitudinal directions. Although initially not planned, it also became possible during the tests to identify the modal parameters of the first vertical mode. To identify these dynamic characteristics of the bridge, frequency sweeps were performed over the range of 0-20 Hz in both the transverse and the longitudinal directions first with the rails in place and then with the rails disconnected. To record the response of the structure, a series of accelerometers were mounted on the bridge as well as on the adjacent roadbed. Due to the symmetry of the bridge and the fact that it consisted of two simply supported spans, only the east span was instrumented. Broad band frequency sweeps led to the identification of peaks corresponding to natural frequencies. Detailed frequency sweeps were then performed around these frequencies and the corresponding experimental response curves for many accelerometers were produced. The experimental response curves of the first vertical mode were obtained from vertically oriented accelerometers during the second series of longitudinal tests. Computer programs were then developed, in order to fit theoretical response curves to the available experimental response curves. The parameters for the theoretical curves, which were calculated by the programs to produce the best possible fit (according to the least squares criteria) with the corresponding experimental curves, were the natural frequencies, the modal damping values and the modal amplitudes. These programs were used with many of the experimental curves, which resulted in

the estimates of the natural frequencies and the corresponding modal damping values. In addition, Fourier analysis of the experimental records was performed to plot the mode shapes of various modes.

Finally, a detailed three dimensional finite element model of the bridge was developed using the program COSMOS/M. A combination of shell and lumped mass elements was used to model the various components of the bridge. The results of this modeling were then compared to the results obtained from the resonance tests. This model will be the first step towards a more detailed system identification study in the future. Discussion of the results was provided in each chapter of this report. The most important results and conclusions are summarized below:

1. Table 7.1 summarizes all the modal parameters that were experimentally identified during the tests. These include the natural frequencies, the modal damping values of the fundamental modes in the transverse, longitudinal and vertical directions with and without the rails, as well as of the second mode in the transverse direction with the rails in place. Details and explanations for these values can be found in the corresponding chapters of the report.

Table 7.1 : Summary of the Experimental Results.

MODE	RAIL UNCUT		RAIL CUT	
	Frequency (Hz)	Damping (%)	Frequency (Hz)	Damping (%)
First Transverse Mode	4.93	2.15	4.80	2.3
Second Transverse Mode	6.75	4.50	-	-
First Longitudinal Mode	6.56	5.00	5.95	5.33
First Vertical Mode	6.06	1.65	5.55	1.45

2. Comparison of the experimental results between the uncut and disconnected rail cases in the first transverse mode, showed that when the rails were cut, a "localized" mode was triggered, which allowed a greater dissipation of energy and significant reduction of the structural acceleration response levels. The exact nature of this mode, which appears to be a variation of the primary fundamental structural mode, could not be identified from the instrumentation scheme and the procedures used in this test. However, in the event of an earthquake, the presence of this mode with a frequency close to that of the primary transverse fundamental mode of the bridge, will probably contribute to higher energy dissipation and reduction of the acceleration response. The structure will probably have an overall "equivalent" fundamental modal damping in the transverse direction of 5.5% at these response amplitudes.

3. It took a distance of about 60 feet on the roadbed for the vibrations to dissipate. This distance is close to the length of the bridge span, a fact that demonstrates a strong interaction and transmission of vibrations between the structure and the adjacent roadbed. This is most likely due to the continuity between the bridge deck and the roadbed provided by the ties, the ballast and the ballast pan. The transmitted vibrations through the soil, were enough to cause the adjacent new bridge, which was under construction at that time to vibrate. In a quick release dynamic field test in 1988, which was performed on the Meloland Road Overcrossing, a two span highway bridge, it was determined that the soil involvement was significant up to a distance of about 30 feet away from the central pier foundation [6], which is approximately 30% of the span length of that bridge. It appears that the interaction between the bridge and the adjacent roadbed is much stronger in the case of the railway bridge.

4. In all cases, cutting of the rails, resulted in lower natural frequencies, which indicates a softer system. No significant effects on the modal damping values were observed, with the exception of the modal damping of the fundamental transverse frequency. This issue was discussed in the first conclusion, as well as in chapter 4. The exact role that the rails play needs to be further investigated through analytical studies, which are currently in

progress. However, it should be mentioned that this was a ballasted bridge with the ballast pan and the ballast itself providing a significant mechanism of continuity between the deck and the roadbed. This makes the effect of the cutting of the rails alone, as it was the case in this test, on the continuity between the deck and the roadbed less significant. Perhaps the effect of cutting the rails would be more significant in open deck bridges. In the longitudinal direction however, it was observed that disconnecting the rails resulted in a sudden decrease of the vibrations which were transmitted to the roadbed. The transmission was smoother and extended away from the bridge a larger distance when the rails were uncut.

5. There was a strong coupling between transverse and torsional vibrations in the second transverse mode. Because of this, it was not possible to match the experimental results for the second transverse mode by using a simple continuous beam model. On the other hand the simple continuous beam model satisfactorily predicted the fundamental vertical frequency of the bridge. However, the second transverse frequency of the bridge predicted by the detailed three dimensional FEM model, was in close agreement with the measured experimental value. This model will be the basis of further system identification studies, which are currently under way.

REFERENCES

1. "A Guide for the Field Testing of Bridges" by American society of Civil Engineers, 1980
2. Bruce M. Douglas, Member, ASCE, Emmanuel A. Maragakis, Associate Member, ASCE, and Bhabananda Nath, " Static Deformations of Bridges from Quick- Release Dynamic Experiments", Journal of Structural Engineering, Vol. 116, No.8, August, 1990, pp. 2201-2213.
3. James Andrew Richardson, " Dynamic Response Analysis of the Dominion Road Bridge Test Data", Eng. Thesis 2426, University of Nevada, Reno.
4. Bruce M. Douglas, Charles D. Drown and Monty L. Gordon, "Experimental Dynamics of Highway Bridges" Proceedings of the second Specialty Conference on Dynamic Response of Structures: Experimentation, Observation, Prediction and Control, Jan. 1981, Atlanta, Georgia.
5. Jean-Guy and Michel Favillier, " Parameter Estimation from Full-Scale Cyclic Testing" Proceedings of the second Specialty Conference on Dynamic Response Structures: Experimentation, Observation, Prediction and Control, Jan. 1981, Atlanta, Georgia.
6. Gerard C. Pardoen, Athol J. Carr and Peter J. Moss, " Bridge Modal Identification Problems" Proceedings of the second Specialty Conference on Dynamic Response of Structures: Experimentation, Observation, Prediction and Control, Jan. 1981, Atlanta, Georgia.
7. Douglas A. Foutch, " A Study of the Vibrational Characteristics of Two Multistory Buildings" Report No. EERL 76-03, California Institute of Technology, Pasadena, California.
8. Douglas A. Foutch, George W. Housner and Paul C. Jennings, " Dynamic Responses of Six Multistory Buildings during the San Fernando Earthquake", Report No. EERL 75-02, California Institute of Technology, Pasadena, California.
9. John C. Wilson, " A Study of Seismic Response of Cable-Stayed Bridge" Proceedings on the second workshop on Bridge Engineering Research in Progress, Oct 1990, Reno, Nevada.
10. Instruction and Maintenance Manual for MK - 12.8A - 4600 Eccentric Mass Shaker System, prepared by ANCO Engineers Inc, Culver City, California.
11. Hooke R., and Jeeves T.A (1961) , "Direct Search Solution of Numerical and Statistical Problems," Journal of the Association For Computing Machinery , Vol. 8, 1961, pp. 212-229.
12. Ray W. Clough and Joseph Penzien, " Dynamics Of Structures" , second edition.
13. S.P. Timoshenko and T.N Goodier, " Theory Of Elasticity", third edition.
14. "COSMOS/M" manual , produced by Structural Research and Analysis Corporation.

APPENDIX

A.1 PROGRAM FOR FITTING A THREE VARIABLE SYSTEM

```
PROGRAM SDOF
INTEGER NTIMES
REAL A(35,2),Q,R(100),YTH(50),SUM
REAL ERR,ZEA1,FRE1,AMP1,ESUM1,ESUM2
REAL A1M,F1M,Z1M
PARAMETER(NTIMES=22)
OPEN(UNIT=12,FILE='RCH2.TXT',STATUS='OLD')
READ(12,*)((A(I,k),k=1,2),I=1,NTIMES)
PRINT*,'ENTER INITIAL F1,D1,A1'
READ*,FRE1,ZEA1,AMP1
DF=.0001
DA=0.01
DD=.0001

*****AMP1*****
100 J=0

    ESUM1=0
    ESUM2=0
110 sum=0
    J=J+1
    DO 10 I=1,NTIMES
        Q=AMP1*FRE1**2
        R(I)=((FRE1**2-A(I,1)**2)**2+(2*ZEA1*A(I,1)*FRE1)**2)**0.5
        YTH(I)=Q/R(I)
c open(unit=10,file='kum.txt',status='OLD')
c write(10,*)YTH(I)
        ERR=(A(I,2)-YTH(I))**2
        SUM=SUM+ERR
    10 CONTINUE
        IF(J.EQ.1) THEN
            ESUM1=SUM
            AMP1=AMP1+DA
            GOTO110
        ELSE
            ESUM2=SUM
        ENDIF
        print*,esum1,esum2
        IF(ESUM2.LT.ESUM1)THEN
            A1M=AMP1
300 ESUM1=ESUM2
            AMP1=AMP1+DA
            SUM=0

        DO 11 I=1,NTIMES
```

```

Q=AMP1*FRE1**2
R(I)=((FRE1**2-A(I,1)**2)**2+(2*ZEA1*A(I,1)*FRE1)**2)**0.5
YTH(I)=Q/R(I)
c  open(unit=10,file='kum.txt',status='OLD')
c  write(10,*)YTH(I)
ERR=(A(I,2)-YTH(I))**2
SUM=SUM+ERR
11 CONTINUE
ESUM2=SUM
IF(ESUM2.LT.ESUM1)THEN
A1M=AMP1
GOTO300
ELSE
A1M=AMP1-DA
ENDIF
ELSE
AMP1=AMP1-DA
500 SUM=0
AMP1=AMP1-DA
DO 12 I=1,NTIMES

Q=AMP1*FRE1**2
R(I)=((FRE1**2-A(I,1)**2)**2+(2*ZEA1*A(I,1)*FRE1)**2)**0.5
YTH(I)=Q/R(I)
c  open(unit=10,file='kum.txt',status='OLD')
c  write(10,*)YTH(I)
ERR=(A(I,2)-YTH(I))**2
SUM=SUM+ERR
12 CONTINUE
ESUM2=SUM
IF(ESUM2.LT.ESUM1)THEN
ESUM1=ESUM2
A1M=AMP1
GOTO500
ELSE
A1M=AMP1+DA
ENDIF
ENDIF
PRINT*, 'AMP1'
print*, esum1, esum2
*****FRE1***A1M*****
ESUM1=0
ESUM2=0
J=0
111 sum=0
J=J+1
DO 20 I=1,NTIMES

Q=A1M*FRE1**2
R(I)=((FRE1**2-A(I,1)**2)**2+(2*ZEA1*A(I,1)*FRE1)**2)**0.5
YTH(I)=Q/R(I)

```

```

c  open(unit=10,file='kum.txt',status='OLD')
c  write(10,*)YTH(I)
  ERR=(A(I,2)-YTH(I))**2
  SUM=SUM+ERR
20 CONTINUE
  IF(J.EQ.1) THEN
    ESUM1=SUM
    FRE1=FRE1+DF
    GOTO 111
  ELSE
    ESUM2=SUM
  ENDIF

  IF(ESUM2.LT.ESUM1) THEN
    F1M=FRE1
301 ESUM1=ESUM2
    FRE1=FRE1+DF
    SUM=0
    DO 21 I=1,NTIMES

      Q=A1M*FRE1**2
      R(I)=((FRE1**2-A(I,1)**2)**2+(2*ZEA1*A(I,1)*FRE1)**2)**0.5
      YTH(I)=Q/R(I)
c  open(unit=10,file='kum.txt',status='OLD')
c  write(10,*)YTH(I)
  ERR=(A(I,2)-YTH(I))**2
  SUM=SUM+ERR
21 CONTINUE
  ESUM2=SUM
  IF(ESUM2.LT.ESUM1) THEN
    F1M=FRE1
    GOTO301
  ELSE
    F1M=FRE1-DF
  ENDIF
  ELSE
    FRE1=FRE1-DF
501 SUM=0
    FRE1=FRE1-DF
    DO 22 I=1,NTIMES
      Q=A1M*FRE1**2
      R(I)=((FRE1**2-A(I,1)**2)**2+(2*ZEA1*A(I,1)*FRE1)**2)**0.5
      YTH(I)=Q/R(I)
c  open(unit=10,file='kum.txt',status='OLD')
c  write(10,*)YTH(I)
  ERR=(A(I,2)-YTH(I))**2
  SUM=SUM+ERR
22 CONTINUE
  ESUM2=SUM
  IF(ESUM2.LT.ESUM1) THEN
    ESUM1=ESUM2

```

```

F1M=FRE1
GOTO501
ELSE
F1M=FRE1+DF
ENDIF
ENDIF
PRINT*,'FRE1'
print*,esum1,esum2
*****ZEA1****A1M***F1M*****
J=0
ESUM1=0
ESUM2=0

112 sum=0
J=J+1
DO 30 I=1,NTIMES

Q=A1M*F1M**2
R(I)=$((F1M**2-A(I,1)**2)**2+(2*ZEA1*A(I,1)*F1M)**2)**0.5
YTH(I)=Q/R(I)
c open(unit=10,file='kum.txt',status='OLD')
c write(10,*)YTH(I)
ERR=(A(I,2)-YTH(I))**2
SUM=SUM+ERR
30 CONTINUE

IF(J.EQ.1) THEN
ESUM1=SUM
ZEA1=ZEA1+DD
GOTO112
ELSE
ESUM2=SUM
ENDIF
IF(ESUM2.LT.ESUM1)THEN
Z1M=ZEA1
302 ESUM1=ESUM2

ZEA1=ZEA1+DD
SUM=0
DO 31 I=1,NTIMES

Q=A1M*F1M**2
R(I)=$((F1M**2-A(I,1)**2)**2+(2*ZEA1*A(I,1)*F1M)**2)**0.5
YTH(I)=Q/R(I)
c open(unit=10,file='kum.txt',status='OLD')
c write(10,*)YTH(I)
ERR=(A(I,2)-YTH(I))**2
SUM=SUM+ERR
31 CONTINUE

```

```

ESUM2=SUM
IF(ESUM2.LT.ESUM1)THEN
Z1M=ZEA1
GOTO302
ELSE
Z1M=ZEA1-DD
ENDIF
ELSE
ZEA1=ZEA1-DD
502 SUM=0

ZEA1=ZEA1-DD

DO 32 I=1,NTIMES
Q=A1M*F1M**2
R(I)=((F1M**2-A(I,1)**2)**2+(2*ZEA1*A(I,1)*F1M)**2)**0.5
YTH(I)=Q/R(I)
c open(unit=10,file='kum.txt',status='OLD')
c write(10,*)YTH(I)
ERR=(A(I,2)-YTH(I))**2
SUM=SUM+ERR
32 CONTINUE
ESUM2=SUM
IF(ESUM2.LT.ESUM1)THEN
ESUM1=ESUM2
Z1M=ZEA1
GOTO502
ELSE
Z1M=ZEA1+DD
ENDIF
ENDIF
PRINT*, 'ZEA1'
print*, esum1, esum2
***A1M,F1M,Z1M*****
IF(ESUM1.LT.350)THEN
GOTO400
ELSE
AMP1=A1M
FRE1=F1M
ZEA1=Z1M
GOTO 100
ENDIF
SUM=0
400 DO 81 I=1,NTIMES
Q=A1M*F1M**2
R(I)=((F1M**2-A(I,1)**2)**2+(2*Z1M*A(I,1)*F1M)**2)**0.5
YTH(I)=Q/R(I)
open(unit=10,file='kum.txt',status='OLD')
write(10,*)YTH(I)
ERR=(A(I,2)-YTH(I))**2
SUM=SUM+ERR

```

```

81 CONTINUE
  PRINT*,E1= ',ESUM1,'E2= ',ESUM2
  PRINT*,F1= ',F1M,'Z1= ',Z1M,'A1= ',A1M
200 END

```

A.2 PROGRAM FOR FITTING A SIX VARIABLE SYSTEM

```

INTEGER NTIMES
REAL A(35,2),Q1,Q2,R1(100),R2(100),YTH(50),SUM
REAL ERR,ZEA1,ZEA2,FRE1,FRE2,AMP1,AMP2,ESUM1,ESUM2
REAL A1M,A2M,F1M,F2M,Z1M,Z2M
PARAMETER(NTIMES=14)
OPEN(UNIT=12,FILE='H5.TXT',STATUS='OLD')
READ(12,*)((A(I,k),k=1,2),I=1,NTIMES)
PRINT*, 'ENTER INITIAL F1,D1,A1,F2,D2,A2'
READ*,FRE1,ZEA1,AMP1,FRE2,ZEA2,AMP2
DF=.0001
DA=0.01
DD=.0001

*****AMP1*****
100 J=0

  ESUM1=0
  ESUM2=0
110 sum=0
  J=J+1
  DO 10 I=1,NTIMES
    Q1=AMP1*FRE1**2
    Q2=AMP2*FRE2**2
    R1(I)=((FRE1**2-A(I,1)**2)**2+(2*ZEA1*A(I,1)*FRE1)**2)**0.5
    R2(I)=((FRE2**2-A(I,1)**2)**2+(2*ZEA2*A(I,1)*FRE2)**2)**0.5
    YTH(I)=Q1/R1(I)+Q2/R2(I)
    ERR=(A(I,2)-YTH(I))**2
    SUM=SUM+ERR
10 CONTINUE
  IF(J.EQ.1) THEN
    ESUM1=SUM
    AMP1=AMP1+DA
    GOTO110
  ELSE
    ESUM2=SUM
  ENDIF
  print*,esum1,esum2
  IF(ESUM2.LT.ESUM1)THEN
    A1M=AMP1
300 ESUM1=ESUM2
    AMP1=AMP1+DA

```

```

SUM=0
DO 11 I=1,NTIMES
Q1=AMP1*FRE1**2
Q2=AMP2*FRE2**2
R1(I)=((FRE1**2-A(I,1)**2)**2+(2*ZEA1*A(I,1)*FRE1)**2)**0.5
R2(I)=((FRE2**2-A(I,1)**2)**2+(2*ZEA2*A(I,1)*FRE2)**2)**0.5
YTH(I)=Q1/R1(I)+Q2/R2(I)
ERR=(A(I,2)-YTH(I))**2
SUM=SUM+ERR
11 CONTINUE
ESUM2=SUM
IF(ESUM2.LT.ESUM1)THEN
A1M=AMP1
GOTO300
ELSE
A1M=AMP1-DA
ENDIF
ELSE
AMP1=AMP1-DA
500 SUM=0
AMP1=AMP1-DA
DO 12 I=1,NTIMES
Q1=AMP1*FRE1**2
Q2=AMP2*FRE2**2
R1(I)=((FRE1**2-A(I,1)**2)**2+(2*ZEA1*A(I,1)*FRE1)**2)**0.5
R2(I)=((FRE2**2-A(I,1)**2)**2+(2*ZEA2*A(I,1)*FRE2)**2)**0.5
YTH(I)=Q1/R1(I)+Q2/R2(I)
ERR=(A(I,2)-YTH(I))**2
SUM=SUM+ERR
12 CONTINUE
ESUM2=SUM
IF(ESUM2.LT.ESUM1)THEN
ESUM1=ESUM2
A1M=AMP1
GOTO500
ELSE
A1M=AMP1+DA
ENDIF
ENDIF
PRINT*, 'AMP1'
print*, esum1, esum2
*****FRE1***A1M*****

```

```

ESUM1=0
ESUM2=0
J=0
111 sum=0
J=J+1
DO 20 I=1,NTIMES
Q1=A1M*FRE1**2

```

```

Q2=AMP2*FRE2**2
R1(I)=((FRE1**2-A(I,1)**2)**2+(2*ZEA1*A(I,1)*FRE1)**2)**0.5
R2(I)=((FRE2**2-A(I,1)**2)**2+(2*ZEA2*A(I,1)*FRE2)**2)**0.5
YTH(I)=Q1/R1(I)+Q2/R2(I)
ERR=(A(I,2)-YTH(I))**2
SUM=SUM+ERR
20 CONTINUE
IF(J.EQ.1) THEN
ESUM1=SUM
FRE1=FRE1+DF
GOTO 111
ELSE
ESUM2=SUM
ENDIF

IF(ESUM2.LT.ESUM1) THEN
F1M=FRE1
301 ESUM1=ESUM2
FRE1=FRE1+DF
SUM=0
DO 21 I=1,NTIMES
Q1=A1M*FRE1**2
Q2=AMP2*FRE2**2
R1(I)=((FRE1**2-A(I,1)**2)**2+(2*ZEA1*A(I,1)*FRE1)**2)**0.5
R2(I)=((FRE2**2-A(I,1)**2)**2+(2*ZEA2*A(I,1)*FRE2)**2)**0.5
YTH(I)=Q1/R1(I)+Q2/R2(I)
ERR=(A(I,2)-YTH(I))**2
SUM=SUM+ERR
21 CONTINUE
ESUM2=SUM
IF(ESUM2.LT.ESUM1) THEN
F1M=FRE1
GOTO301
ELSE
F1M=FRE1-DF
ENDIF
ELSE
FRE1=FRE1-DF
501 SUM=0
FRE1=FRE1-DF
DO 22 I=1,NTIMES
Q1=A1M*FRE1**2
Q2=AMP2*FRE2**2
R1(I)=((FRE1**2-A(I,1)**2)**2+(2*ZEA1*A(I,1)*FRE1)**2)**0.5
R2(I)=((FRE2**2-A(I,1)**2)**2+(2*ZEA2*A(I,1)*FRE2)**2)**0.5
YTH(I)=Q1/R1(I)+Q2/R2(I)
ERR=(A(I,2)-YTH(I))**2
SUM=SUM+ERR
22 CONTINUE
ESUM2=SUM
IF(ESUM2.LT.ESUM1) THEN

```

```

ESUM1=ESUM2
F1M=FRE1
GOTO501
ELSE
F1M=FRE1+DF
ENDIF
ENDIF
PRINT*, 'FRE1'
print*, esum1, esum2
*****ZEA1****A1M***F1M*****
J=0
ESUM1=0
ESUM2=0

112 sum=0
J=J+1
DO 30 I=1,NTIMES
Q1=A1M*F1M**2
Q2=AMP2*FRE2**2
R1(I)=((F1M**2-A(I,1)**2)**2+(2*ZEA1*A(I,1)*F1M)**2)**0.5
R2(I)=((FRE2**2-A(I,1)**2)**2+(2*ZEA2*A(I,1)*FRE2)**2)**0.5
YTH(I)=Q1/R1(I)+Q2/R2(I)
ERR=(A(I,2)-YTH(I))**2
SUM=SUM+ERR
30 CONTINUE

IF(J.EQ.1) THEN
ESUM1=SUM
ZEA1=ZEA1+DD
GOTO112
ELSE
ESUM2=SUM
ENDIF
IF(ESUM2.LT.ESUM1)THEN
Z1M=ZEA1
302 ESUM1=ESUM2

ZEA1=ZEA1+DD
SUM=0
DO 31 I=1,NTIMES
Q1=A1M*F1M**2
Q2=AMP2*FRE2**2
R1(I)=((F1M**2-A(I,1)**2)**2+(2*ZEA1*A(I,1)*F1M)**2)**0.5
R2(I)=((FRE2**2-A(I,1)**2)**2+(2*ZEA2*A(I,1)*FRE2)**2)**0.5
YTH(I)=Q1/R1(I)+Q2/R2(I)
ERR=(A(I,2)-YTH(I))**2
SUM=SUM+ERR
31 CONTINUE
ESUM2=SUM
IF(ESUM2.LT.ESUM1)THEN
Z1M=ZEA1

```

```

GOTO302
ELSE
Z1M=ZEA1-DD
ENDIF
ELSE
ZEA1=ZEA1-DD
502 SUM=0

ZEA1=ZEA1-DD

DO 32 I=1,NTIMES
Q1=A1M*F1M**2
Q2=AMP2*FRE2**2
R1(I)=((F1M**2-A(I,1)**2)**2+(2*ZEA1*A(I,1)*F1M)**2)**0.5
R2(I)=((FRE2**2-A(I,1)**2)**2+(2*ZEA2*A(I,1)*FRE2)**2)**0.5
YTH(I)=Q1/R1(I)+Q2/R2(I)
ERR=(A(I,2)-YTH(I))**2
SUM=SUM+ERR
32 CONTINUE
ESUM2=SUM

IF(ESUM2.LT.ESUM1)THEN
ESUM1=ESUM2
Z1M=ZEA1
GOTO502
ELSE
Z1M=ZEA1+DD
ENDIF
ENDIF
PRINT*,ZEA1'
print*,esum1,esum2
*****AMP2****A1M,F1M,Z1M*****
J=0

ESUM1=0
ESUM2=0

113 sum=0
J=J+1
DO 40 I=1,NTIMES
Q1=A1M*F1M**2
Q2=AMP2*FRE2**2
R1(I)=((F1M**2-A(I,1)**2)**2+(2*Z1M*A(I,1)*F1M)**2)**0.5
R2(I)=((FRE2**2-A(I,1)**2)**2+(2*ZEA2*A(I,1)*FRE2)**2)**0.5
YTH(I)=Q1/R1(I)+Q2/R2(I)
ERR=(A(I,2)-YTH(I))**2
SUM=SUM+ERR
40 CONTINUE
IF(J.EQ.1) THEN
ESUM1=SUM
AMP2=AMP2+DA

```

```

GOTO113
ELSE
ESUM2=SUM
ENDIF
IF(ESUM2.LT.ESUM1) THEN
A2M=AMP2
303 ESUM1=ESUM2
AMP2=AMP2+DA
SUM=0
DO 41 I=1,NTIMES
Q1=A1M*F1M**2
Q2=AMP2*FRE2**2
R1(I)=((F1M**2-A(I,1)**2)**2+(2*Z1M*A(I,1)*F1M)**2)**0.5
R2(I)=((FRE2**2-A(I,1)**2)**2+(2*ZEA2*A(I,1)*FRE2)**2)**0.5
YTH(I)=Q1/R1(I)+Q2/R2(I)
ERR=(A(I,2)-YTH(I))**2
SUM=SUM+ERR
41 CONTINUE
ESUM2=SUM
IF(ESUM2.LT.ESUM1)THEN
A2M=AMP2
GOTO303
ELSE
A2M=AMP2-DA
ENDIF
ELSE
AMP2=AMP2-DA
503 SUM=0
AMP2=AMP2-DA

DO 42 I=1,NTIMES
Q1=A1M*F1M**2
Q2=AMP2*FRE2**2
R1(I)=((F1M**2-A(I,1)**2)**2+(2*Z1M*A(I,1)*F1M)**2)**0.5
R2(I)=((FRE2**2-A(I,1)**2)**2+(2*ZEA2*A(I,1)*FRE2)**2)**0.5
YTH(I)=Q1/R1(I)+Q2/R2(I)
ERR=(A(I,2)-YTH(I))**2
SUM=SUM+ERR
42 CONTINUE
ESUM2=SUM

IF(ESUM2.LT.ESUM1) THEN
ESUM1=ESUM2
A2M=AMP2
GOTO503
ELSE
A2M=AMP2+DA
ENDIF
ENDIF
PRINT*, 'AMP2'

```

```

print*,esum1,esum2
*****FRE2*****A1M,F1M,Z1M,A2M*****
J=0

ESUM1=0
ESUM2=0

114 sum=0
J=J+1
DO 50 I=1,NTIMES
Q1=A1M*F1M**2
Q2=A2M*FRE2**2
R1(I)=((F1M**2-A(I,1)**2)**2+(2*Z1M*A(I,1)*F1M)**2)**0.5
R2(I)=((FRE2**2-A(I,1)**2)**2+(2*ZEA2*A(I,1)*FRE2)**2)**0.5
YTH(I)=Q1/R1(I)+Q2/R2(I)
ERR=(A(I,2)-YTH(I))**2
SUM=SUM+ERR
50 CONTINUE

IF(J.EQ.1) THEN
ESUM1=SUM
FRE2=FRE2+DF
GOTO114
ELSE
ESUM2=SUM
ENDIF
IF(ESUM2.LT.ESUM1)THEN
F2M=FRE2
304 ESUM1=ESUM2

FRE2=FRE2+DF
SUM=0
DO 51 I=1,NTIMES
Q1=A1M*F1M**2
Q2=A2M*FRE2**2
R1(I)=((F1M**2-A(I,1)**2)**2+(2*Z1M*A(I,1)*F1M)**2)**0.5
R2(I)=((FRE2**2-A(I,1)**2)**2+(2*ZEA2*A(I,1)*FRE2)**2)**0.5
YTH(I)=Q1/R1(I)+Q2/R2(I)
ERR=(A(I,2)-YTH(I))**2
SUM=SUM+ERR
51 CONTINUE
ESUM2=SUM
IF(ESUM2.LT.ESUM1)THEN
F2M=FRE2
GOTO304
ELSE
F2M=FRE2-DF
ENDIF
ELSE
FRE2=FRE2-DF

```

```

504 SUM=0
* PRINT*,ESUM(J),J
FRE2=FRE2-DF
DO 52 I=1,NTIMES
Q1=A1M*F1M**2
Q2=A2M*FRE2**2
R1(I)=((F1M**2-A(I,1)**2)**2+(2*Z1M*A(I,1)*F1M)**2)**0.5
R2(I)=((FRE2**2-A(I,1)**2)**2+(2*ZEA2*A(I,1)*FRE2)**2)**0.5
YTH(I)=Q1/R1(I)+Q2/R2(I)
ERR=(A(I,2)-YTH(I))**2
SUM=SUM+ERR
52 CONTINUE
ESUM2=SUM

IF(ESUM2.LT.ESUM1)THEN
ESUM1=ESUM2
F2M=FRE2
GOTO504
ELSE
F2M=FRE2+DF
ENDIF
ENDIF
PRINT*,'FRE2'
print*,esum1,esum2
*****ZEA2*****A1M,F1M,Z1M,A2M,F2M*****
J=0

ESUM1=0
ESUM2=0

115 sum=0
J=J+1
DO 60 I=1,NTIMES
Q1=A1M*F1M**2
Q2=A2M*F2M**2
R1(I)=((F1M**2-A(I,1)**2)**2+(2*Z1M*A(I,1)*F1M)**2)**0.5
R2(I)=((F2M**2-A(I,1)**2)**2+(2*ZEA2*A(I,1)*F2M)**2)**0.5
YTH(I)=Q1/R1(I)+Q2/R2(I)
ERR=(A(I,2)-YTH(I))**2
SUM=SUM+ERR
60 CONTINUE

IF(J.EQ.1) THEN
ESUM1=SUM
ZEA2=ZEA2+DD
GOTO115
ELSE
ESUM2=SUM
ENDIF
IF(ESUM2.LT.ESUM1)THEN
Z2M=ZEA2

```

305 ESUM1=ESUM2

ZEA2=ZEA2+DD

SUM=0

DO 61 I=1,NTIMES

Q1=A1M*F1M**2

Q2=A2M*F2M**2

R1(I)=((F1M**2-A(I,1)**2)**2+(2*Z1M*A(I,1)*F1M)**2)**0.5

R2(I)=((F2M**2-A(I,1)**2)**2+(2*ZEA2*A(I,1)*F2M)**2)**0.5

YTH(I)=Q1/R1(I)+Q2/R2(I)

ERR=(A(I,2)-YTH(I))**2

SUM=SUM+ERR

61 CONTINUE

ESUM2=SUM

IF(ESUM2.LT.ESUM1)THEN

Z2M=ZEA2

GOTO305

ELSE

Z2M=ZEA2-DD

ENDIF

ELSE

ZEA2=ZEA2-DD

505 SUM=0

* PRINT*,ESUM(J),J

ZEA2=ZEA2-DD

DO 62 I=1,NTIMES

Q1=A1M*F1M**2

Q2=A2M*F2M**2

R1(I)=((F1M**2-A(I,1)**2)**2+(2*Z1M*A(I,1)*F1M)**2)**0.5

R2(I)=((F2M**2-A(I,1)**2)**2+(2*ZEA2*A(I,1)*F2M)**2)**0.5

YTH(I)=Q1/R1(I)+Q2/R2(I)

ERR=(A(I,2)-YTH(I))**2

SUM=SUM+ERR

62 CONTINUE

ESUM2=SUM

IF(ESUM2.LT.ESUM1)THEN

ESUM1=ESUM2

Z2M=ZEA2

GOTO505

ELSE

Z2M=ZEA2+DD

ENDIF

ENDIF

PRINT*,ZEA2'

print*,esum1,esum2

*****A1M,F1M,Z1M,A2M,F2M,Z2M*****

IF(ESUM1.LT.30)THEN

GOTO400

```

ELSE
AMP1=A1M
FRE1=F1M
ZEA1=Z1M
AMP2=A2M
FRE2=F2M
ZEA2=Z2M
GOTO 100
ENDIF
400 DO 81 I=1,NTIMES
Q1=A1M*F1M**2
Q2=A2M*F2M**2
R1(I)=((F1M**2-A(I,1)**2)**2+(2*Z1M*A(I,1)*F1M)**2)**0.5
R2(I)=((F2M**2-A(I,1)**2)**2+(2*Z2M*A(I,1)*F2M)**2)**0.5
YTH(I)=Q1/R1(I)+Q2/R2(I)
OPEN(UNIT=11,FILE='OUT.TXT',STATUS='old')
WRITE(11,*)YTH(I)
ERR=(A(I,2)-YTH(I))**2
SUM=SUM+ERR
81 CONTINUE
PRINT*,E1= 'ESUM1',E2= 'ESUM2
PRINT*,F1= 'F1M',Z1= 'Z1M',A1= 'A1M',F2= 'F2M,
-Z2= 'Z2M,
-A2= 'A2M
200 END

```

A.3 PROGRAM FOR FITTING A NINE VARIABLE SYSTEM

```

INTEGER NTIMES
REAL A(35,2),Q1,Q2,R1(100),R2(100),R3(100),YTH(50),SUM
REAL ERR,ZEA1,ZEA2,FRE1,FRE2,AMP1,AMP2,ESUM1,ESUM2
REAL FRE3,AMP3,ZEA3
REAL A1M,A2M,F1M,F2M,Z1M,Z2M,A3M,F3M,Z3M
PARAMETER(NTIMES=25)
OPEN(UNIT=12,FILE='CH2RL.TXT',STATUS='OLD')
READ(12,*)((A(I,k),k=1,2),I=1,NTIMES)
PRINT*,ENTER INITIAL F1,D1,A1,F2,D2,A2,F3,D3,A3'
READ*,FRE1,ZEA1,AMP1,FRE2,ZEA2,AMP2,FRE3,ZEA3,AMP3
DF=.0001
DA=0.01
DD=.0001

*****AMP1*****
100 J=0

ESUM1=0
ESUM2=0
110 sum=0

```

```

J=J+1
DO 10 I=1,NTIMES
Q1=AMP1*FRE1**2
Q2=AMP2*FRE2**2
Q3=AMP3*FRE3**2
R1(I)=((FRE1**2-A(I,1)**2)**2+(2*ZEA1*A(I,1)*FRE1)**2)**0.5
R2(I)=((FRE2**2-A(I,1)**2)**2+(2*ZEA2*A(I,1)*FRE2)**2)**0.5
R3(I)=((FRE3**2-A(I,1)**2)**2+(2*ZEA3*A(I,1)*FRE3)**2)**0.5
YTH(I)=Q1/R1(I)+Q2/R2(I)+Q3/R3(I)
ERR=(A(I,2)-YTH(I))**2
SUM=SUM+ERR
10 CONTINUE
IF(J.EQ.1) THEN
ESUM1=SUM
AMP1=AMP1+DA
GOTO110
ELSE
ESUM2=SUM
ENDIF
print*,esum1,esum2
IF(ESUM2.LT.ESUM1)THEN
A1M=AMP1
300 ESUM1=ESUM2
AMP1=AMP1+DA
SUM=0
DO 11 I=1,NTIMES
Q1=AMP1*FRE1**2
Q2=AMP2*FRE2**2
Q3=AMP3*FRE3**2
R1(I)=((FRE1**2-A(I,1)**2)**2+(2*ZEA1*A(I,1)*FRE1)**2)**0.5
R2(I)=((FRE2**2-A(I,1)**2)**2+(2*ZEA2*A(I,1)*FRE2)**2)**0.5
R3(I)=((FRE3**2-A(I,1)**2)**2+(2*ZEA3*A(I,1)*FRE3)**2)**0.5
YTH(I)=Q1/R1(I)+Q2/R2(I)+Q3/R3(I)
ERR=(A(I,2)-YTH(I))**2
SUM=SUM+ERR
11 CONTINUE
ESUM2=SUM
IF(ESUM2.LT.ESUM1)THEN
A1M=AMP1
GOTO300
ELSE
A1M=AMP1-DA
ENDIF
ELSE
AMP1=AMP1-DA
500 SUM=0
AMP1=AMP1-DA
DO 12 I=1,NTIMES
Q1=AMP1*FRE1**2
Q2=AMP2*FRE2**2
Q3=AMP3*FRE3**2

```

```

R1(I)=((FRE1**2-A(I,1)**2)**2+(2*ZEA1*A(I,1)*FRE1)**2)**0.5
R2(I)=((FRE2**2-A(I,1)**2)**2+(2*ZEA2*A(I,1)*FRE2)**2)**0.5
R3(I)=((FRE3**2-A(I,1)**2)**2+(2*ZEA3*A(I,1)*FRE3)**2)**0.5
YTH(I)=Q1/R1(I)+Q2/R2(I)+Q3/R3(I)
ERR=(A(I,2)-YTH(I))**2
SUM=SUM+ERR
12 CONTINUE
ESUM2=SUM
IF(ESUM2.LT.ESUM1)THEN
ESUM1=ESUM2
A1M=AMP1
GOTO500
ELSE
A1M=AMP1+DA
ENDIF
ENDIF
PRINT*, 'AMP1'
print*, esum1, esum2
*****FRE1**A1M*****

```

```

ESUM1=0
ESUM2=0
J=0
111 sum=0
J=J+1
DO 20 I=1,NTIMES
Q1=A1M*FRE1**2
Q2=AMP2*FRE2**2
Q3=AMP3*FRE3**2
R1(I)=((FRE1**2-A(I,1)**2)**2+(2*ZEA1*A(I,1)*FRE1)**2)**0.5
R2(I)=((FRE2**2-A(I,1)**2)**2+(2*ZEA2*A(I,1)*FRE2)**2)**0.5
R3(I)=((FRE3**2-A(I,1)**2)**2+(2*ZEA3*A(I,1)*FRE3)**2)**0.5
YTH(I)=Q1/R1(I)+Q2/R2(I)+Q3/R3(I)
ERR=(A(I,2)-YTH(I))**2
SUM=SUM+ERR
20 CONTINUE
IF(J.EQ.1) THEN
ESUM1=SUM
FRE1=FRE1+DF
GOTO 111
ELSE
ESUM2=SUM
ENDIF

IF(ESUM2.LT.ESUM1) THEN
F1M=FRE1
301 ESUM1=ESUM2
FRE1=FRE1+DF
SUM=0
DO 21 I=1,NTIMES

```

```

Q1=A1M*FRE1**2
Q2=AMP2*FRE2**2
Q3=AMP3*FRE3**2
R1(I)=((FRE1**2-A(I,1)**2)**2+(2*ZEA1*A(I,1)*FRE1)**2)**0.5
R2(I)=((FRE2**2-A(I,1)**2)**2+(2*ZEA2*A(I,1)*FRE2)**2)**0.5
R3(I)=((FRE3**2-A(I,1)**2)**2+(2*ZEA3*A(I,1)*FRE3)**2)**0.5
YTH(I)=Q1/R1(I)+Q2/R2(I)+Q3/R3(I)
ERR=(A(I,2)-YTH(I))**2
SUM=SUM+ERR
21 CONTINUE
ESUM2=SUM
IF(ESUM2.LT.ESUM1) THEN
F1M=FRE1
GOTO301
ELSE
F1M=FRE1-DF
ENDIF
ELSE
FRE1=FRE1-DF
501 SUM=0
FRE1=FRE1-DF
DO 22 I=1,NTIMES
Q1=A1M*FRE1**2
Q2=AMP2*FRE2**2
Q3=AMP3*FRE3**2
R1(I)=((FRE1**2-A(I,1)**2)**2+(2*ZEA1*A(I,1)*FRE1)**2)**0.5
R2(I)=((FRE2**2-A(I,1)**2)**2+(2*ZEA2*A(I,1)*FRE2)**2)**0.5
R3(I)=((FRE3**2-A(I,1)**2)**2+(2*ZEA3*A(I,1)*FRE3)**2)**0.5
YTH(I)=Q1/R1(I)+Q2/R2(I)+Q3/R3(I)
ERR=(A(I,2)-YTH(I))**2
SUM=SUM+ERR
22 CONTINUE
ESUM2=SUM
IF(ESUM2.LT.ESUM1) THEN
ESUM1=ESUM2
F1M=FRE1
GOTO501
ELSE
F1M=FRE1+DF
ENDIF
ENDIF
PRINT*, 'FRE1'
print*, esum1, esum2
*****ZEA1****A1M***F1M*****
J=0
ESUM1=0
ESUM2=0

112 sum=0
J=J+1
DO 30 I=1,NTIMES

```

```

Q1=A1M*F1M**2
Q2=AMP2*FRE2**2
Q3=AMP3*FRE3**2
R1(I)=((F1M**2-A(I,1)**2)**2+(2*ZEA1*A(I,1)*F1M)**2)**0.5
R2(I)=((FRE2**2-A(I,1)**2)**2+(2*ZEA2*A(I,1)*FRE2)**2)**0.5
R3(I)=((FRE3**2-A(I,1)**2)**2+(2*ZEA3*A(I,1)*FRE3)**2)**0.5
YTH(I)=Q1/R1(I)+Q2/R2(I)+Q3/R3(I)
ERR=(A(I,2)-YTH(I))**2
SUM=SUM+ERR
30 CONTINUE

```

```

IF(J.EQ.1) THEN
ESUM1=SUM
ZEA1=ZEA1+DD
GOTO112
ELSE
ESUM2=SUM
ENDIF
IF(ESUM2.LT.ESUM1)THEN
Z1M=ZEA1
302 ESUM1=ESUM2

```

```

ZEA1=ZEA1+DD
SUM=0
DO 31 I=1,NTIMES
Q1=A1M*F1M**2
Q2=AMP2*FRE2**2
Q3=AMP3*FRE3**2
R1(I)=((F1M**2-A(I,1)**2)**2+(2*ZEA1*A(I,1)*F1M)**2)**0.5
R2(I)=((FRE2**2-A(I,1)**2)**2+(2*ZEA2*A(I,1)*FRE2)**2)**0.5
R3(I)=((FRE3**2-A(I,1)**2)**2+(2*ZEA3*A(I,1)*FRE3)**2)**0.5
YTH(I)=Q1/R1(I)+Q2/R2(I)+Q3/R3(I)
ERR=(A(I,2)-YTH(I))**2
SUM=SUM+ERR

```

```

31 CONTINUE
ESUM2=SUM
IF(ESUM2.LT.ESUM1)THEN
Z1M=ZEA1
GOTO302
ELSE
Z1M=ZEA1-DD
ENDIF
ELSE
ZEA1=ZEA1-DD

```

```

502 SUM=0

```

```

ZEA1=ZEA1-DD

```

```

DO 32 I=1,NTIMES
Q1=A1M*F1M**2
Q2=AMP2*FRE2**2

```

```

Q3=AMP3*FRE3**2
R1(I)=((F1M**2-A(I,1)**2)**2+(2*ZEA1*A(I,1)*F1M)**2)**0.5
R2(I)=((FRE2**2-A(I,1)**2)**2+(2*ZEA2*A(I,1)*FRE2)**2)**0.5
R3(I)=((FRE3**2-A(I,1)**2)**2+(2*ZEA3*A(I,1)*FRE3)**2)**0.5
YTH(I)=Q1/R1(I)+Q2/R2(I)+Q3/R3(I)
ERR=(A(I,2)-YTH(I))**2
SUM=SUM+ERR
32 CONTINUE
ESUM2=SUM

IF(ESUM2.LT.ESUM1)THEN
ESUM1=ESUM2
Z1M=ZEA1
GOTO502
ELSE
Z1M=ZEA1+DD
ENDIF
ENDIF
PRINT*, 'ZEA1'
print*, esum1, esum2
*****AMP2***A1M,F1M,Z1M*****
J=0

ESUM1=0
ESUM2=0

113 sum=0
J=J+1
DO 40 I=1,NTIMES
Q1=A1M*F1M**2
Q2=AMP2*FRE2**2
Q3=AMP3*FRE3**2
R1(I)=((F1M**2-A(I,1)**2)**2+(2*Z1M*A(I,1)*F1M)**2)**0.5
R2(I)=((FRE2**2-A(I,1)**2)**2+(2*ZEA2*A(I,1)*FRE2)**2)**0.5
R3(I)=((FRE3**2-A(I,1)**2)**2+(2*ZEA3*A(I,1)*FRE3)**2)**0.5
YTH(I)=Q1/R1(I)+Q2/R2(I)+Q3/R3(I)
ERR=(A(I,2)-YTH(I))**2
SUM=SUM+ERR
40 CONTINUE
IF(J.EQ.1) THEN
ESUM1=SUM
AMP2=AMP2+DA
GOTO113
ELSE
ESUM2=SUM
ENDIF
IF(ESUM2.LT.ESUM1) THEN
A2M=AMP2
303 ESUM1=ESUM2
AMP2=AMP2+DA
SUM=0

```

```

DO 41 I=1,NTIMES
Q1=A1M*F1M**2
Q2=AMP2*FRE2**2
Q3=AMP3*FRE3**2
R1(I)=((F1M**2-A(I,1)**2)**2+(2*Z1M*A(I,1)*F1M)**2)**0.5
R2(I)=((FRE2**2-A(I,1)**2)**2+(2*ZEA2*A(I,1)*FRE2)**2)**0.5
R3(I)=((FRE3**2-A(I,1)**2)**2+(2*ZEA3*A(I,1)*FRE3)**2)**0.5
YTH(I)=Q1/R1(I)+Q2/R2(I)+Q3/R3(I)
ERR=(A(I,2)-YTH(I))**2
SUM=SUM+ERR
41 CONTINUE
ESUM2=SUM
IF(ESUM2.LT.ESUM1)THEN
A2M=AMP2
GOTO303
ELSE
A2M=AMP2-DA
ENDIF
ELSE
AMP2=AMP2-DA
503 SUM=0
AMP2=AMP2-DA

DO 42 I=1,NTIMES
Q1=A1M*F1M**2
Q2=AMP2*FRE2**2
Q3=AMP3*FRE3**2
R1(I)=((F1M**2-A(I,1)**2)**2+(2*Z1M*A(I,1)*F1M)**2)**0.5
R2(I)=((FRE2**2-A(I,1)**2)**2+(2*ZEA2*A(I,1)*FRE2)**2)**0.5
R3(I)=((FRE3**2-A(I,1)**2)**2+(2*ZEA3*A(I,1)*FRE3)**2)**0.5
YTH(I)=Q1/R1(I)+Q2/R2(I)+Q3/R3(I)
ERR=(A(I,2)-YTH(I))**2
SUM=SUM+ERR
42 CONTINUE
ESUM2=SUM

IF(ESUM2.LT.ESUM1) THEN
ESUM1=ESUM2
A2M=AMP2
GOTO503
ELSE
A2M=AMP2+DA
ENDIF
ENDIF
PRINT*, 'AMP2'
print*, esum1, esum2
*****FRE2*****A1M,F1M,Z1M,A2M*****
J=0

ESUM1=0

```

```

ESUM2=0

114 sum=0
  J=J+1
  DO 50 I=1,NTIMES
    Q1=A1M*F1M**2
    Q2=A2M*FRE2**2
    Q3=AMP3*FRE3**2
    R1(I)=((F1M**2-A(I,1)**2)**2+(2*Z1M*A(I,1)*F1M)**2)**0.5
    R2(I)=((FRE2**2-A(I,1)**2)**2+(2*ZEA2*A(I,1)*FRE2)**2)**0.5
    R3(I)=((FRE3**2-A(I,1)**2)**2+(2*ZEA3*A(I,1)*FRE3)**2)**0.5
    YTH(I)=Q1/R1(I)+Q2/R2(I)+Q3/R3(I)
    ERR=(A(I,2)-YTH(I))**2
    SUM=SUM+ERR
  50 CONTINUE

  IF(J.EQ.1) THEN
    ESUM1=SUM
    FRE2=FRE2+DF
    GOTO114
  ELSE
    ESUM2=SUM
  ENDIF
  IF(ESUM2.LT.ESUM1)THEN
    F2M=FRE2
304 ESUM1=ESUM2

    FRE2=FRE2+DF
    SUM=0
    DO 51 I=1,NTIMES
      Q1=A1M*F1M**2
      Q2=A2M*FRE2**2
      Q3=AMP3*FRE3**2
      R1(I)=((F1M**2-A(I,1)**2)**2+(2*Z1M*A(I,1)*F1M)**2)**0.5
      R2(I)=((FRE2**2-A(I,1)**2)**2+(2*ZEA2*A(I,1)*FRE2)**2)**0.5
      R3(I)=((FRE3**2-A(I,1)**2)**2+(2*ZEA3*A(I,1)*FRE3)**2)**0.5
      YTH(I)=Q1/R1(I)+Q2/R2(I)+Q3/R3(I)
      ERR=(A(I,2)-YTH(I))**2
      SUM=SUM+ERR
    51 CONTINUE
    ESUM2=SUM
    IF(ESUM2.LT.ESUM1)THEN
      F2M=FRE2
      GOTO304
    ELSE
      F2M=FRE2-DF
    ENDIF
    ELSE
      FRE2=FRE2-DF
504 SUM=0

```

```

* PRINT*,ESUM(J),J
FRE2=FRE2-DF
DO 52 I=1,NTIMES
Q1=A1M*F1M**2
Q2=A2M*FRE2**2
Q3=AMP3*FRE3**2
R1(I)=((F1M**2-A(I,1)**2)**2+(2*Z1M*A(I,1)*F1M)**2)**0.5
R2(I)=((FRE2**2-A(I,1)**2)**2+(2*ZEA2*A(I,1)*FRE2)**2)**0.5
R3(I)=((FRE3**2-A(I,1)**2)**2+(2*ZEA3*A(I,1)*FRE3)**2)**0.5
YTH(I)=Q1/R1(I)+Q2/R2(I)+Q3/R3(I)
ERR=(A(I,2)-YTH(I))**2
SUM=SUM+ERR
52 CONTINUE
ESUM2=SUM

IF(ESUM2.LT.ESUM1)THEN
ESUM1=ESUM2
F2M=FRE2
GOTO504
ELSE
F2M=FRE2+DF
ENDIF
ENDIF
PRINT*, 'FRE2'
print*,esum1,esum2
*****ZEA2*****A1M,F1M,Z1M,A2M,F2M*****

J=0

ESUM1=0
ESUM2=0

115 sum=0
J=J+1
DO 60 I=1,NTIMES
Q1=A1M*F1M**2
Q2=A2M*F2M**2
Q3=AMP3*FRE3**2
R1(I)=((F1M**2-A(I,1)**2)**2+(2*Z1M*A(I,1)*F1M)**2)**0.5
R2(I)=((F2M**2-A(I,1)**2)**2+(2*ZEA2*A(I,1)*F2M)**2)**0.5
R3(I)=((FRE3**2-A(I,1)**2)**2+(2*ZEA3*A(I,1)*FRE3)**2)**0.5
YTH(I)=Q1/R1(I)+Q2/R2(I)+Q3/R3(I)
ERR=(A(I,2)-YTH(I))**2
SUM=SUM+ERR
60 CONTINUE

IF(J.EQ.1) THEN
ESUM1=SUM
ZEA2=ZEA2+DD
GOTO115
ELSE
ESUM2=SUM

```

```

ENDIF
IF(ESUM2.LT.ESUM1)THEN
Z2M=ZEA2
305 ESUM1=ESUM2

```

```

ZEA2=ZEA2+DD
SUM=0
DO 61 I=1,NTIMES
Q1=A1M*F1M**2
Q2=A2M*F2M**2
Q3=AMP3*FRE3**2
R1(I)=((F1M**2-A(I,1)**2)**2+(2*Z1M*A(I,1)*F1M)**2)**0.5
R2(I)=((F2M**2-A(I,1)**2)**2+(2*ZEA2*A(I,1)*F2M)**2)**0.5
R3(I)=((FRE3**2-A(I,1)**2)**2+(2*ZEA3*A(I,1)*FRE3)**2)**0.5
YTH(I)=Q1/R1(I)+Q2/R2(I)+Q3/R3(I)
ERR=(A(I,2)-YTH(I))**2
SUM=SUM+ERR

```

```

61 CONTINUE
ESUM2=SUM
IF(ESUM2.LT.ESUM1)THEN
Z2M=ZEA2
GOTO305
ELSE
Z2M=ZEA2-DD
ENDIF
ELSE

```

```

ZEA2=ZEA2-DD
505 SUM=0
* PRINT*,ESUM(J),J
ZEA2=ZEA2-DD

```

```

DO 62 I=1,NTIMES
Q1=A1M*F1M**2
Q2=A2M*F2M**2
Q3=AMP3*FRE3**2
R1(I)=((F1M**2-A(I,1)**2)**2+(2*Z1M*A(I,1)*F1M)**2)**0.5
R2(I)=((F2M**2-A(I,1)**2)**2+(2*ZEA2*A(I,1)*F2M)**2)**0.5
R3(I)=((FRE3**2-A(I,1)**2)**2+(2*ZEA3*A(I,1)*FRE3)**2)**0.5
YTH(I)=Q1/R1(I)+Q2/R2(I)+Q3/R3(I)
ERR=(A(I,2)-YTH(I))**2
SUM=SUM+ERR

```

```

62 CONTINUE
ESUM2=SUM

```

```

IF(ESUM2.LT.ESUM1)THEN
ESUM1=ESUM2
Z2M=ZEA2
GOTO505
ELSE
Z2M=ZEA2+DD

```

```

ENDIF
ENDIF
PRINT*, 'ZEA2'
print*, esum1, esum2
*****AMP3*****A1M, F1M, Z1M, A2M, F2M, Z2M*****
J=0

ESUM1=0
ESUM2=0

116 sum=0
J=J+1
DO 70 I=1, NTIMES
Q1=A1M*F1M**2
Q2=A2M*F2M**2
Q3=AMP3*FRE3**2
R1(I)=[(F1M**2-A(I,1)**2)**2+(2*Z1M*A(I,1)*F1M)**2]**0.5
R2(I)=[(F2M**2-A(I,1)**2)**2+(2*Z2M*A(I,1)*F2M)**2]**0.5
R3(I)=[(FRE3**2-A(I,1)**2)**2+(2*ZEA3*A(I,1)*FRE3)**2]**0.5
YTH(I)=Q1/R1(I)+Q2/R2(I)+Q3/R3(I)
ERR=(A(I,2)-YTH(I))**2
SUM=SUM+ERR
70 CONTINUE
IF(J.EQ.1) THEN
ESUM1=SUM
AMP3=AMP3+DA
GOTO116
ELSE
ESUM2=SUM
ENDIF
IF(ESUM2.LT.ESUM1) THEN
A3M=AMP3
306 ESUM1=ESUM2
AMP3=AMP3+DA
SUM=0
DO 71 I=1, NTIMES
Q1=A1M*F1M**2
Q2=A2M*F2M**2
Q3=AMP3*FRE3**2
R1(I)=[(F1M**2-A(I,1)**2)**2+(2*Z1M*A(I,1)*F1M)**2]**0.5
R2(I)=[(F2M**2-A(I,1)**2)**2+(2*Z2M*A(I,1)*F2M)**2]**0.5
R3(I)=[(FRE3**2-A(I,1)**2)**2+(2*ZEA3*A(I,1)*FRE3)**2]**0.5
YTH(I)=Q1/R1(I)+Q2/R2(I)+Q3/R3(I)
ERR=(A(I,2)-YTH(I))**2
SUM=SUM+ERR
71 CONTINUE
ESUM2=SUM
IF(ESUM2.LT.ESUM1) THEN
A3M=AMP3
GOTO306
ELSE

```

```

A3M=AMP3-DA
ENDIF
ELSE

AMP3=AMP3-DA
506 SUM=0
AMP3=AMP3-DA

DO 72 I=1,NTIMES
Q1=A1M*F1M**2
Q2=A2M*F2M**2
Q3=AMP3*FRE3**2
R1(I)=$((F1M**2-A(I,1)**2)**2+(2*Z1M*A(I,1)*F1M)**2)**0.5
R2(I)=$((F2M**2-A(I,1)**2)**2+(2*Z2M*A(I,1)*F2M)**2)**0.5
R3(I)=$((FRE3**2-A(I,1)**2)**2+(2*ZEA3*A(I,1)*FRE3)**2)**0.5
YTH(I)=Q1/R1(I)+Q2/R2(I)+Q3/R3(I)
ERR=(A(I,2)-YTH(I))**2
SUM=SUM+ERR
72 CONTINUE
ESUM2=SUM

IF(ESUM2.LT.ESUM1) THEN
ESUM1=ESUM2
A3M=AMP3
GOTO506
ELSE
A3M=AMP3+DA
ENDIF
ENDIF
PRINT*, 'AMP3'
print*, esum1, esum2
*****FRE3*****A1M, F1M, Z1M, A2M, F2M, Z2M, A3M*****
J=0

ESUM1=0
ESUM2=0

117 sum=0
J=J+1
DO 80 I=1,NTIMES
Q1=A1M*F1M**2
Q2=A2M*F2M**2
Q3=A3M*FRE3**2
R1(I)=$((F1M**2-A(I,1)**2)**2+(2*Z1M*A(I,1)*F1M)**2)**0.5
R2(I)=$((F2M**2-A(I,1)**2)**2+(2*Z2M*A(I,1)*F2M)**2)**0.5
R3(I)=$((FRE3**2-A(I,1)**2)**2+(2*ZEA3*A(I,1)*FRE3)**2)**0.5
YTH(I)=Q1/R1(I)+Q2/R2(I)+Q3/R3(I)
ERR=(A(I,2)-YTH(I))**2
SUM=SUM+ERR
80 CONTINUE

```

```

IF(J.EQ.1) THEN
ESUM1=SUM
FRE3=FRE3+DF
GOTO117
ELSE
ESUM2=SUM
ENDIF
IF(ESUM2.LT.ESUM1)THEN
F3M=FRE3
307 ESUM1=ESUM2

FRE3=FRE3+DF
SUM=0
DO 81 I=1,NTIMES
Q1=A1M*F1M**2
Q2=A2M*F2M**2
Q3=A3M*FRE3**2
R1(I)=((F1M**2-A(I,1)**2)**2+(2*Z1M*A(I,1)*F1M)**2)**0.5
R2(I)=((F2M**2-A(I,1)**2)**2+(2*Z2M*A(I,1)*F2M)**2)**0.5
R3(I)=((FRE3**2-A(I,1)**2)**2+(2*ZEA3*A(I,1)*FRE3)**2)**0.5
YTH(I)=Q1/R1(I)+Q2/R2(I)+Q3/R3(I)
ERR=(A(I,2)-YTH(I))**2
SUM=SUM+ERR
81 CONTINUE
ESUM2=SUM
IF(ESUM2.LT.ESUM1)THEN
F3M=FRE3
GOTO307
ELSE
F3M=FRE3-DF
ENDIF
ELSE
FRE3=FRE3-DF
507 SUM=0
* PRINT*,ESUM(J),J
FRE3=FRE3-DF
DO 82 I=1,NTIMES
Q1=A1M*F1M**2
Q2=A2M*F2M**2
Q3=A3M*FRE3**2
R1(I)=((F1M**2-A(I,1)**2)**2+(2*Z1M*A(I,1)*F1M)**2)**0.5
R2(I)=((F2M**2-A(I,1)**2)**2+(2*Z2M*A(I,1)*F2M)**2)**0.5
R3(I)=((FRE3**2-A(I,1)**2)**2+(2*ZEA3*A(I,1)*FRE3)**2)**0.5
YTH(I)=Q1/R1(I)+Q2/R2(I)+Q3/R3(I)
ERR=(A(I,2)-YTH(I))**2
SUM=SUM+ERR
82 CONTINUE
ESUM2=SUM

IF(ESUM2.LT.ESUM1)THEN

```

```

ESUM1=ESUM2
F3M=FRE3
GOTO507
ELSE
F3M=FRE3+DF
ENDIF
ENDIF
PRINT*, 'FRE3'
print*, esum1, esum2
*****ZEA3*****A1M, F1M, Z1M, A2M, F2M, Z2M, A3M, F3M*****
J=0

ESUM1=0
ESUM2=0

118 sum=0
J=J+1
DO 90 I=1, NTIMES
Q1=A1M*F1M**2
Q2=A2M*F2M**2
Q3=A3M*F3M**2
R1(I)=((F1M**2-A(I,1)**2)**2+(2*Z1M*A(I,1)*F1M)**2)**0.5
R2(I)=((F2M**2-A(I,1)**2)**2+(2*Z2M*A(I,1)*F2M)**2)**0.5
R3(I)=((F3M**2-A(I,1)**2)**2+(2*ZEA3*A(I,1)*F3M)**2)**0.5
YTH(I)=Q1/R1(I)+Q2/R2(I)+Q3/R3(I)
ERR=(A(I,2)-YTH(I))**2
SUM=SUM+ERR
90 CONTINUE

IF(J.EQ.1) THEN
ESUM1=SUM
ZEA3=ZEA3+DD
GOTO118
ELSE
ESUM2=SUM
ENDIF
IF(ESUM2.LT.ESUM1) THEN
Z3M=ZEA3
308 ESUM1=ESUM2

ZEA3=ZEA3+DD
SUM=0
DO 91 I=1, NTIMES
Q1=A1M*F1M**2
Q2=A2M*F2M**2
Q3=A3M*F3M**2
R1(I)=((F1M**2-A(I,1)**2)**2+(2*Z1M*A(I,1)*F1M)**2)**0.5
R2(I)=((F2M**2-A(I,1)**2)**2+(2*Z2M*A(I,1)*F2M)**2)**0.5
R3(I)=((F3M**2-A(I,1)**2)**2+(2*ZEA3*A(I,1)*F3M)**2)**0.5
YTH(I)=Q1/R1(I)+Q2/R2(I)+Q3/R3(I)
ERR=(A(I,2)-YTH(I))**2

```

```

SUM=SUM+ERR
91 CONTINUE
ESUM2=SUM
IF(ESUM2.LT.ESUM1)THEN
Z3M=ZEA3
GOTO308
ELSE
Z3M=ZEA3-DD
ENDIF
ELSE
ZEA3=ZEA3-DD
508 SUM=0
* PRINT*,ESUM(J),J
ZEA3=ZEA3-DD

DO 92 I=1,NTIMES
Q1=A1M*F1M**2
Q2=A2M*F2M**2
Q3=A3M*F3M**2
R1(I)=$((F1M**2-A(I,1)**2)**2+(2*Z1M*A(I,1)*F1M)**2)**0.5
R2(I)=$((F2M**2-A(I,1)**2)**2+(2*Z2M*A(I,1)*F2M)**2)**0.5
R3(I)=$((F3M**2-A(I,1)**2)**2+(2*ZEA3*A(I,1)*F3M)**2)**0.5
YTH(I)=Q1/R1(I)+Q2/R2(I)+Q3/R3(I)
ERR=(A(I,2)-YTH(I))**2
SUM=SUM+ERR
92 CONTINUE
ESUM2=SUM

IF(ESUM2.LT.ESUM1)THEN
ESUM1=ESUM2
Z3M=ZEA3
GOTO508
ELSE
Z3M=ZEA3+DD
ENDIF
ENDIF
PRINT*, 'ZEA3'
print*, esum1, esum2
*****A1M,F1M,Z1M,A2M,F2M,Z2M,A3M,F3M,Z3M*****
IF(ESUM1.LT.10000)THEN
GOTO400
ELSE
AMP1=A1M
FRE1=F1M
ZEA1=Z1M
AMP2=A2M
FRE2=F2M
ZEA2=Z2M
AMP3=A3M
FRE3=F3M

```

```

ZEA3=Z3M
GOTO 100
ENDIF
SUM=0
400 DO 401 I=1,NTIMES
  Q1=A1M*F1M**2
  Q2=A2M*F2M**2
  Q3=A3M*F3M**2
  R1(I)=((F1M**2-A(I,1)**2)**2+(2*Z1M*A(I,1)*F1M)**2)**0.5
  R2(I)=((F2M**2-A(I,1)**2)**2+(2*Z2M*A(I,1)*F2M)**2)**0.5
  R3(I)=((F3M**2-A(I,1)**2)**2+(2*Z3M*A(I,1)*F3M)**2)**0.5
  YTH(I)=Q1/R1(I)+Q2/R2(I)+Q3/R3(I)
  OPEN(UNIT=11,FILE='OUT.TXT',STATUS='old')
  WRITE(11,*)YTH(I)
  ERR=(A(I,2)-YTH(I))**2
  SUM=SUM+ERR
401 CONTINUE
  PRINT*,E1= ',ESUM1,E2= ',ESUM2
  PRINT*,F1=',F1M,Z1=',Z1M,A1=',A1M,F2=',F2M,
  -Z2=',Z2M,A2=',A2M,F3=',F3M,Z3=',Z3M,A3=',A3M
200 END

```

LIST OF CCEER PUBLICATIONS

Report No.	Publication
CCEER-84-1	Saiidi, M., and R. Lawver, "User's Manual for LZAK-C64, A Computer Program to Implement the Q-Model on Commodore 64," Civil Engineering Department, Report No. CCEER-84-1, University of Nevada, Reno, January 1984.
CCEER-84-1 Reprint	Douglas, B., Norris, G., Saiidi, M., Dodd, L., Richardson, J. and Reid, W., "Simple Bridge Models for Earthquakes and Test Data," Civil Engineering Department, Report No. CCEER-84-1 Reprint, University of Nevada, Reno, January 1984.
CCEER-84-2	Douglas, B. and T. Iwasaki, "Proceedings of the First USA-Japan Bridge Engineering Workshop," held at the Public Works Research Institute, Tsukuba, Japan, Civil Engineering Department, Report No. CCEER-84-2, University of Nevada, Reno, April 1984.
CCEER-84-3	Saiidi, M., J. Hart, and B. Douglas, "Inelastic Static and Dynamic Analysis of Short R/C Bridges Subjected to Lateral Loads," Civil Engineering Department, Report No. CCEER-84-3, University of Nevada, Reno, July 1984.
CCEER-84-4	Douglas, B., "A Proposed Plan for a National Bridge Engineering Laboratory," Civil Engineering Department, Report No. CCEER-84-4, University of Nevada, Reno, December 1984.
CCEER-85-1	Norris, G. and P. Abdollaholiae, "Laterally Loaded Pile Response: Studies with the Strain Wedge Model," Civil Engineering Department, Report No. CCEER-85-1, University of Nevada, Reno, April 1985.
CCEER-86-1	Ghusn, G. and M. Saiidi, "A Simple Hysteretic Element for Biaxial Bending of R/C in NEABS-86," Civil Engineering Department, Report No. CCEER-86-1, University of Nevada, Reno, July 1986.
CCEER-86-2	Saiidi, M., R. Lawver, and J. Hart, "User's Manual of ISADAB and SIBA, Computer Programs for Nonlinear Transverse Analysis of Highway Bridges Subjected to Static and Dynamic Lateral Loads," Civil Engineering Department, Report No. CCEER-86-2, University of Nevada, Reno, September 1986.
CCEER-87-1	Siddharthan, R., "Dynamic Effective Stress Response of Surface and Embedded Footings in Sand," Civil engineering Department, Report No. CCEER-86-2, University of Nevada, Reno, June 1987.
CCEER-87-2	Norris, G. and R. Sack, "Lateral and Rotational Stiffness of Pile Groups for Seismic Analysis of Highway Bridges," Civil Engineering Department, Report No. CCEER-87-2, University of Nevada, Reno, June 1987.
CCEER-88-1	Orie, J. and M. Saiidi, "A Preliminary Study of One-Way Reinforced Concrete Pier Hinges Subjected to Shear and Flexure," Civil Engineering Department, Report No. CCEER-88-1, University of Nevada, Reno, January 1988.
CCEER-88-2	Orie, D., M. Saiidi, and B. Douglas, "A Micro-CAD System for Seismic Design of Regular Highway Bridges," Civil Engineering Department, Report No. CCEER-88-2, University of Nevada, Reno, June 1988.
CCEER-88-3	Orie, D. and M. Saiidi, "User's Manual for Micro-SARB, a Microcomputer Program for Seismic Analysis of Regular Highway Bridges," Civil Engineering Department, Report No. CCEER-88-3, University of Nevada, Reno, October 1988.

- CCEER-89-1 Douglas, B., M. Saiidi, R. Hayes, and G. Holcomb, "A Comprehensive Study of the Loads and Pressures Exerted on Wall Forms by the Placement of Concrete," Civil Engineering Department, Report No. CCEER-89-1, University of Nevada, Reno, February 1989.
- CCEER-89-2 Richardson, J. and B. Douglas, "Dynamic Response Analysis of the Dominion Road Bridge Test Data," Civil Engineering Department, Report No. CCEER-89-2, University of Nevada, Reno, March 1989.
- CCEER-89-2 Vrontinos, S., M. Saiidi, and B. Douglas, "A Simple Model to Predict the Ultimate Response of R/C Beams with Concrete Overlays," Civil Engineering Department, Report NO. CCEER-89-2, University of Nevada, Reno, June 1989.
- CCEER-89-3 Ebrahimpour, A. and P. Jagadish, "Statistical Modeling of Bridge Traffic Loads - A Case Study," Civil Engineering Department, Report No. CCEER-89-3, University of Nevada, Reno, December 1989.
- CCEER-89-4 Shields, J. and M. Saiidi, "Direct Field Measurement of Prestress Losses in Box Girder Bridges," Civil Engineering Department, Report No. CCEER-89-4, University of Nevada, Reno, December 1989.
- CCEER-90-1 Saiidi, M., E. Maragakis, G. Ghosn, Y. Jiang, and D. Schwartz, "Survey and Evaluation of Nevada's Transportation Infrastructure, Task 7.2 - Highway Bridges, Final Report," Civil Engineering Department, Report No. CCEER 90-1, University of Nevada, Reno, October 1990.
- CCEER-90-2 Abdel-Ghaffar, S., E. Maragakis, and M. Saiidi, "Analysis of the Response of Reinforced Concrete Structures During the Whittier Earthquake 1987," Civil Engineering Department, Report No. CCEER 90-2, University of Nevada, Reno, October 1990.
- CCEER-91-1 Saiidi, M., E. Hwang, E. Maragakis, and B. Douglas, "Dynamic Testing and the Analysis of the Flamingo Road Interchange," Civil Engineering Department, Report No. CCEER-91-1, University of Nevada, Reno, February 1991.
- CCEER-91-2 Norris, G., R. Siddharthan, Z. Zafir, S. Abdel-Ghaffar, and P. Gowda, "Soil-Foundation-Structure Behavior at the Oakland Outer Harbor Wharf," Civil Engineering Department, Report No. CCEER-91-2, University of Nevada, Reno, July 1991.
- CCEER-91-3 Norris, G., "Seismic Lateral and Rotational Pile Foundation Stiffnesses at Cypress," Civil Engineering Department, Report No. CCEER-91-3, University of Nevada, Reno, August 1991.
- CCEER-91-4 O'Connor, D. and M. Saiidi, "A Study of Protective Overlays for Highway Bridge Decks in Nevada, with Emphasis on Polyester-Styrene Polymer Concrete," Civil Engineering Department, Report No. CCEER-91-4, University of Nevada, Reno, October 1991.
- CCEER-91-5 O'Connor, D.N. and M. Saiidi, "Laboratory Studies of Polyester-Styrene Polymer Concrete Engineering Properties," Civil Engineering Department, Report No. CCEER-91-5, University of Nevada, Reno, November 1991.
- CCEER-92-1 Straw, D.L. and M. Saiidi, "Scale Model Testing of One-Way Reinforced Concrete Pier Hinges Subject to Combined Axial Force, Shear and Flexure," edited by D.N. O'Connor, Civil Engineering Department, Report No. CCEER-92-1, University of Nevada, Reno, March 1992.
- CCEER-92-2 Wehbe, N., M. Saiidi, and F. Gordaninejad, "Basic Behavior of Composite Sections Made of Concrete Slabs and Graphite Epoxy Beams," Civil Engineering Department, Report No. CCEER-92-2, University of Nevada, Reno, August 1992.

- CCEER-92-3 Saiidi, M. and E. Hutchens, "A Study of Prestress Changes in A Post-Tensioned Bridge During the First 30 Months," Civil Engineering Department, Report No. CCEER-92-3, University of Nevada, Reno, April 1992.
- CCEER-92-4 Saiidi, M., B. Douglas, S. Feng, E. Hwang, and E. Maragakis, "Effects of Axial Force on Frequency of Prestressed Concrete Bridges," Civil Engineering Department, Report No. CCEER-92-4, University of Nevada, Reno, August 1992.
- CCEER-92-5 Siddharthan, R., and Z. Zafir, "Response of Layered Deposits to Traveling Surface Pressure Waves," Civil Engineering Department, Report No. CCEER-92-5, University of Nevada, Reno, September 1992.
- CCEER-92-6 Norris, G., and Z. Zafir, "Liquefaction and Residual Strength of Loose Sands from Drained Triaxial Tests," Civil Engineering Department, Report No. CCEER-92-6, University of Nevada, Reno, September 1992.
- CCEER-92-7 Douglas, B., "Some Thoughts Regarding the Improvement of the University of Nevada, Reno's National Academic Standing," Civil Engineering Department, Report No. CCEER-92-7, University of Nevada, Reno, September 1992.
- CCEER-92-8 Saiidi, M., E. Maragakis, and S. Feng, "An Evaluation of the Current Caltrans Seismic Restrainer Design Method," Civil Engineering Department, Report No. CCEER-92-8, University of Nevada, Reno, October 1992.
- CCEER-92-9 O'Connor, D., M. Saiidi, and E. Maragakis, "Effect of Hinge Restrainers on the Response of the Madrone Drive Undercrossing During the Loma Prieta Earthquake," Civil Engineering Department, Report No. CCEER-92-9, University of Nevada, Reno, February 1993.
- CCEER-92-10 O'Connor, D., and M. Saiidi, "Laboratory Studies of Polyester Concrete: Compressive Strength at Elevated Temperatures and Following Temperature Cycling, Bond Strength to Portland Cement Concrete, and Modulus of Elasticity," Civil Engineering Department, Report No. CCEER-92-10, University of Nevada, Reno, February 1993.
- CCEER-92-11 Wehbe, N., M. Saiidi, and D. O'Connor, "Economic Impact of Passage of Spent Fuel Traffic on Two Bridges in Northeast Nevada," Civil Engineering Department, Report No. CCEER-92-11, University of Nevada, Reno, December 1992.
- CCEER-93-1 Jiang, Y., and M. Saiidi, "Behavior, Design, and Retrofit of Reinforced Concrete One-way Bridge Column Hinges," edited by D. O'Connor, Civil Engineering Department, Report No. CCEER-93-1, University of Nevada, Reno, March 1993.
- CCEER-93-2 Abdel-Ghaffar, S., E. Maragakis, and M. Saiidi, "Evaluation of the Response of the Aptos Creek Bridge During the 1989 Loma Prieta Earthquake," Civil Engineering Department, Report No. CCEER-93-2, University of Nevada, Reno, June 1993.
- CCEER-93-3 Sanders, D.H., B.M. Douglas, and T.L. Martin, "Seismic Retrofit Prioritization of Nevada Bridges," Civil Engineering Department, Report No. CCEER-93-3, University of Nevada, Reno, July 1993.
- CCEER-93-4 Abdel-Ghaffar, S., E. Maragakis, and M. Saiidi, "Performance of Hinge Restrainers in the Huntington Avenue Overhead During the 1989 Loma Prieta Earthquake," Civil Engineering Department, Report No. CCEER-93-4, University of Nevada, Reno, June 1993 (in final preparation).

- CCEER-93-5 Maragakis, E., M. Saiidi, S. Feng, and L. Flournoy, "Effects of Hinge Restrainers on the Response of the San Gregorio Bridge During the Loma Prieta Earthquake," (in final preparation) Civil Engineering Department, Report No. CCEER-93-5, University of Nevada, Reno.
- CCEER-93-6 Saiidi, M., E. Maragakis, S. Abdel-Ghaffar, S. Feng, and D. O'Connor, "Response of Bridge Hinge Restrainers During Earthquakes -Field Performance, Analysis, and Design," Civil Engineering Department, Report No. CCEER-93-6, University of Nevada, Reno, May 1993.
- CCEER-93-7 Wehbe, N., Saiidi, M., Maragakis, E., and Sanders, D., "Adequacy of Three Highway Structures in Southern Nevada for Spent Fuel Transportation, Civil Engineering Department, Report No. CCEER-93-7, University of Nevada, Reno, August 1993.
- CCEER-93-8 Roybal, J., Sanders, D.H., and Maragakis, E., "Vulnerability Assessment of Masonry in the Reno-Carson City Urban Corridor," Civil Engineering Department, Report No. CCEER-93-8, University of Nevada, Reno, May 1993.
- CCEER-93-9 Zafir, Z. and Siddharthan, R., "MOVLOAD: A Program to Determine the Behavior of Nonlinear Horizontally Layered Medium Under Moving Load," Civil Engineering Department, Report No. CCEER-93-9, University of Nevada, Reno, August 1993.
- CCEER-93-10 O'Connor, D.N., Saiidi, M., and Maragakis, E.A., "A Study of Bridge Column Seismic Damage Susceptibility at the Interstate 80/U.S. 395 Interchange in Reno, Nevada," Civil Engineering Department, Report No. CCEER-93-10, University of Nevada, Reno, October 1993.
- CCEER-94-1 Maragakis, E., B. Douglas, and E. Abdelwahed, "Preliminary Dynamic Analysis of a Railroad Bridge," Report CCEER-94-1, January 1994.
- CCEER-94-2 Douglas, B.M., Maragakis, E.A., and Feng, S., "Stiffness Evaluation of Pile Foundation of Cazenovia Creek Overpass," Civil Engineering Department, Report No. CCEER-94-2, University of Nevada, Reno, March 1994.
- CCEER-94-3 Douglas, B.M., Maragakis, E.A., and Feng, S., "Summary of Pretest Analysis of Cazenovia Creek Bridge," Civil Engineering Department, Report No. CCEER-94-3, University of Nevada, Reno, April 1994.
- CCEER-94-4 Norris, G.M. and Madhu, R., "Liquefaction and Residual Strength of Sands from Drained Triaxial Tests, Report 2," Civil Engineering Department, CCEER-94-4, University of Nevada, Reno, August 1994.
- CCEER-94-5 Saiidi, M., Hutchens, E., and Gardella, D., "Prestress Losses in a Post-Tensioned R/C Box Girder Bridge in Southern Nevada," Civil Engineering Department, CCEER-94-5, University of Nevada, Reno, August 1994.
- CCEER-95-1 Siddharthan, R., El-Gamal, M., and Maragakis, E.A., "Nonlinear Bridge Abutment, Verification, and Design Curves," Civil Engineering Department, CCEER-95-1, University of Nevada, Reno, January 1995.
- CCEER-95-2 Norris, G.M., Madhu, R., Valceschini, R., and Ashour, M., "Liquefaction and Residual Strength of Loose Sands from Drained Triaxial Tests," Report 2, Civil Engineering Department, Report No. CCEER-95-2, University of Nevada, Reno, February 1995.
- CCEER-95-3 Wehbe, N., Saiidi, M., Sanders, D., and Douglas, B., "Ductility of Rectangular Reinforced Concrete Bridge Columns with Moderate Confinement," Civil Engineering Department, Report No. CCEER-95-3, University of Nevada, Reno, July 1995.

- CCEER-95-4 Martin, T., Saiidi, M., and Sanders, D., "Seismic Retrofit of Column-Pier Cap Connections in Bridges in Northern Nevada," Civil Engineering Department, Report No. CCEER-95-4, University of Nevada, Reno, August 1995.
- CCEER-95-5 Darwish, I., Saiidi, M., and Sanders, D., "Experimental Study of Seismic Susceptibility Column-Footing Connections," Civil Engineering Department, Report No. CCEER-95-5, University of Nevada, Reno, September 1995.
- CCEER-95-6 Griffin, G., Saiidi, M., and Maragakis, E., "Nonlinear Seismic Response of Isolated Bridges and Effects of Pier Ductility Demand," Civil Engineering Department, Report No. CCEER-95-6, University of Nevada, Reno, November 1995.
- CCEER-95-7 Acharya, S., Saiidi, M., and Sanders, D., "Seismic Retrofit of Bridge Footings and Column-Footing Connections," Report for the Nevada Department of Transportation, Civil Engineering Department, Report No. CCEER-95-7, University of Nevada, Reno, November 1995.
- CCEER-95-8 Maragakis, E., Douglas, B., and Sandirasegaram, U., "Full-Scale Field Resonance Tests of a Railway Bridge," A Report to the Association of American Railroads, Civil Engineering Department, Report No. CCEER-95-8, University of Nevada, Reno, December 1995.
- CCEER-95-9 Douglas, B., Maragakis, E., and Feng, S., "System Identification Studies on Cazenovia Creek Overpass," Report for the National Center for Earthquake Engineering Research, Civil Engineering Department, Report No. CCEER-95-9, University of Nevada, Reno, October 1995.
- CCEER-96-1 El-Gamal, M.E. and Siddharthan, R.V., "Programs to Computer Translational Stiffness of Seat-Type Bridge Abutment," Civil Engineering Department, Report No. CCEER-96-1, University of Nevada, Reno, March 1996.
- CCEER-96-2 Labia, Y., Saiidi, M., and Douglas, B., "Evaluation and Repair of Full-Scale Prestressed Concrete Box Girders," A Report to the National Science Foundation, Research Grant CMS-9201908, Civil Engineering Department, Report No. CCEER-96-2, University of Nevada, Reno, May 1996.
- CCEER-96-3 Darwish, I., Saiidi, M., and Sanders, D., "Seismic Retrofit of R/C Oblong Tapered Bridge Columns with Inadequate Bar Anchorage in Columns and Footings," A Report to the Nevada Department of Transportation, Civil Engineering Department, Report No. CCEER-96-3, University of Nevada, Reno, May 1996.
- CCEER-96-4 Ashour, M., Pilling, P., Norris, G., and Perez, H., "The Prediction of Lateral Load Behavior of Single Piles and Pile Groups Using the Strain Wedge Model," A Report to the California Department of Transportation, Civil Engineering Department, Report No. CCEER-96-4, University of Nevada, Reno, June, 1996.
- CCEER-97-1-A Rimal, P. and Itani, A. "Sensitivity Analysis of Fatigue Evaluations of Steel Bridges", Center for Earthquake Research, Department of Civil Engineering, University of Nevada, Reno, Nevada Report No. CCEER-97-1-A, September, 1997.
- CCEER-97-1-B Maragakis, E., Douglas, B., and Sandirasegaram, U. "Full-Scale Field Resonance Tests of a Railway Bridge," A Report to the Association of American Railroads, Civil Engineering Department, University of Nevada, Reno, May, 1996.

